GROUND MOTION SCALING FOR THE PREDICTION OF THE SEISMIC
RESPONSE OF CONCRETE GRAVITY DAMS

A THESIS SUBMITTED TO
THE GRADUATE SCHOOL OF NATURAL AND APPLIED SCIENCES
OF
MIDDLE EAST TECHNICAL UNIVERSITY

BY

MUSTAFA BERK DUYGU

IN PARTIAL FULFILLMENT OF THE REQUIREMENTS
FOR
THE DEGREE OF MASTER OF SCIENCE
IN
CIVIL ENGINEERING

DECEMBER 2014

Approval of the thesis:

GROUND MOTION SCALING FOR THE PREDICTION OF THE SEISMIC RESPONSE OF CONCRETE GRAVITY DAMS

submitted by **MUSTAFA BERK DUYGU** in partial fulfillment of the requirements for the degree of **Master of Science in Civil Engineering Department, Middle East Technical University** by,

Prof. Dr. Gülbin Dural Ünver   _____
Dean, Graduate School of **Natural and Applied Sciences**

Prof. Dr. Ahmet Cevdet Yalçıner   _____
Head of Department, **Civil Engineering**

Assoc. Prof. Dr. Yalın Arıcı   _____
Supervisor, **Civil Engineering Dept., METU**

Examining Committee Members:

Prof. Dr. Barış Binici   _____
Civil Engineering Dept., METU

Assoc. Prof. Dr. Yalın Arıcı   _____
Civil Engineering Dept., METU

Prof. Dr. Murat Altuğ Erberik   _____
Civil Engineering Dept., METU

Assoc. Prof. Dr. Ayşegül Askan Gündoğan   _____
Civil Engineering Dept., METU

Assist. Prof. Dr. Mustafa Tolga Yılmaz   _____
Engineering Science Dept., METU

DATE: 03.12.2014

I hereby declare that all information in this document has been obtained and presented in accordance with academic rules and ethical conduct. I also declare that, as required by these rules and conduct, I have fully cited and referenced all material and results that are not original to this work.

Name, Last name : Mustafa Berk Duygu

Signature   :

ABSTRACT

GROUND MOTION SCALING FOR THE PREDICTION OF THE SEISMIC
RESPONSE OF CONCRETE GRAVITY DAMS

Duygu, Mustafa Berk

M.S., Department of Civil Engineering

Supervisor : Assoc. Prof. Dr. Yalın Arıcı

December 2014, 124 pages

Designing dams for seismic safety gains importance as the number of dams are increasing as a result of increasing need in water storage and hydropower. To define a structure's seismic safety, scaling of accelerograms should be considered as one of the most crucial elements. Appropriate scaling of ground motion records is required to better estimate the linear and nonlinear structural response of a structure. Although, in literature, there exist numerous methods dealing with this issue, it is required to determine the most suitable ones for designing concrete gravity dams. In this study, in order to compare the effectiveness of different ground motion scaling procedures, four different ground motion scaling procedures were used. The scaling methods used in this thesis are namely, non-stationary spectral matching, scaling for ASCE-7-10, scaling of records to arithmetic mean of maximum incremental velocity and Modal Pushover Based Scaling. The two dimensional Concrete Gravity Dam models are analyzed by utilizing non-linear dynamic analyses for the selected and scaled records.

Keywords: Ground Motion Scaling, Concrete Gravity Dam, Nonlinear Dynamic Analysis.

ÖZ

BETON AĞIRLIK BARAJLARININ SİSMİK DAVRANIŞLARININ TAHMİN EDİLMESİ İÇİN YER HAREKETLERİNİN ÖLÇEKLENDİRİLMESİ

Duygu, Mustafa Berk

Yüksek Lisans, İnşaat Mühendisliği Bölümü

Tez Yöneticisi: Doç. Dr. Yalın Arıcı

Aralık 2014, 124 sayfa

Sismik güvenlik için barajların tasarımı, su depolama ve su gücü ihtiyacının artmasıyla barajların sayıları çoğaldıkça önem kazanmaktadır. Bir yapının sismik güvenliğini tanımlamak için deprem ivme kayıtlarının ölçeklendirilmesi en önemli unsurlardan biri olarak düşünülmelidir. Bir yapının doğrusal ve doğrusal olmayan yapısal tepkisini daha iyi hesaplamak için yer hareketlerinin kayıtlarının uygun bir şekilde ölçeklendirilmesi gerekmektedir. Literatürde bu konuyla ilgili çok sayıda yöntem bulunmasına rağmen beton ağırlık barajlarının tasarlanması için en uygun yöntemlerin belirlenmesi esastır. Bu çalışmada, farklı yer hareketleri ölçeklendirme tekniklerinin etkililiğini karşılaştırmak için dört farklı yer hareketi ölçeklendirme prosedürü kullanılmıştır. Bu tezde kullanılan ölçeklendirme yöntemleri, durağan olmayan spektral eşleştirme, ASCE7-10 standartlarına göre ölçeklendirme, kayıtların maksimum artan hızının aritmetik ortalamasına göre ölçeklendirilmesi ve modsal itme tabanlı ölçeklendirmedir. İki boyutlu beton ağırlık baraj modelleri, seçilen ve ölçeklendirilen kayıtlar için lineer olmayan dinamik analizler kullanılarak analiz edilmiştir.

Anahtar Kelimeler: Yer hareketlerinin ölçeklendirilmesi, Beton Ağırlık Barajı, Doğrusal Olmayan Dinamik Analiz.

To My Wife

ACKNOWLEDGEMENTS

TABLE OF CONTENTS

LIST OF TABLES

TABLES

LIST OF FIGURES

FIGURES

CHAPTER 1

INTRODUCTION

1.1 GENERAL

Selecting and scaling of accelerograms is one of the most important issues in earthquake engineering as the ground motion records are widely being used in the design and evaluation of structures by engineers and academicians in lieu of the spectral analysis techniques. The choice and combination of the ground motions adds a significant layer of uncertainty on the prediction of the response of a structural system which can seldomly be addressed by trial and error methods even using today's powerful computers. As such, well-established, proven and documented methods are necessary for the selecting and scaling of the accelerograms in order to better estimate the nonlinear structural response of a structure for a target hazard by using real earthquake records.

A number of methods and procedures have been developed to deal with the issue of scaling and selecting accelerograms for the nonlinear analysis of structural systems. The selection of a suitable method, as given above, is in order to ascertain the accurate prediction of the response of a structure and hence can be changed for different systems. The important issue, however, is perhaps to define what an "accurate" prediction entails. Given that in comparison to a code based spectral analysis, a set of time history analyses will always include a stochastic component, an accurate analysis would mean: Capturing the mean performance level intended for the performance of the structure which can be chosen in terms of different engineering parameters, obtaining the aforementioned performance level with a level of certainty implying a limited variance in the analysis results - given the increase in the variance could mean questionable predictions and using a limited number of analyses to reach the evaluation or design goal.

Concrete gravity dams are very important structures as the failure comprises a huge risk to the society both for life safety and economic costs. Concrete gravity dams can be very tall as in the example of the Grande Dixence Dam which has an height of 285m (Ali et al., 2012). These imposing structures must be designed not only for the hydrostatic forces, but to also for dynamic and hydrodynamic forces that an earthquake may create. The design and evaluation of these systems is increasingly done using time history analyses given the need for the accurate prediction of the performance level of existing old dam stock as well as the newer systems. Thus, for both evaluation and design, the ground motion selection is a very important part of the process.

In this thesis, the performance of four different ground motion scaling procedures for the time history analyses of concrete gravity monoliths were investigated. A set of 35 different ground motions were used on 3 different dam systems with the heights of 50, 100 and 150m's. Possible variation in the material strength was considered by evaluating these systems at two different strength values. The performance of these procedures are quantified in terms of their proximity to the benchmark goals in terms of mean values, as well as the obtained variances from each method displaying a measure of reliability of the procedure. In order to justify their further use for the prediction of the performance of these systems in an efficient manner, combination rules are sought to provide the practicing engineers with the optimal number of motions to be used for design purposes.

1.2   LITERATURE REVIEW

With performance based seismic design gaining significant popularity and reputation, using non-linear response history analysis becomes more important especially for irregular and uncommon structures such as concrete gravity dams. In this respect, a set of ground motions which are appropriately scaled and modified to the target hazard is required. In most basic terms, the selection and scaling of ground motions affects the results obtained from any nonlinear analyses. Unfortunately, seismic design and building codes provide very little information for selection and scaling of earthquakes. This situation yields to a range of problems in seismic design due to this vague and unresolved nature, such as 1) unexperienced engineers are

overwhelmed by the complexity of the situation with loss of judgment on the accuracy even the correctness of the analyses 2) due to the time and resource required to obtain a reasonable solution using ground motions, the design is conducted with elastic, static methods 3) the choices during the analyses may lead to completely irrelevant misrepresentation of an hazard situation by voluntary of involuntary selection of the input ground motions.

As the occurrence of variability in the structural response due to the nature of input ground motions is unavoidable and as yet not fully quantifiable, the guidelines showing the appropriate ways of selecting and scaling suitable suites of accelerograms have not come to a desirable level yet (Bommer and Acevedo, 2004; Haselton, 2009). As in most design and evaluation methods, the analyst has to know the target of the analysis very well before choosing a method. Most of the selection methods can still not provide accurate estimates on the engineering demand parameters for some conditions and depend both on the nature of strong motion and the site characteristics (Kalkan and Chopra, 2009). It should also not be forgotten that the determination of the effectiveness of these ground motion scaling methods is a complicated issue because evaluations made by using numerical simulations may provide limited information and there are only a few studies performed with the experimental data (Kalkan and Chopra, 2011).

The performance of concrete gravity dams, along with the required evaluation technique, is significantly different than common structures comprised of prismatic, well reinforced beam and column systems. The ground motion excitations affecting a concrete gravity dam produce high stresses on the dam which can exceed the strength limit, causing the dam to go beyond its elastic limit, thereby producing a high structural damage (Asteris and Tzamtzis, 2003). The structural damage occurs in terms of crack propagation, which initiates on the downstream and the upstream slopes of the monolith propagating towards the other side (Araujo and Awruch, 1998). This is a phenomenon which can be investigated using nonlinear structural analyses, since in nonlinear analyses, tensile cracking of concrete can be observed which can change the stiffness of the system (Araujo and Awruch, 1998). A number of dams has undergone significant damage: the well-known cases of the Koyna Dam

and Shih Kang Dam are examples of severely damaged dam systems due to earthquakes (Nuss, et. al. 2012).

1.3   GROUND MOTION INTENSITY MEASURES

Ground motion intensity measures are mostly scalar indices developed in order to quantify the characteristics of the significantly random and non-stationary ground motions, with particular attention in development devoted to the impact of the given index especially on buildings' performances. There are many ground motion intensity measures; although, the basic measures, such as Peak Ground Acceleration (PGA), Peak Ground Velocity (PGV), and Peak Ground Displacement (PGD), can provide sufficient information on the ground motion characteristics, they still cannot provide sufficient information by themselves on the damage potential of a ground motion for a specific structure (Baker and Cornell, 2006).

Researchers and practitioners mostly use 5% - damped spectral acceleration, S_a, as the ground motion intensity measure although it has many limitations to characterize the nonlinear response of a building. Besides S_a, the main ground motion properties that will affect structural response are the spectral shape, strong motion duration and presence of velocity pulses which is also related to the distance of fault (NEHRP,2011). More complex and rarely-used measures include the inelastic responses of a single-degree-of-freedom system and vector-based (multiple) intensity measures (e.g., elastic spectral accelerations at two periods, the inelastic spectral displacement at the first-mode period, and the elastic spectral displacement at the second-mode period) (Baker and Cornell, 2006).

There are three primary types of horizontal spectral acceleration S_a: (1) arbitrary component (S_{aarb}), (2) geometric mean ($S_{agm.}$), and (3) maximum direction ($S_{amaxDir}$). One of these definitions can be selected, and the performance estimation will not depend on the selection. However, the procedure used to select and scale ground motions must be consistent with the definition used for the target spectrum (Baker and Cornell, 2006).

In this study, S_{aarb} values of ground motions are considered in scaling and for the target spectra, S_{agm} is selected for the target spectrum as it is one of the most common

methods for defining a target spectrum. ASCE 7-10 - Minimum Design Loads for Buildings and Other Structures also recommends using S_{agm} (ASCE, 2010).

1.4 GROUND MOTION SCALING PROCEDURES AND APPROACHES

As mentioned above, there are many ground motion scaling procedures. Current methodologies used to design and evaluate structures utilize mainly intensity-based scaling methods which make use of spectral matching techniques that modify the frequency content of the ground motion record in order to match its response spectrum to the target spectrum. The main objective of intensity-based methods is to provide scale factors for ground motion records to produce accurate Response History Analysis (RHA) of the structures for the scaled ground motion records (Fahjan, 2008).

Scaling ground motions to a target Peak Ground Acceleration (PGA) is one of the oldest and simplest methods. This method produces inaccurate and scattered estimates on Engineering Demand Parameters (EDP) (Nau and Hall, 1984; Miranda, 1993; Vidic et al., 1994; Shome and Cornell, 1998). In addition, other scalar intensity measures (IM) (such as effective peak acceleration, Arias intensity and effective peak velocity, etc.) were also stated to be inaccurate and inefficient (Kurama and Farrow, 2003).

The main problem of scalar intensity measures is that they do not consider any property of the structure to be analyzed. For example, including a vibration property of the structure can lead to improved methods to scale ground motions. A previous study shows that scaling ground motion records to a target value of the elastic spectral acceleration, $A(T_1)$ from the code-based design spectrum or PSHA-based uniform hazard spectrum at the fundamental vibration period of the structure, T_1, provides better results for structures whose response is dominated by their first-mode (Shome et al., 1998). Nevertheless, other studies indicate that this ground motion scaling method is not accurate for higher vibration modes and not efficient in the inelastic range of structural response (Mehanny, 1999), (Alavi and Krawinkler, 2000), (Kurama and Farrow, 2003).

In order to consider higher mode responses, a "scalar IM" that combines the spectral accelerations at the first two periods ($A(T_1)$ and $A(T_2)$), and a "vector IM" which is based on $A(T_1)$ and $A(T_1)/A(T_2)$ ratio were investigated (Bazzurro, 1998) and (Shome and Cornell, 1999). However, according to Baker and his coworkers, although this vector IM improves accuracy, it is not efficient for "near-fault" records having dominant velocity pulse (Baker and Cornell, 2006). As the near-fault and far-fault characteristics of strong motions are quite different, efficient ground motion scaling procedures must take into account the site distance characteristics.

In order to consider the properties of structures in the scaling procedures of ground motions, a new scaling procedure named "Modal Pushover Based Ground Motion Scaling" was proposed (Kalkan and Chopra, 2011). This method tries to match the maximum deformation of a first mode inelastic single degree of freedom system to the target inelastic deformation. The force - deformation relation of the system can be obtained from the first mode pushover curve.

One of the main problems with the ground motion scaling procedures is that they can cause dispersion on the inelastic structural response. There are many studies in the literature to determine the sources of dispersion and methods to reduce it. Different scaling factors based both on ground-motion data and spectrum intensities were investigated, leading to the finding that scaling with respect to spectrum intensities result in less dispersion (Nau and Hall, 1984). The scaling of records within a bin to the bin-median spectral acceleration reduces dispersion in structural response. If the dispersion in ground-motion intensities is decreased by 50%, the required number of nonlinear response history analysis will be decreased by a factor of 4 (Shome et al., 1998). Additionally, other studies revealed that scaling factors based on various spectrum intensities and an ensemble of records compatible with the design spectrum should be used to reduce dispersion (Martinez-Rueda, 1998). Scaling based on a goodness-of-fit criterion to the target spectrum was shown to produce smaller coefficient of variation for scaling of ground motions in bi-directional analysis (Beyer and Bommer, 2007).

The magnitude is usually regarded as the most dominant and effective parameter in ground motion selection (Bommer and Acevedo, 2004). The importance of magnitude and distance parameters on non-linear structural response was

investigated by Iervolino and Cornell (2005). There are several ground motion selection criteria proposed by different studies, based on magnitude, distance and site class (Kappos and Kyriakakis, 2000, Watson-Lamprey and Abrahamson, 2006). There are also different suggestions on scaling procedures focusing on minimizing the differences between elastic response spectrum and the target spectrum (Kennedy et al., 1984; Malhotra, 2003; Alavi and Krawinkler, 2004; Naeim et al., 2004; Youngs et al., 2007).

1.4.1 TIME BASED GROUND MOTION SCALING

In time based ground motion scaling procedure, the recorded motion is scaled (up or down) uniformly in order to match the target spectrum within a predefined period range. This procedure does not change the frequency content of the record. If there exist more than one ground motion time history, the analyst can both utilize the same procedure to fit the records separately, or best-fit the average of the generated spectra to the target spectrum. (Fahjan, 2008)

1.4.1.1 TIME BASED GROUND MOTION SCALING FOR SINGLE TIME HISTORY

This procedure aims to minimize the difference in a least-square sense between the response spectrum of the scaled ground motion and target spectrum. The difference defined in this method can be calculated as follows. (Fahjan, 2008)

Equation 1.1: $|Difference| = \int_{T_A}^{T_B} \left[\alpha S_a^{actual}(T) - \alpha S_a^{target}(T) \right]^2 dT$

To minimize the difference, the first derivative of the difference with respect to the scaling factor has to be zero as follows:

Equation 1.2: $min|Difference| \rightarrow \frac{d|Difference|}{d\alpha} = 0$

Combination of Equations 1 and 2, leads to a new equation for the scaling factor (α) as follows.

Equation 1.3: $\alpha = \frac{\sum_{T=T_A}^{T_B} S_a^{actual} - \alpha S_a^{target}}{\sum_{T=T_A}^{T_B} \left(S_a^{actual} \right)^2}$

where,

S_a^{target} :target acceleration response spectrum,

S_a^{actual} :acceleration spectrum of the given (actual) time history

T   :period of oscillator

T_A :period that scaling starts

T_B :period that scaling ends

1.4.1.2   TIME BASED GROUND MOTION SCALING FOR MULTIPLE TIME HISTORY RECORDS

As discussed previously, if there are more than one ground motion time histories to be scaled, the analyst can either utilize the same procedure to fit the records separately, or best-fit the average of the generated spectra to the target spectrum (Fahjan, 2008). There are three main approaches for multiple time histories.

For the first approach, the average of the time histories is used to fit to target spectra using a unique scaling factor for all time histories. In this approach, as all time histories are modified by the same factor, their average can match the target spectrum very well.

In the second approach, the procedure which is described previously for the single time histories is utilized to each time history, separately. In this approach, all the time histories can be perfectly scaled, but the average may not match the target spectrum very well.

The third approach is to match the time histories to the target spectra by utilizing different scaling factors for each one of them. In order to make the average spectrum of the scaled motions fit the target spectrum, a set of scaling factors are obtained in this method. However, in this approach, although a best fit average spectrum can be achieved, the scaling factors determined for the different input time histories may become insignificant as very high or very low (including negative) values can be obtained. (Fahjan, 2008)

In this study, some of the time based scaling approaches were used. All of these approaches fit to the third approach of multiple time histories defined above, which utilizes different scaling factors for each time history. Details of the ground motion scaling procedures used in this study are discussed in Chapter 2 of this thesis.

1.4.2 FREQUENCY BASED SCALING

In frequency based scaling methodology, real ground motion records are utilized to produce time histories in order to match the target spectrum. Frequency based scaling methodology is more appropriate with respect to classical artificial record generation because the physical properties of ground motions remain unchanged (Nikolaou, 1998).

In frequency based scaling methodology, by using a spectral ratio obtained using the target spectrum, a real ground motion can be filtered in its own frequency domain. Furthermore, the procedure does not alter the Fourier phases of the motions. This iterative procedure can be repeated until the ground motion matches the target spectra perfectly for certain period ranges. Therefore ground motions that can perfectly fit to target spectrum can be obtained by using a real ground motion data as an input. However, it is important that the spectra obtained by using this procedure must produce consistent results in terms of structural analysis, for example in longer periods, structural factor should be equal to average ductility factor (i.e. Equal Displacement Rule) for velocity and displacement sensitive spectral regions. (Özdemir and Fahjan, 2007)

1.4.3 NON-STATIONARY SPECTRAL MATCHING

In non-stationary spectral matching procedures, time domain spectral matching is utilized to generate acceleration time histories. In this method, spectral accelerations of each generated acceleration time histories is fitted to the target spectrum almost exactly. Although, in some cases, the generated motions may not be realistic, this is not considered to be a problem for structural analyses (Abrahamson, 1992).

In this thesis, RSPMatch program is used for the purpose of spectral matching (Abrahamson, 1992). The procedure used in this method is a modification of Lilhanand and Tseng Algorithm (Lilhanand and Tseng, 1988) and for a wider range

of time histories it can preserve the non-stationary character of the reference ground motion. Although non-stationary spectral matching procedures are more complicated than the frequency domain scaling procedures, their convergence properties are better and they preserve the non-stationary character of the reference time history (Abrahamson, 1992).

1.4.4 SCALING OF GROUND CONSIDERING MAXIMUM INCREMENTAL VELOCITY (MIV)

Incremental Velocity (IV) refers to the area under the acceleration time history between two points of accelerations which are equal to zero. In this scaling method, ground motions are scaled to the arithmetic mean of MIV's of ground motions.

A study conducted in 2003 suggests that Maximum Incremental Velocity (MIV) is good at representing the damage potential since it better represents the impulsive characteristics of the earthquakes (Kurama and Farrow, 2003). Using MIV as a scaling method was shown to outperform many of the other scaling procedures for the non-linear response history of building structures (O'Donnell et al., 2013).

1.4.5 MODAL PUSHOVER BASED SCALING PROCEDURE

In Modal Pushover Based Scaling Procedure, ground motions are scaled to match a target value of an inelastic deformation of the first mode inelastic single degree of freedom (SDF) system. The properties of the SDF system are determined by the first mode pushover analysis. (Kalkan and Chopra, 2011)

In this method, firstly, the target earthquake spectrum and the structural periods of the structure to be analyzed are determined. The pushover curve of the structure is obtained by using non-linear static analyses. The obtained pushover curve is idealized in order to use in a SDF analysis. A target deformation is obtained using the yield strength reduction factor (R_y) and the empirical relations, or through the use of the utilized unscaled motions in SDF analyses. If the SDF analysis is chosen, the mean of the displacement results of the set of runs using the unscaled motions is the

target displacement goal. The empirical procedure was shown to yield very similar results to the mean displacement results obtained using the unscaled set of ground motions.

The scale factor for each motion is obtained using the SDF with the idealized force deformation relation in transient analysis. The scale factor is increased until the target displacement ($\bar{D}_1'$) is obtained in the analysis. If more than one factor is obtained, the smaller of the two is used as the scaling factor. A unique factor for each motion is obtained using this procedure by minimizing the difference between the SDF deformation using the idealized pushover relation and the target value of deformation (Kalkan and Chopra, 2011).

1.4.6 SCALING OF GROUND MOTIONS USING CODE SPECIFICATIONS

In addition to the various scaling approaches generated by a number of researchers, there exist several standards and procedures in various building codes and official documents which make their methods obligatory in the assessment and evaluation of structures. For instance, building codes like International Building Code (IBC) (ICC, 2006) require that earthquake records must be scaled with respect to the ASCE-7 (ASCE, 2010) provisions. The provisions given in the Turkish Earthquake Resistant Design Code and the American Society of Civil Engineers ASCE/SEI 7-10 are summarized below.

1.4.6.1 TURKISH SEISMIC CODE STANDARDS (2007)

Turkish seismic code (DBYBHY, 2007) allows using artificial, recorded or simulated time histories as the input ground motions for linear and nonlinear seismic analyses. According to Turkish seismic code (DBYBHY, 2007), the duration of the ground motion time history shall not be shorter than 5 times the fundamental period of the building. This duration should also not be shorter than 15 seconds. For zero periods, mean spectral acceleration of generated ground motions shall not be less than A_og. For 5% damping ratio, the mean spectral accelerations of artificially generated acceleration records shall not be less than 90 % of the elastic spectral accelerations ($S_{ae}(T)$) in the period range between $0.2T_1$ and $2T_1$ with respect to

dominant natural period (T_1) of the building in the considered direction of earthquake.

The local site conditions should be taken into account for any recorded earthquake or ground motions simulated physically. For time domain analyses, at least three ground motions should be utilized and the maximum of these results shall be used. If at least seven ground motions are used, for design, the mean values of the results should be considered (DBYBHY, 2007).

1.4.6.2 ASCE/SEI STANDARD 7-10 (ASCE, 2010)

ASCE-7 (ASCE, 2010) indicates that earthquake records shall be selected from the events whose fault distance, magnitudes and source mechanisms comply with the maximum earthquake considered. If the required number of suitable records is not available, appropriate simulated ground motions may be included in order to make up the required total number. For 2D analysis of symmetric-plan buildings, ASCE-7 requires intensity-based scaling of ground motion records using appropriate scale factors so that the mean value of the 5 percent-damped response spectra for the set of scaled records is not less than the design response spectrum over $0.2T_1$ to $1.5T_1$ period range. The design value of an engineering demand parameter (EDP)— member deformations, story drifts or member forces—is used as EDP average value over seven or more ground motions, or its maximum value over all ground motions, as long as the analysis of the system is performed for fewer than seven ground motions. A unique scaling factor is not guaranteed by the ASCE-7 scaling procedure for each record. Various scaling factor combinations can be described in order to make sure that the average spectrum of scaled records are above the design spectrum (or amplified spectrum for 3-D analyses) over the specified period range (Kalkan and Chopra, 2009).

In this thesis, record selection and scaling process is also investigated by means of ASCE-7 approach and further details are provided in the following chapters.

1.5 SELECTION OF EARTHQUAKE SPECTRA

Selection of earthquake spectra is usually based on probabilistic seismic hazard analyses which yield a cumulative aggregated earthquake hazard at the site due to a

12

number of faults posing risk nearby. The results of the analysis are traditionally given in terms of an earthquake spectrum. Different spectra are provided for different hazard levels which are selected usually in accordance with structure specific performance goals. The provision of the ground motions to be used is sometimes considered an integral part of such a study, most often not.

The seismic hazard at the site is traditionally given in terms of a design spectrum although it is well known that such a spectrum has significant limitations for the prediction of the nonlinear performance of most structures. The specific nature of the earthquake reflected on the time history, such as the nature of the pulse, the frequency content and duration is not present on a response spectrum. While the site effects are somewhat represented in terms of period elongation or amplitude change, it should be kept in mind that for almost all cases, these assumptions are based on specific statistical relations and not the real site conditions.

While the determination of the spectrum introduces certain uncertainty to a design/evaluation process, this uncertainty is mostly handled through selection of the hazard levels and the quantification of the risks that the active faults near the site causes. However, this uncertainty is different from the variance in the analysis introduced by the time history analyses. As given above, the characteristics of the record and the related variance in the pulse, frequency and duration characteristics are the major variable in time history selection. The uncertainty regarding the selection of the response spectrum is not within the scope of this thesis: the focus is kept on the time history selection.

1.6   SELECTION OF TIME HISTORY RECORDS

In order to obtain good results in the scaling of the ground motions, the real set of ground motions and the target spectrum to which those motions will be scaled should be selected in a proper manner. Most of the record selection approaches and many building codes (e.g. (ATC, 2011)) suggest selection of ground motions by filtering them using a magnitude interval which can represent different scenarios.

The purpose of selecting real earthquake records is to include the specific features of the ground motion into the analyses. This matching can be based on an elastic

response spectrum or an earthquake scenario with the minimum parameters including the magnitude, distance and site class. According to the guidance given in the seismic design codes, compatibility of the record with the response spectrum is generally more important than seismological parameters for the selection of proper actual records. As a result, the selection of the records is most often conducted by means of ground motion parameters such as the peak ground acceleration, the peak ground velocity, and the duration. Additionally, the selection of the records in a specified magnitude range is important since the magnitude is one of the main features of a ground motion and it affects the frequency content as well as the duration of the strong motion. It is desirable to use earthquake magnitudes within ± 0.25 magnitude units of the target magnitude (Stewart et al., 2001).

Fault distance is also one of the important parameters; it may affect ground motion characteristics because especially near-fault motions may have different properties than other ground motions mainly due to the velocity pulses. Site conditions may also affect the main characteristics of a ground motion such as the frequency content and amplitude. It has been observed in many studies that velocity pulses may affect many near-fault ground motion records and there is a relationship between pulse period and earthquake magnitude (Alavi and Krawinkler, 2000; Somerville et al., 2004; Mavroeidis and Papageorgiou, 2003; Bray and Rodriguez-Marek, 2004; Fu and Menun, 2004; Baker, 2007; Shahi and Baker, 2011).

Acceleration time histories can be produced in several ways. They can be obtained by using artificial records which are compatible with the design response spectrum, from synthetic records obtained from seismological models and from accelerograms recorded in real earthquakes.

1.6.1   ARTIFICIAL ACCELEROGRAMS

The reason why artificial accelerograms are generated is to match a target response spectrum by obtaining a power spectral density function using the smoothed response spectrum. In this method, sinusoidal signals including random phase angles and amplitudes are derived. Next, the sinusoidal motions are summed, followed by an iterative procedure. This procedure can be used to improve the match with the target response spectrum, by calculating the ratio between actual response ordinates and the

target at selected frequencies. Supplementary information rather than the response spectrum, such as the duration related to the expected earthquake motion, is required to obtain other characteristics of artificial spectrum compatible record. Although acceleration time-series that are almost totally compatible with the elastic design spectrum could be obtained, in most cases, the generated accelerograms have an excessive number of cycles of strong motion. As a result, these accelerograms have a high energy content which makes them unrealistic. (Bahar et. al., 2012)

Another difficulty with respect to artificial time history generation is observed upon trying to match an individual ground motion to a design spectrum which is not intended to represent the motion from a single earthquake (Naeim and Kelly, 1999). In general, the design response spectrum results from a statistical analysis considering the effect of several seismic sources at the same time. Thus, earthquakes in different sources may drive the response at various periods. Additionally, the spectrum consists of spectra corresponding to scenarios in each of the sources (Reiter, 1990; Bommer et al., 2000).

1.6.2   SYNTHETIC ACCELEROGRAMS

Seismological source models accounting for path and site effects can generate synthetic accelerograms. In general, the real difficulties lie in defining suitable input parameters, for example the source, site characteristics and path. A definition of a specific earthquake scenario in terms of magnitude, rupture mechanism in addition to the location of the site and geological conditions is required in order to generate synthetic accelerograms. Most of these parameters are not always available, especially upon utilization of seismic design codes (Bommer et al., 2003).

1.6.3   REAL ACCELEROGRAMS

Real strong ground motion accelerograms bear a lot of information related to the nature of the ground shaking and have all of the ground-motion characteristics (frequency, amplitude, and duration, energy content and phase characteristics). Additionally, they reflect all the factors affecting accelerograms (characteristics of the source, site and path). Upon the significant increase in the number of measured ground motions in the last decade, using and scaling real recorded accelerograms

turned out to be one of most referenced contemporary research areas in this field. Although the global strong motion databank continuously grow, there exists numerous combinations of earthquake parameters such as the rupture mechanism, magnitude, source-to site distance and the site classification that remain not represented well, which, in some cases, can make gathering appropriate records difficult (Bommer et al., 2003).

1.7 OBJECTIVES AND SCOPE

The primary goal of this study is to investigate the four different ground motion scaling procedures that can be used for the analyses of concrete gravity dams to predict the seismic response.

In order to assess the effectiveness of the ground motion scaling methods, the following steps were taken:

❖ Six different concrete gravity dam models were created for nonlinear time history analyses of scaled and unscaled motions. The structural models represents three dam models having 50m, 100m and 150m's of total height for two different strength conditions.

❖ A suite of 35 different ground motions were selected as the ground motion set for determining the efficacy and accuracy of the prediction of these four methods on the selected dam systems.

❖ The maximum displacement and acceleration at the top of the monolith , the maximum base shear and the ratio of the cracked area to the total monolith area are taken as the EDP's in study representing the performance of the structure in different scalars.

❖ Unscaled set of original selected motions was used in nonlinear analyses of the given systems in order to determine the benchmark results which would set the theoretical goal of the analysis results, representing the mean and the variance in the aforementioned EDP levels.

❖ The different ground motions are scaled according to four different procedures. Nonlinear analyses were conducted on the selected systems in order to compare the efficacy of the procedures in yielding the benchmark analysis goals. The scaling procedures are investigated by means of the

scatter (variance) and accuracy (mean) in the output EDPs of the non-linear dynamic analyses.

This study is organized in four different chapters. First, the ground motion selection and scaling procedures used for the analyses and general methodology are presented in Chapter 2. The results of the non-linear dynamic analyses are presented in Chapter 3. Evaluation of the analyses results are presented in Chapter 4. The conclusions from this study and future aspects of the research are summarized in Chapter 5.

CHAPTER 2

GROUND MOTION SELECTION AND METHODOLOGY

2.1   INTRODUCTION

Ground motions to be used for seismic design and evaluation are usually selected by considering the magnitude, distance and the site conditions. Some other factors including the directivity or basin effects are sometimes taken into account. The ground motions records selected for this study were taken from PEER Ground Motion Database (PEER, 1998). In order to have compatible results with the other studies on ground motion scaling, a ground motion suite used in many other studies (Kurama and Farrow, 2003; O'Donnell et al., 2013) which compare the effectiveness of ground motion scaling methods was selected. However, only 35 of the 38 motions which were selected in these studies were available for use in the PEER Ground Motion Database (PEER, 1998) and these 35 motions are taken as the original ground motion suite. The remaining three strong motions were removed from PEER database due to some problems in raw data. (PEER, 1998)

2.2   GROUND MOTION SELECTION

O'Donnell and coworkers (2011) distinguished the earthquake records by means of their characteristic properties related to source, directivity, site and basin effects which includes cyclic versus impulsive records, records with high, mid, or low frequency content, short or long duration records. Frequency domain analyses were utilized to investigate basin, duration, and pulse attributes of the records. Near fault motions (having a maximum fault distance of 20km.) were preferred for the motion suite. The motion suite is compiled after the refinement process (O'Donnell et al., 2013). Properties of the motions selected are given in Table 2-1 and accelerograms of the original motions are given in Figure 2-1.

Table 2-1 Ground Motion Records Used in the Analyses

ID	Event	Date	PGA (g)	PGV (cm/sec)	Magnitude	Rjb (km)	Rrup (km)	V_{s30} (m/s)	Station	File ID
1	Loma Prieta	1989	0.526	41.92	6.93	3.9	10.7	376.1	BRAN	BRN090
2	Loma Prieta	1989	0.529	35.014	6.93	8.7	15.2	288.6	Capitola	CAP000
3	Loma Prieta	1989	0.644	55.148	6.93	0.1	3.9	462.2	Corralitos	CLS000
4	Loma Prieta	1989	0.106	8.767	6.93	39.3	39.5	367.6	Fremont - Mission San Jose	SJTE225
5	Loma Prieta	1989	0.357	28.616	6.93	9.2	10	729.6	Gilroy - Gavilan Coll.	GIL067
6	Loma Prieta	1989	0.284	41.964	6.93	10.3	11	338.5	Gilroy - Historic Bldg.	GOF160
7	Loma Prieta	1989	0.367	32.907	6.93	10.4	11.1	270.8	Gilroy Array #2	G02000
8	Loma Prieta	1989	0.555	35.684	6.93	12.2	12.8	349.9	Gilroy Array #3	G03000
9	Loma Prieta	1989	0.417	38.755	6.93	13.8	14.3	221.8	Gilroy Array #4	G04000
10	Loma Prieta	1989	0.17	14.175	6.93	17.9	18.3	663.3	Gilroy Array #6	G06090
11	Loma Prieta	1989	0.587	47.042	6.93	0	3.9	477.7	LGPC	LGP090
12	Loma Prieta	1989	0.512	41.151	6.93	7.6	8.5	370.8	Saratoga - Aloha Ave	STG000
13	Loma Prieta	1989	0.332	61.54	6.93	8.5	9.3	370.8	Saratoga - W Valley Coll.	WVC270
14	Loma Prieta	1989	0.386	15.396	6.93	12.2	18.5	714	UCSC	UC2090
15	Loma Prieta	1989	0.45	18.669	6.93	12	18.4	714	UCSC Lick Observatory	LOB000
16	Loma Prieta	1989	0.672	34.98	6.93	11	17.5	376.1	WAHO	WAH090
17	Cape Mendocino	1992	1.497	125.133	7.01	0	7	513.7	Cape Mendocino	CPM000

Table 2-1 Ground Motion Records Used in the Analyses (Continued)

ID	Event	Date	PGA (g)	PGV (cm/sec)	Magnitude	Rjb (km)	Rrup (km)	V_{s30} (m/s)	Station	File ID
18	Cape Mendocino	1992	0.116	29.934	7.01	16	19.9	457.1	Fortuna - Fortuna Blvd	FOR000
19	Cape Mendocino	1992	0.662	89.684	7.01	0	8.2	712.8	Petrolia	PET090
20	Cape Mendocino	1992	0.549	41.875	7.01	7.9	14.3	311.8	Rio Dell Overpass - FF	RIO360
21	Kobe- Japan	1995	0.042	5.306	6.9	158.1	158.6	256	FUK	FKS090
22	Kobe- Japan	1995	0.821	81.302	6.9	0.9	1	312	KJMA	KJM000
23	Kobe- Japan	1995	0.503	36.623	6.9	7.1	7.1	609	Nishi-Akashi	NIS090
24	Kobe- Japan	1995	0.243	37.795	6.9	19.1	19.1	256	Shin-Osaka	SHI000
25	Kobe- Japan	1995	0.694	85.298	6.9	0	0.3	312	Takarazuka	TAZ090
26	Kobe- Japan	1995	0.616	120.73	6.9	1.5	1.5	256	Takatori	TAK090
27	Duzce- Turkey	1999	0.822	62.101	7.14	12	12	326	Bolu	BOL090
28	Duzce- Turkey	1999	0.535	83.506	7.14	0	6.6	276	Duzce	DZC270
29	Duzce- Turkey	1999	0.111	14.204	7.14	0.2	0.2	424.8	Lamont 1058	1058-E
30	Duzce- Turkey	1999	0.147	11.978	7.14	4.2	4.2	424.8	Lamont 1059	1059-N
31	Duzce- Turkey	1999	0.134	13.685	7.14	11.5	11.5	481	Lamont 1061	1061-E
32	Duzce- Turkey	1999	0.257	16.313	7.14	9.2	9.2	338	Lamont 1062	1062-E
33	Duzce- Turkey	1999	0.97	36.501	7.14	3.9	3.9	424.8	Lamont 375	375-N
34	Duzce- Turkey	1999	0.159	12.953	7.14	8	8	659.6	Lamont 531	531-N
35	Hector Mine	1999	0.337	41.743	7.13	10.3	11.7	684.9	Hector	HEC090
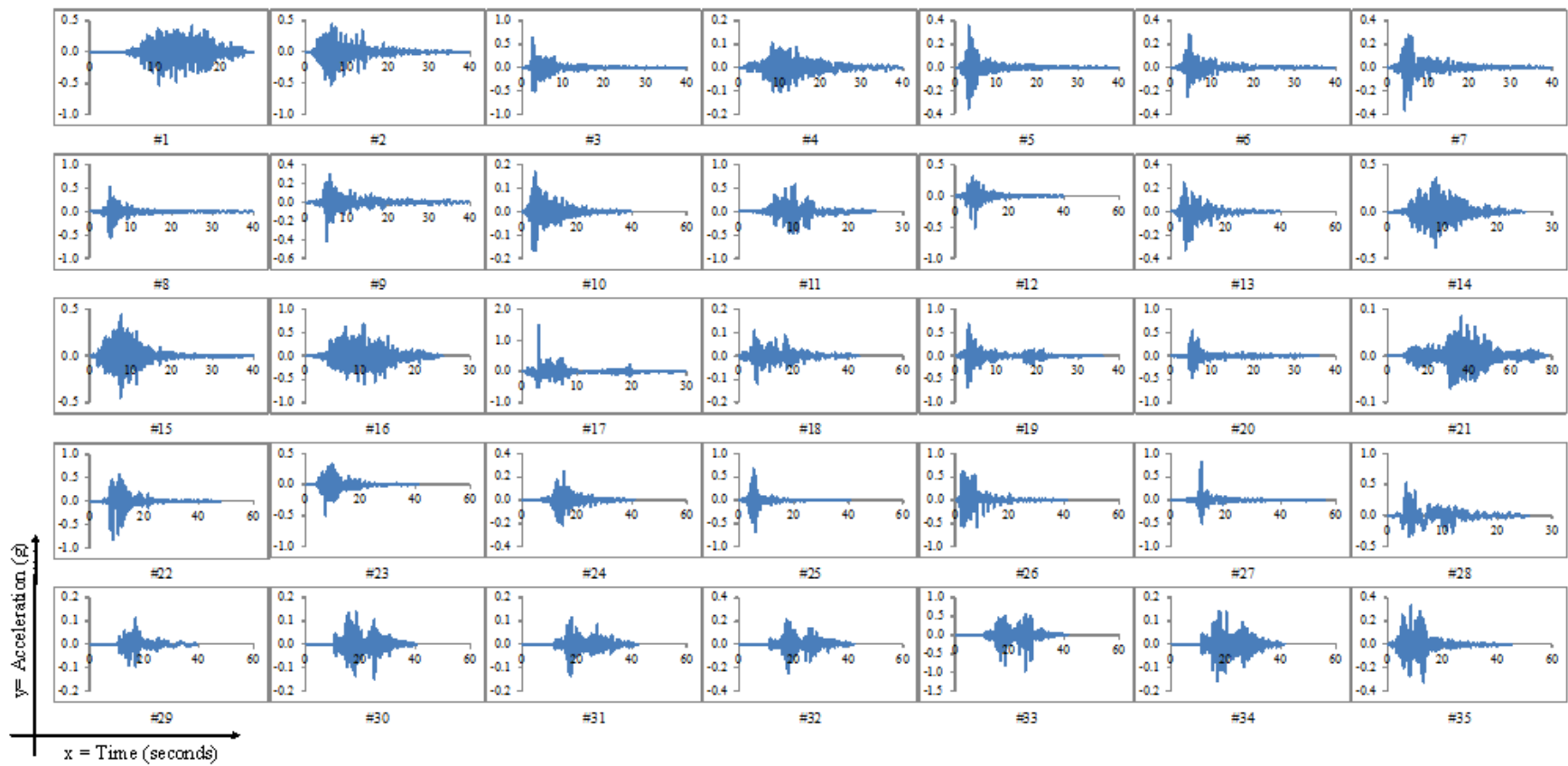
Figure 2-1 Acceleration Time Histories of Selected Motions

2.3 TARGET EARTHQUAKE SPECTRUM

In this study, the scaling of records are carried out by utilizing the target spectra which is obtained by taking the geometric mean of all of the motions selected for the analyses. While the selection of a target spectrum is usually carried out using a seismic hazard analyses, such a spectra was not sought, as an hazard study would involve further difficulties regarding the recurrence periods, fault information and uncertainty related to the attenuation relationships which is not within the scope of this study. The target earthquake spectrum generated by using the spectra of all of the selected motions is given in Figure 2-2
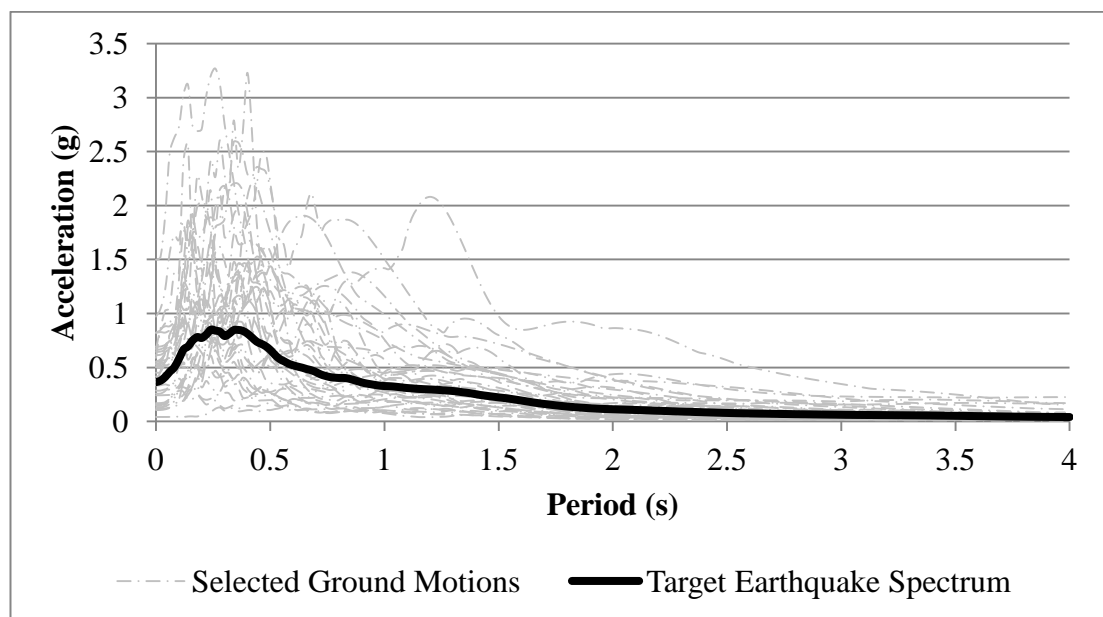
Figure 2-2 Target Earthquake Spectrum

2.4 SCALING OF GROUND MOTIONS

Four different ground motion scaling procedures were utilized in this study in order to compare the effectiveness of different ground motion scaling procedures for the nonlinear analysis of concrete gravity dams. The scaling methods used in this study are:

1) Non-stationary spectral matching (RSPM)
2) Scaling for the ASCE-7-10 specifications (ASCE)

3) Scaling of records to the arithmetic mean of maximum incremental velocity (MIV)

4) Modal Pushover Based Scaling Procedure (MPS)

A short summary of each procedure is given below.

2.4.1 NON-STATIONARY SPECTRAL MATCHING (RSPM)

For the purpose of conducting non-stationary spectral matching of ground motion records, the well-known RSPMatch software was used in this study (Abrahamson, 1992).

All of the ground motion records were scaled to the target spectra defined above using the aforementioned software. The scaling process was made for 10% tolerance for maximum mismatch between 0.1 and 100 hertz of frequencies. For each scaled motion, maximum of 50 iterations were made. After each matching, the authenticity of the ground motion developed is checked in order not to have any unrealistic pulse or duration content within the ground motion. The final spectra were compared to the target spectrum.

The pseudo-velocities, the accelerograms and the response spectra of the scaled motions are shown in Figure 2-3, Figure 2-4 and Figure 2-5, respectively. It can be seen that the ground motions are satisfactorily matched to the target earthquake spectrum.
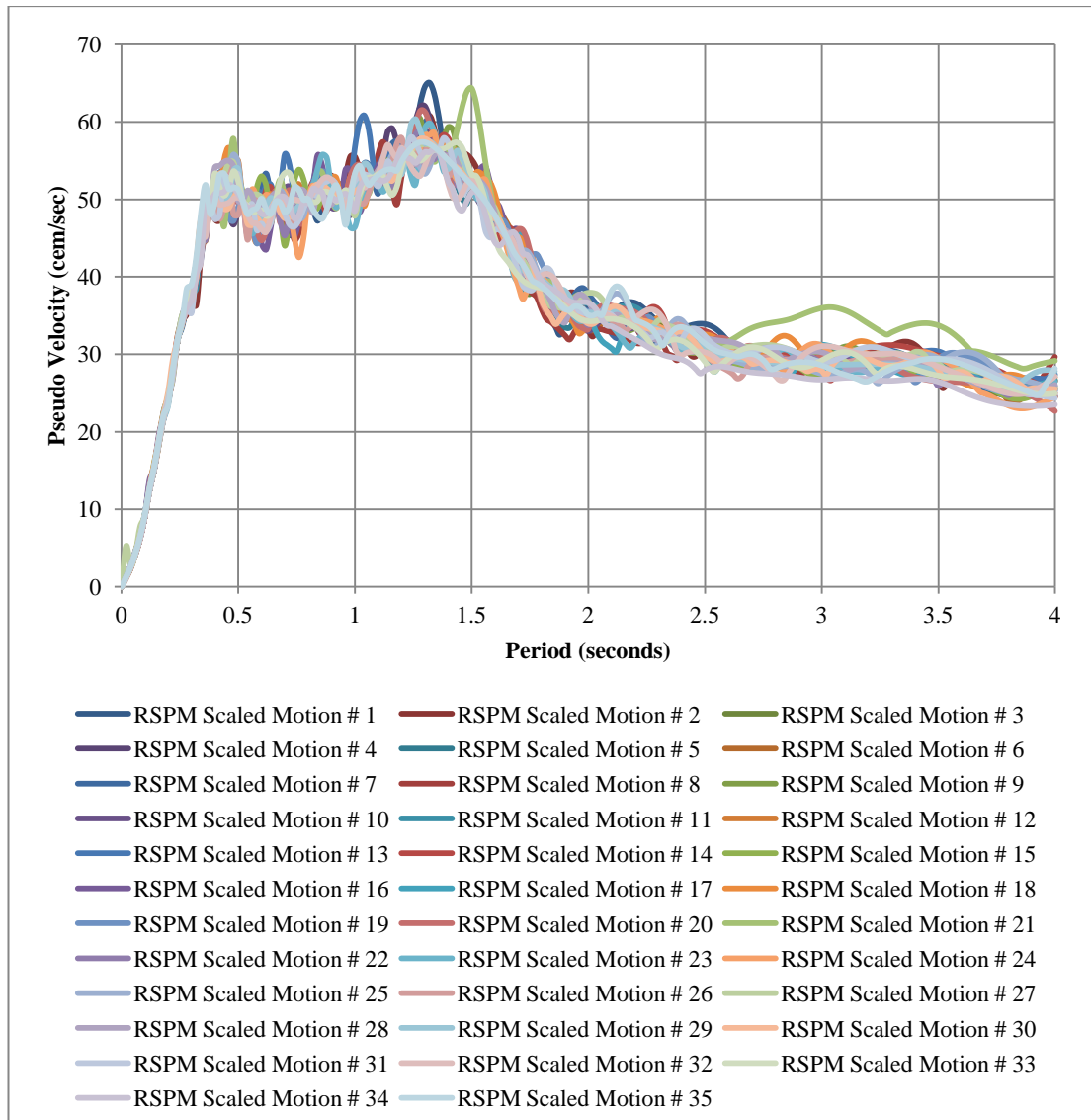
Figure 2-3 Spectral Velocities of the Scaled Motions
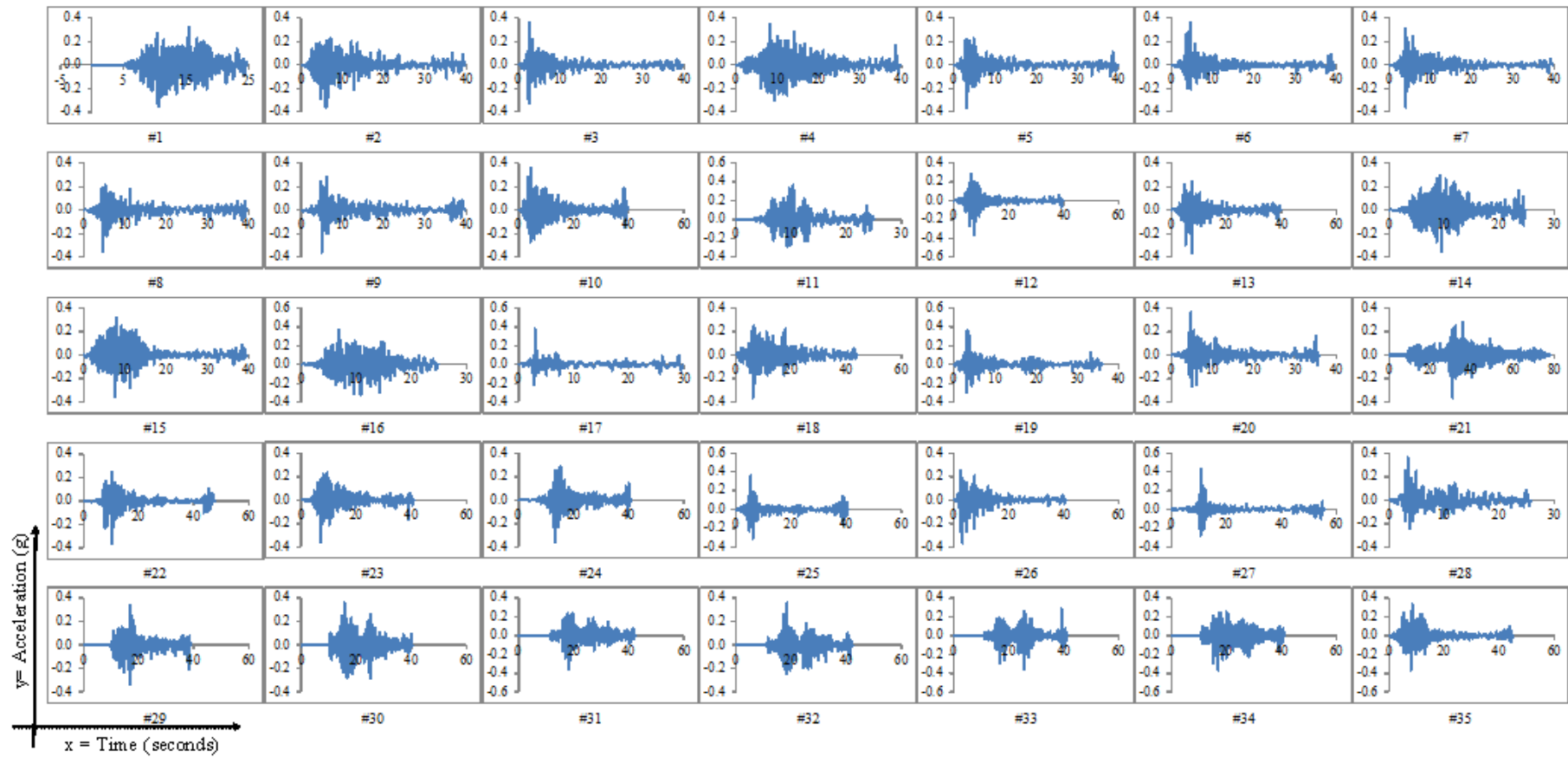
Figure 2-4 Acceleration Time Histories of the Motions Scaled by RSPM
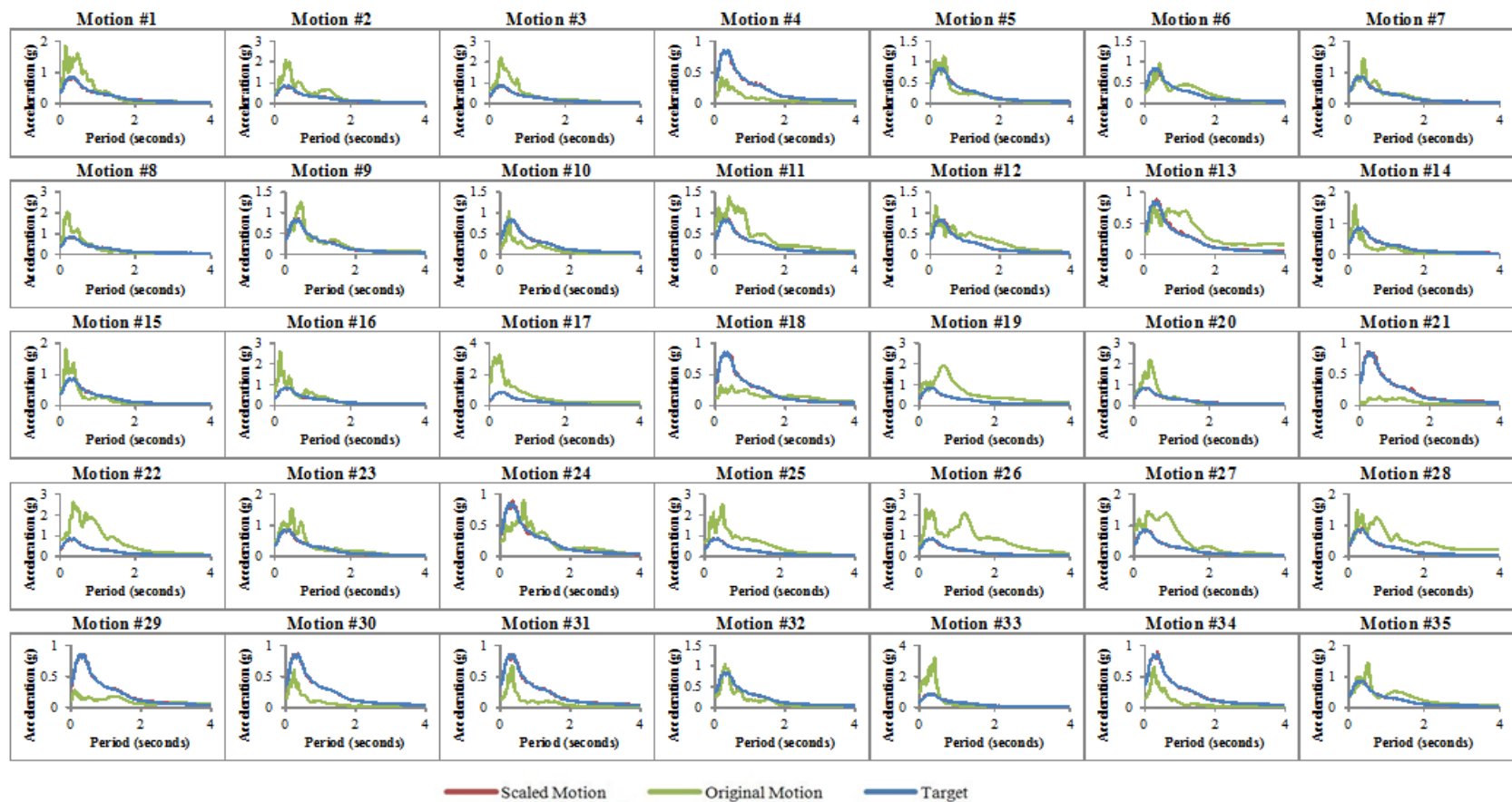
Figure 2-5 Response Spectra of the Motions Scaled by RSPM

The peak acceleration of the matched time histories are compared in Figure 2-6 also showing the peak accelerations of the original motions. It can be seen that the maximum acceleration of the matched accelerations are very similar.
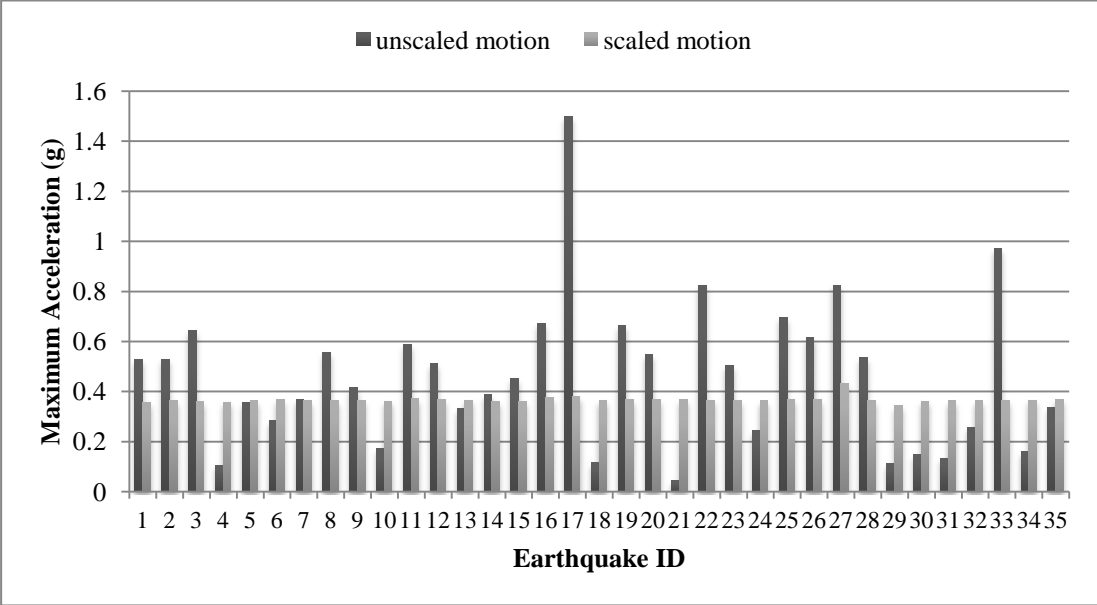
Figure 2-6 Maximum Accelerations of the Scaled Motions (RSPM)

The maximum accelerations of the matched time histories are compared in Figure 2-7 also showing the maximum accelerations of the original motions.
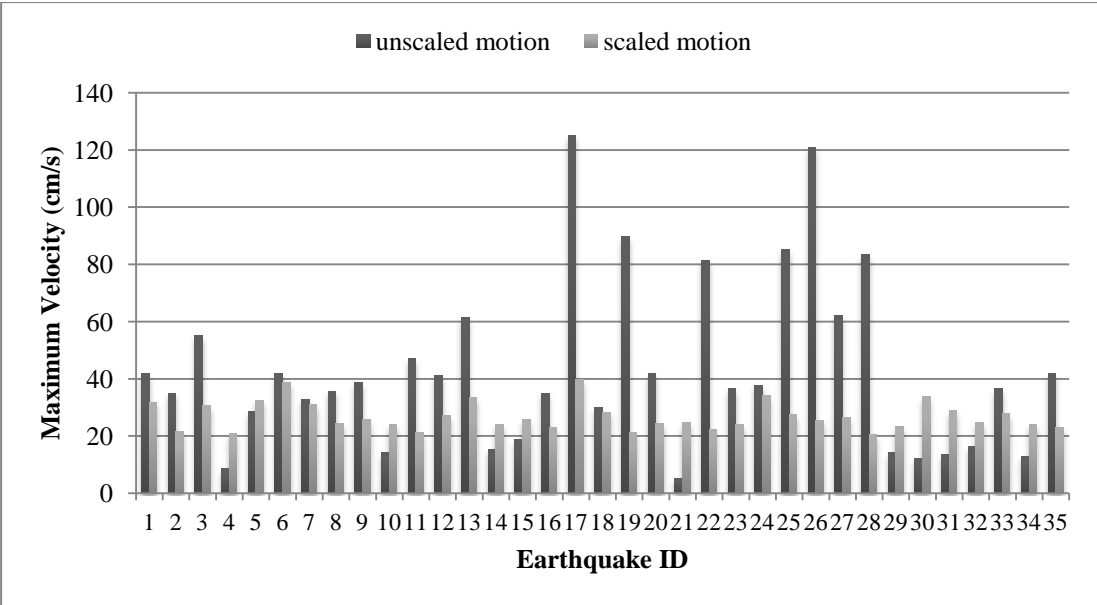
Figure 2-7 Maximum Velocities of the Scaled Motions (RSPM)

The sustained maximum accelerations (Third maximum acceleration of an acceleration time history) of the matched time histories are compared in Figure 2-8 also showing the sustained maximum accelerations of the original motions.
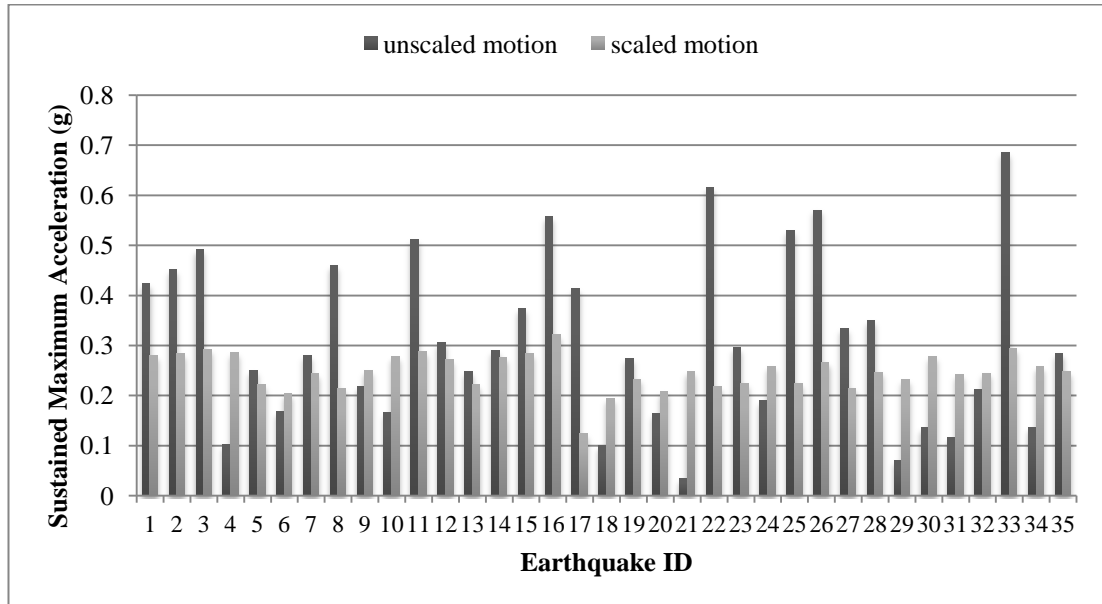
Figure 2-8 Sustained Maximum Accelerations of the Scaled Motions (RSPM)

The sustained maximum velocities of the matched time histories are compared in Figure 2-9 also showing the sustained maximum velocities of the original motions.
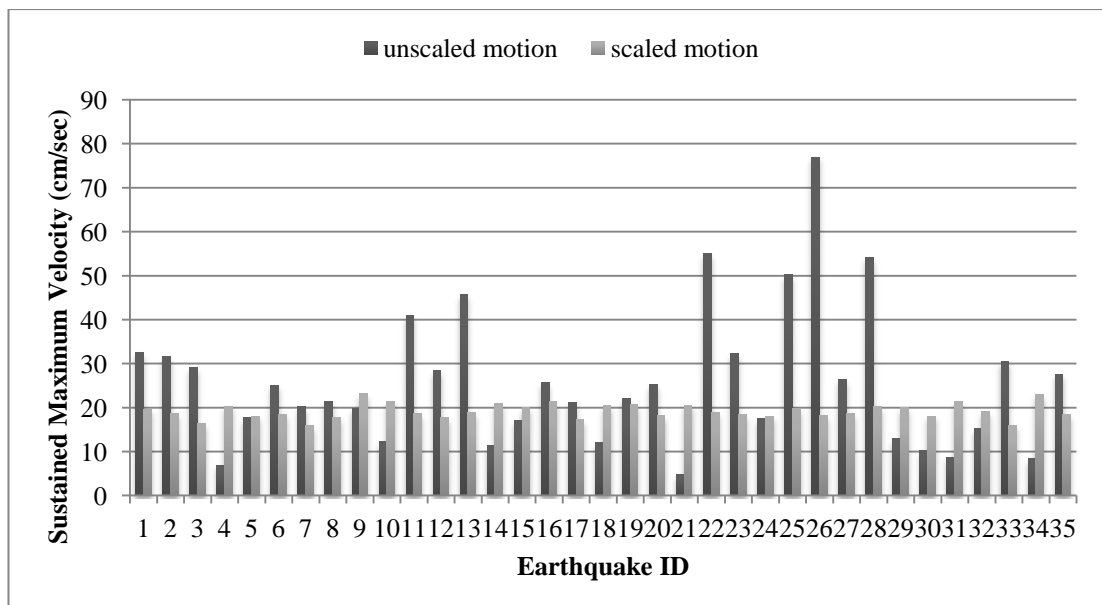
Figure 2-9 Sustained Maximum Velocities of the Scaled Motions (RSPM)

2.4.2 SCALING OF RECORDS USING ASCE-7-10 SPECIFICATIONS AND TIME BASED SCALING PROCEDURES (ASCE)

For the scaling of more than seven records, ASCE-7 requires intensity-based scaling using appropriate scale factors so that the average value of the 5 percent-damped response spectra for the set of scaled records is not less than the design response spectrum over the $0.2T_1$ to $1.5T_1$ period range. As the procedure for scaling is not explicitly provided in ASCE-07, the procedure defined in a study conducted in 2010 (Kalkan and Chopra, 2010) was used in this thesis. This procedure suggests obtaining a scale factor (SF_1) for each of the motions through a least square fit method. After each motion is scaled for these factors, the average spectrum is calculated. According to ASCE-07, the average spectrum should not be less than the target spectrum between periods of $0.2T_1$ to $1.5T_1$. To address this issue, the minimum of the spectrum is compared to the target spectrum once more and a new scale factor (SF_2) is defined to cover the maximum difference between the average and target spectra (ε_{asce}). This scaling procedure is illustrated by Reyes and Kalkan in 2012 as shown in Figure 2-10 and Figure 2-11.The final average spectrum may lie somewhat above the target spectrum as a result of the scale factor SF_2 as given in Figure 2-11.
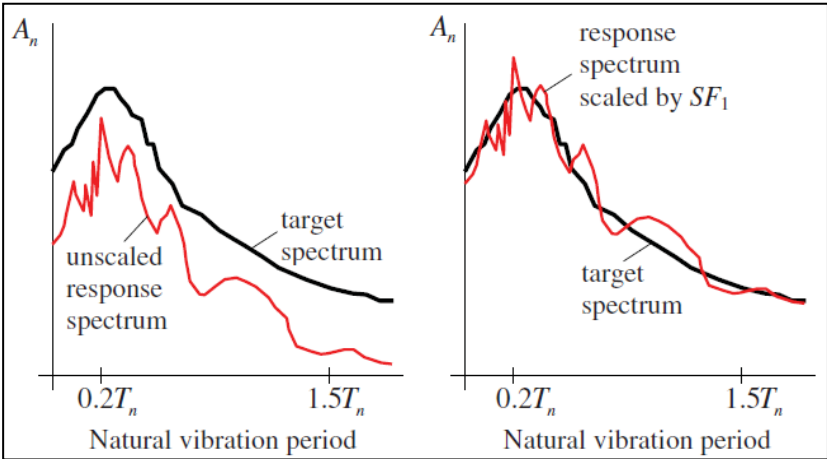
Figure 2-10 Response Spectrum Scaled by SF_1 (Reyes and Kalkan, 2012)
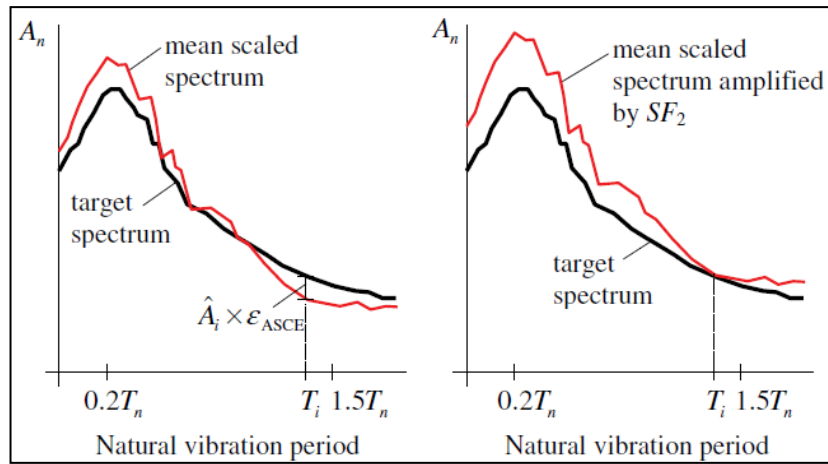
Figure 2-11 Response Spectrum Amplified by SF₂ (Reyes and Kalkan, 2012)

Three different concrete gravity dam models are used in this study (along with two different material strength values), leading to demand values at three different points on the spectrum. The fundamental frequencies for the 50m, 100m and 150m monoliths were determined as 0.17 (Model-1), 0.33(Model-2) and 0.5 (Model-3) seconds, respectively, and three different scale factors and ground motion sets were used for these different models. The scale factors for each motion are given in Figure 2-12 for the three models. The average spectrum obtained for Model 3 is shown in Figure 2-13. The individual spectra are given with the target spectrum for model 3 in Figure 2-14 and separately in Figure 2-15. Scaled accelerograms are shown further in Figure 2-16.
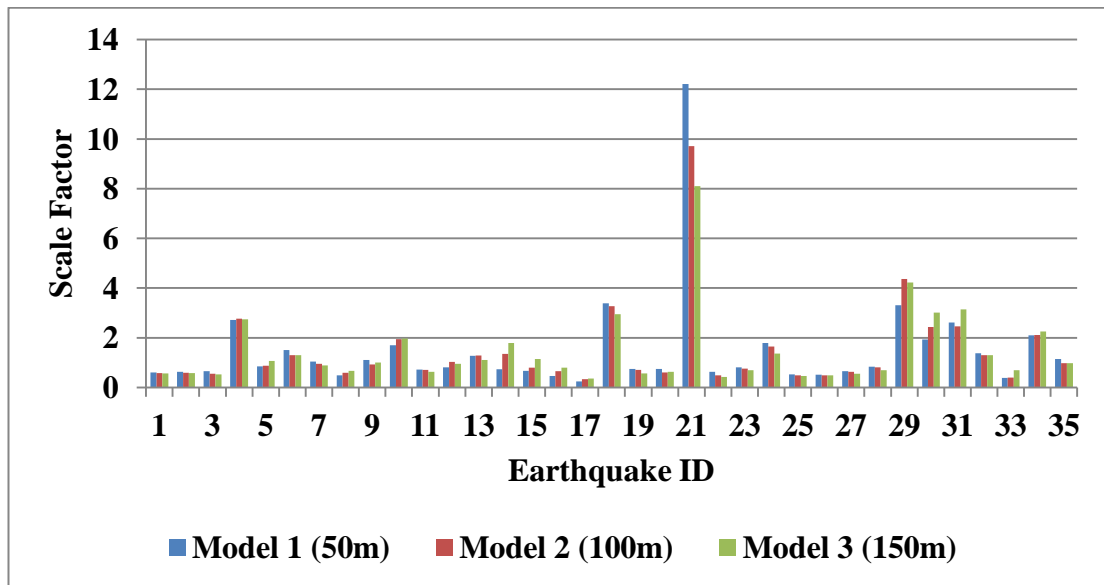
Figure 2-12 Scale Factors for Ground Motion Records (ASCE - 07)
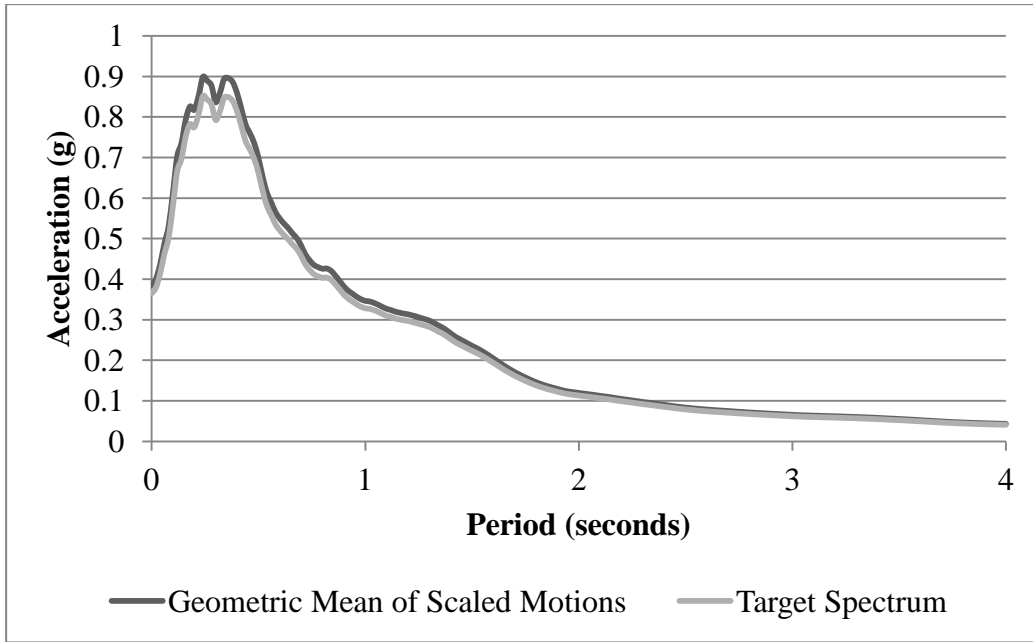
Figure 2-13 Mean Spectrum of Ground Motions and the Target Spectrum - Motion Set of Model 3
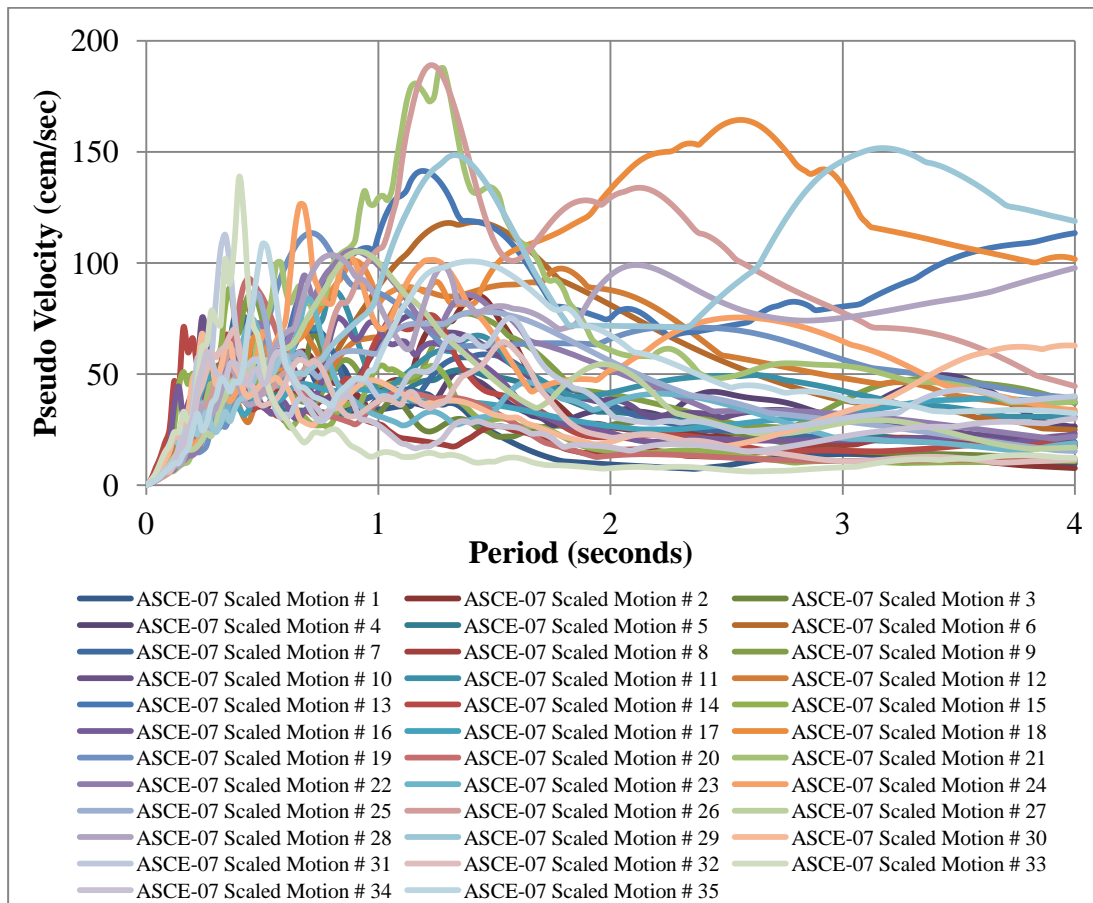
Figure 2-14 Pseudo Velocities of Motions Scaled for ASCE - 07 of Model 3
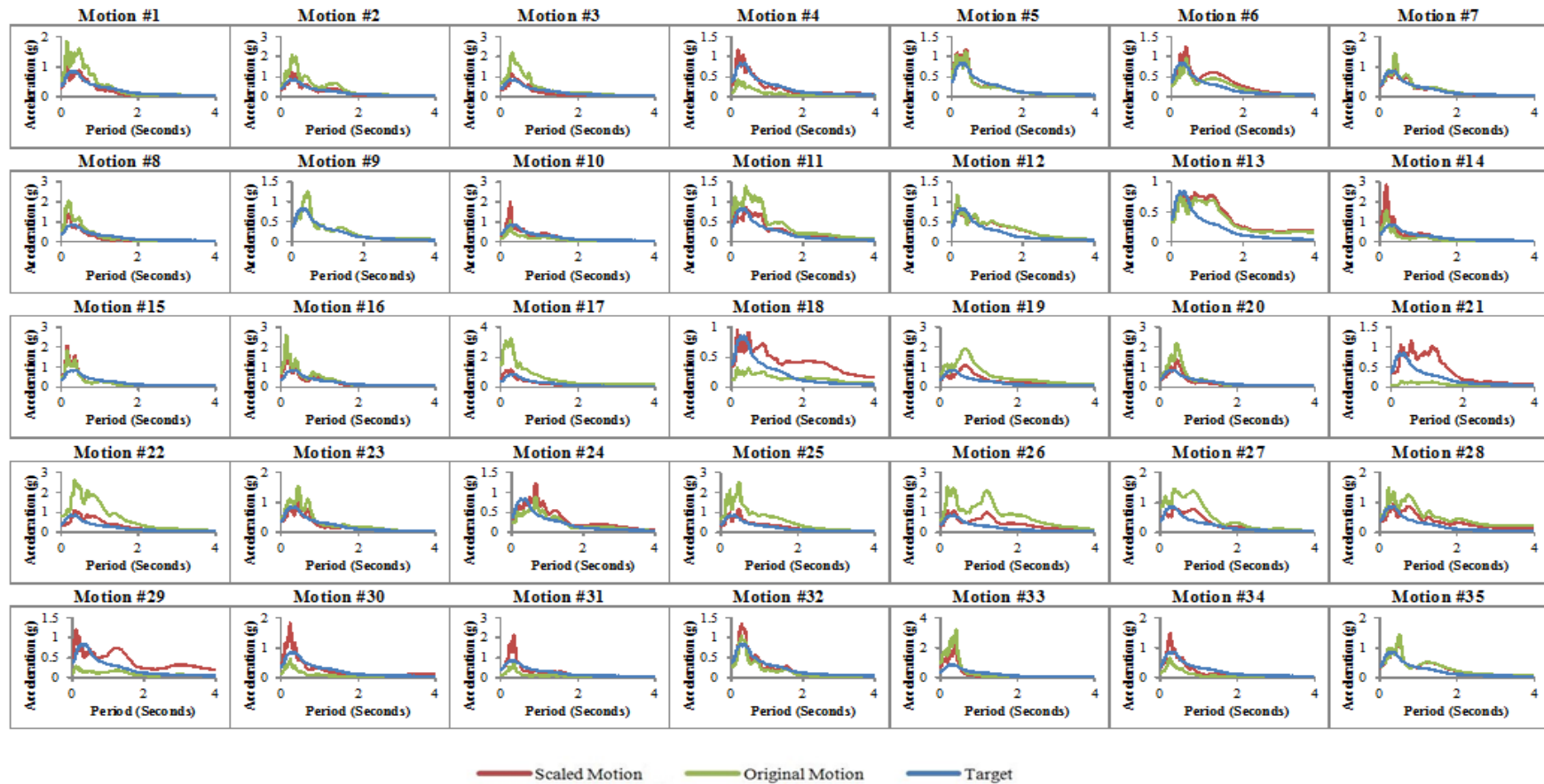
Figure 2-15 Response Spectra of Motions Scaled for ASCE - 07 of Model 3
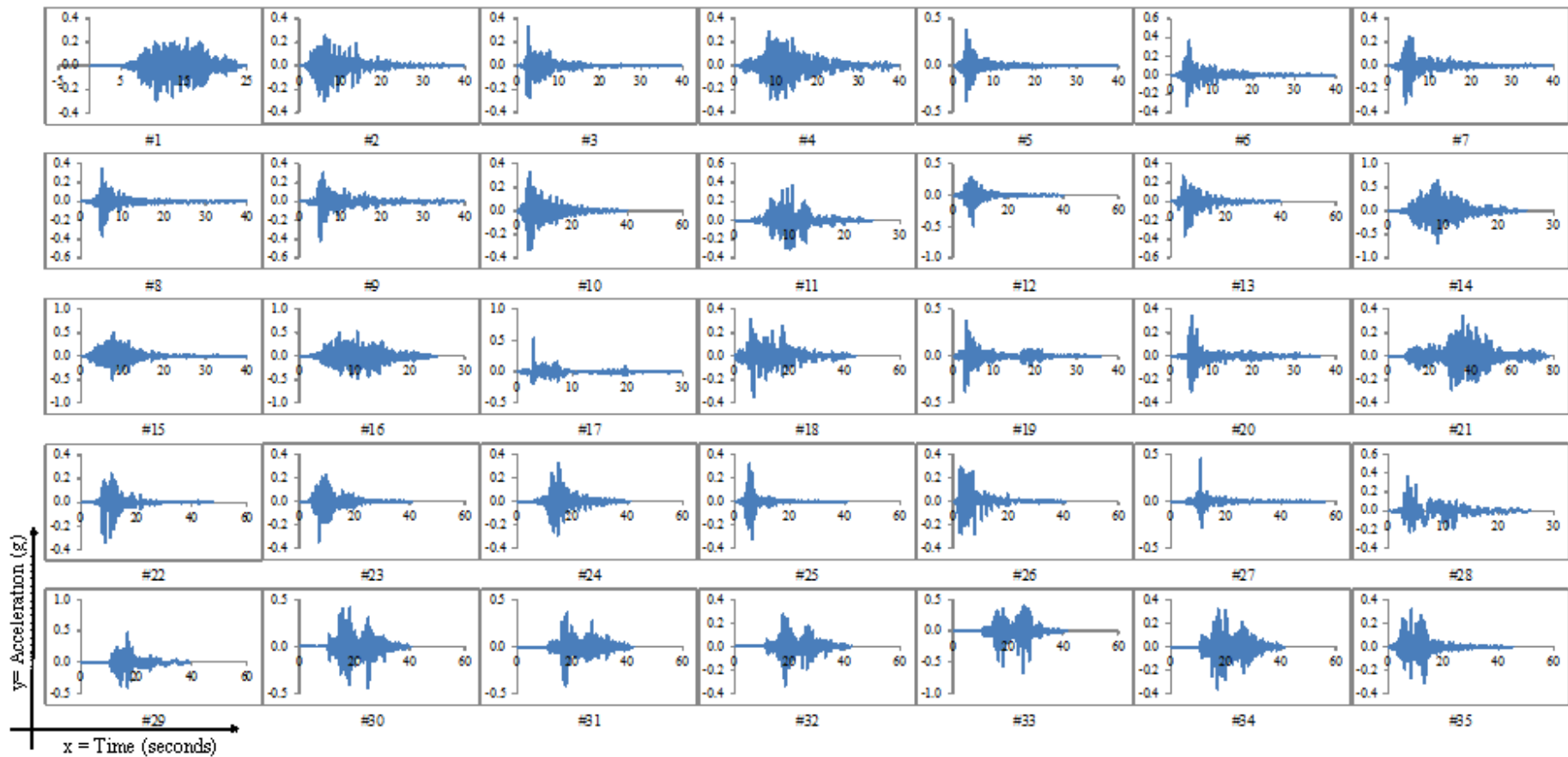
Figure 2-16 Acceleration Time Histories of Motions Scaled for ASCE - 07 of Model 3

34

The peak acceleration of the matched time histories are compared in Figure 2-17 also showing the peak accelerations of the original motions.
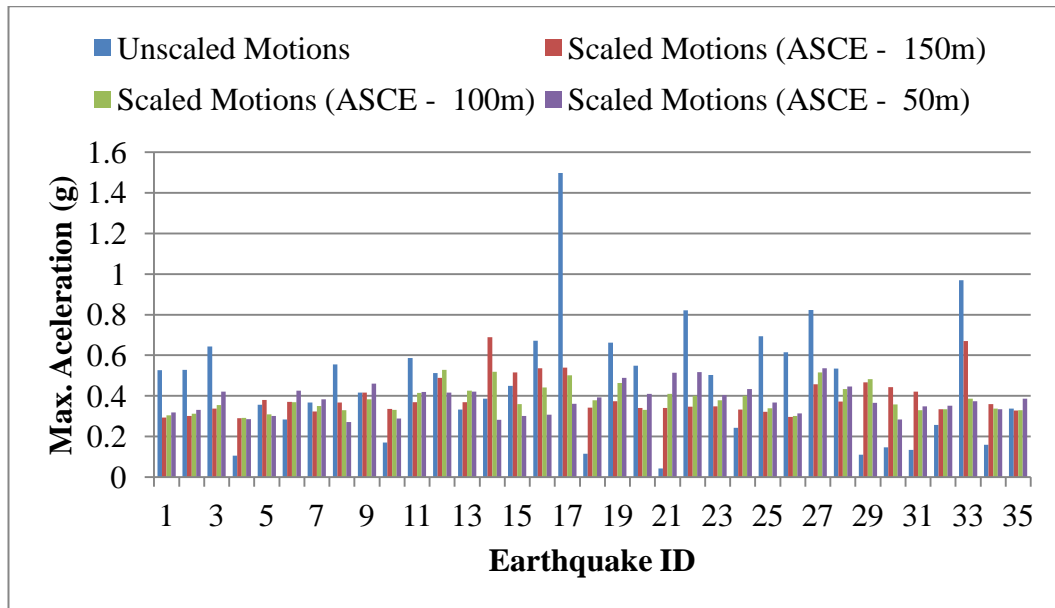

Figure 2-17 Maximum Accelerations of the Scaled Motions (ASCE - 07)

The maximum velocities of the matched time histories are compared in Figure 2-18 also showing the maximum velocities of the original motions.
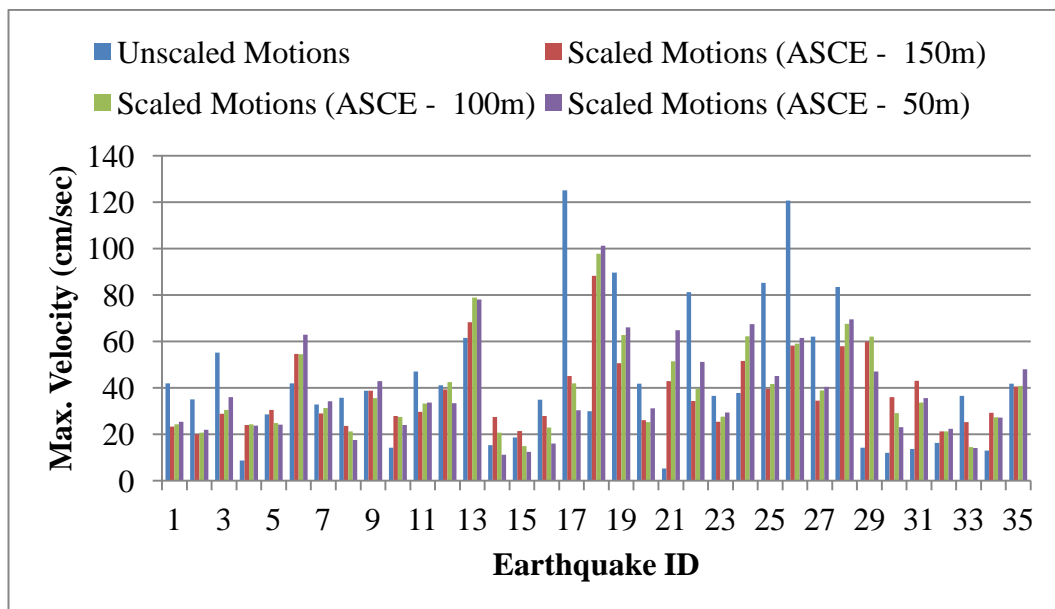
Figure 2-18 Maximum Velocities of the Scaled Motions (ASCE - 07)

The sustained maximum acceleration of the matched time histories are compared in Figure 2-19 also showing the sustained maximum acceleration of the original motions.

Figure 2-19 Sustained Maximum Accelerations of Scaled Motions (ASCE - 07)

The sustained maximum velocities of the matched time histories are compared in Figure 2-20 also showing the sustained maximum velocities of the original motions.


Figure 2-20   Sustained Maximum Velocities of Scaled Motions (ASCE - 07)

36

2.4.3 SCALING OF RECORDS TO ARITHMETIC MEAN OF MAXIMUM INCREMENTAL VELOCITY (MIV)

For the purpose of scaling of the records to the arithmetic mean of maximum incremental velocity, the procedure defined by O'Donnell and coworkers (2013) was utilized. In this procedure, the ground motions are scaled to the average MIV of the ground motion suite. MIV is defined by Kurama and Farrow (2013) as the maximum area under the acceleration time history between two consecutive zero acceleration crossings. All of the motions were scaled to have the average MIV value of 0.626(cm/sec) and their scale factors are shown in Table 2-2.

Table 2-2 MIV Values of Motions and Their Scale Factors

ID	MIV (cm/sec)	Scale Factor	ID	MIV (cm/sec)	Scale Factor
1	0.7375	0.848	19	1.2937	0.484
2	0.6247	1.001	20	0.7468	0.838
3	0.8283	0.755	21	0.0891	7.02
4	0.1115	5.608	22	1.5746	0.397
5	0.3309	1.891	23	0.5908	1.059
6	0.7770	0.805	24	0.5010	1.249
7	0.5079	1.232	25	1.0537	0.594
8	0.5363	1.166	26	1.8635	0.336
9	0.5467	1.144	27	1.2384	0.505
10	0.2076	3.013	28	1.1073	0.565
11	0.6364	0.983	29	0.2558	2.446
12	0.5878	1.064	30	0.1034	6.051
13	0.6729	0.93	31	0.1438	4.351
14	0.2056	3.042	32	0.2564	2.44
15	0.2910	2.15	33	0.6195	1.01
16	0.4229	1.479	34	0.1602	3.904
17	1.4213	0.44	35	0.4801	1.303
18	0.3705	1.688			

The MIV values of the matched time histories are compared in Figure 2-21 also showing the peak accelerations of the original motions. It can be seen from this

figure that the MIV values of all of the motions are equal to average MIV of unscaled motions. The pseudo-velocities, the accelerograms and the response spectra of the scaled motions are shown in Figure 2-22, Figure 2-23 and Figure 2-24, respectively.
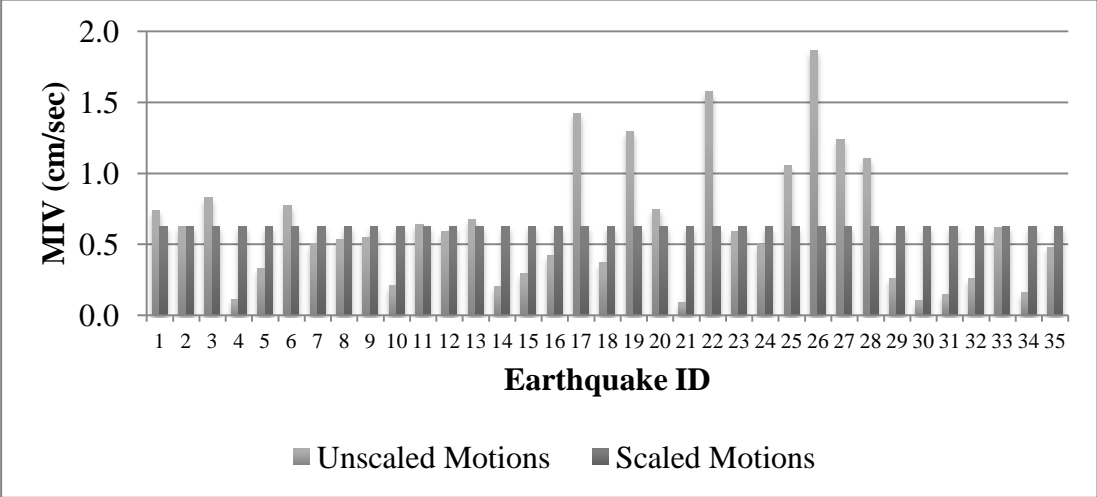
Figure 2-21   MIV values of scaled motions and the original motions
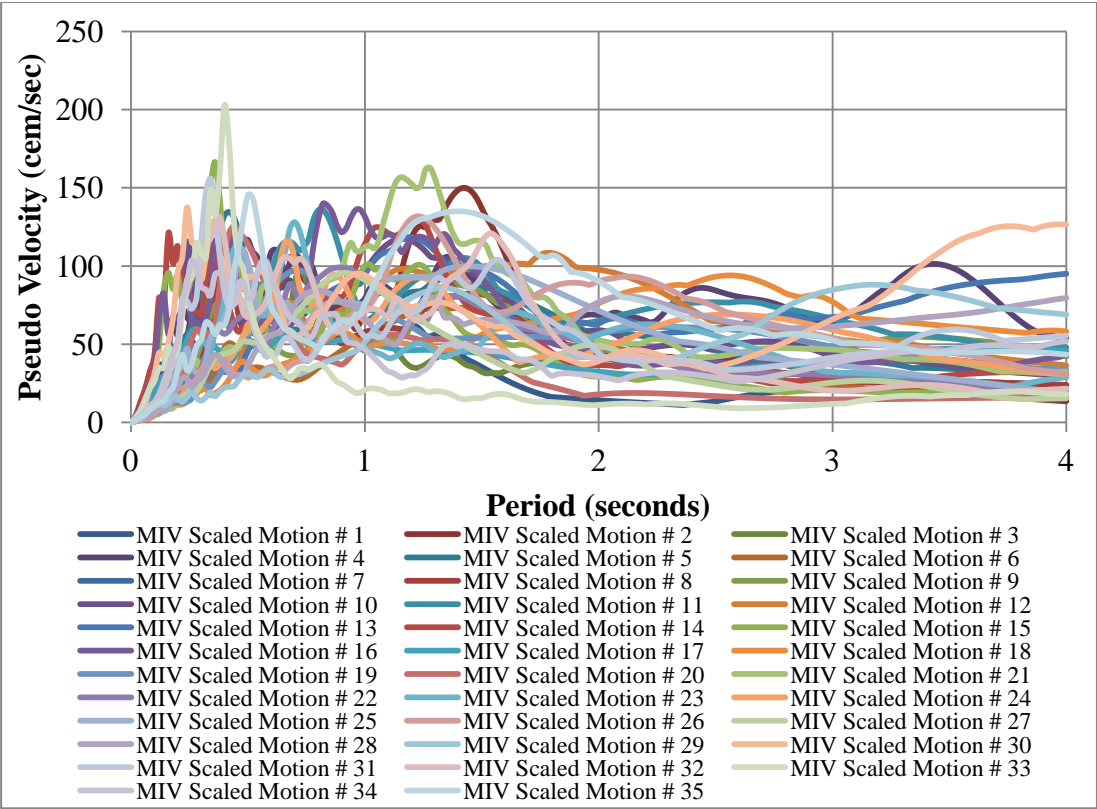
Figure 2-22 Pseudo Velocities of Motions Scaled by Maximum Incremental Velocity
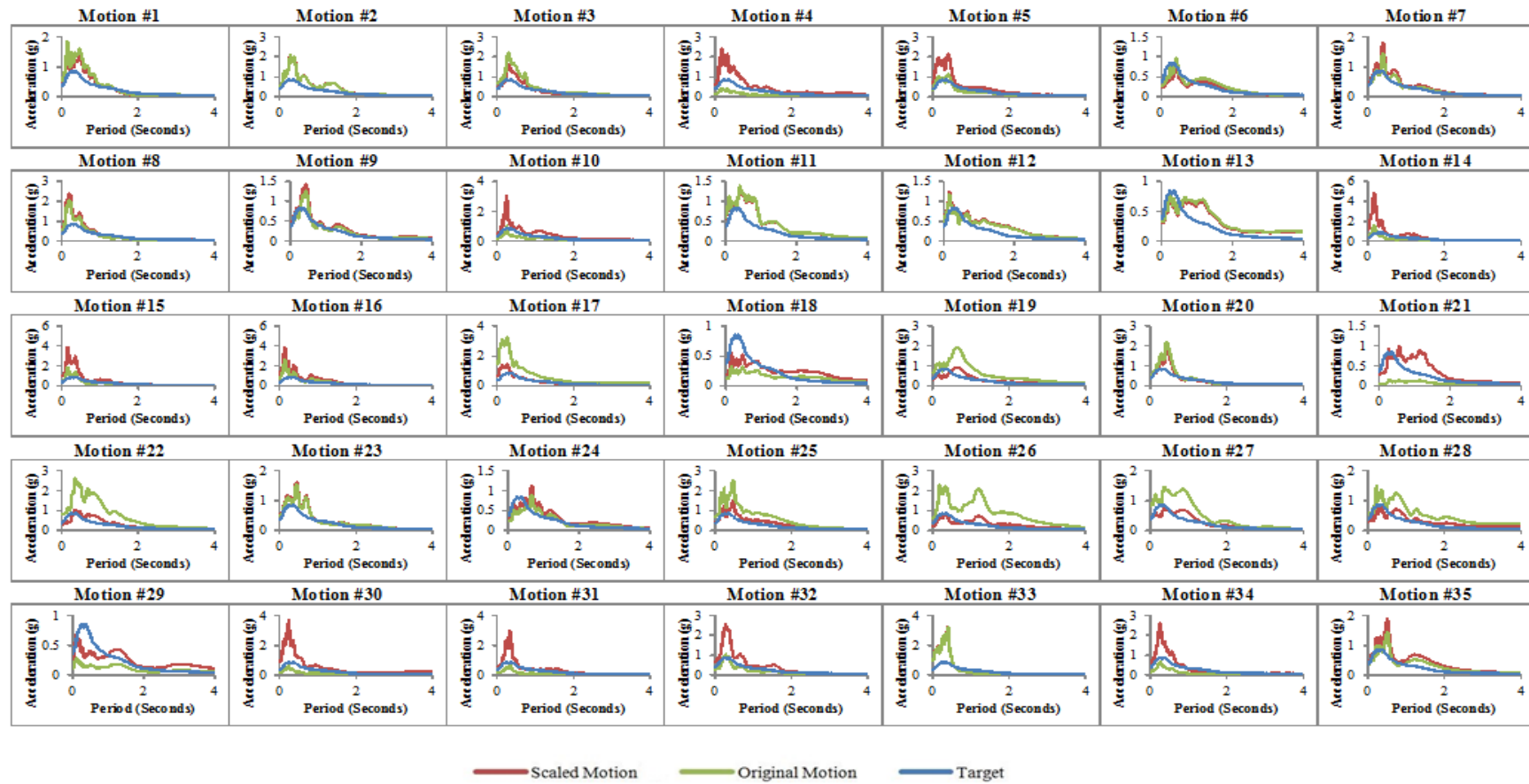
Figure 2-23 Response Spectra of Motions Scaled by Maximum Incremental Velocity
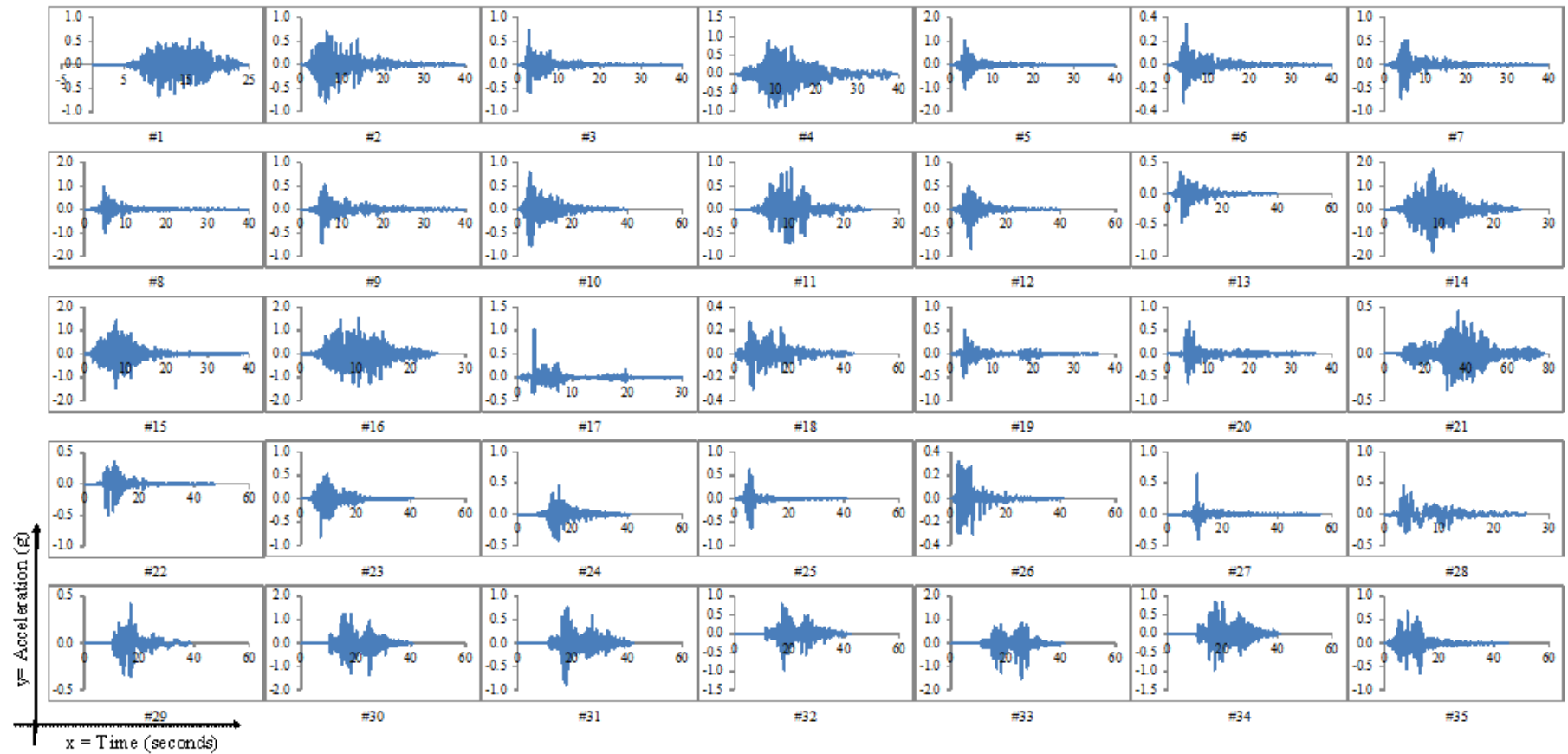
Figure 2-24 Acceleration Time Histories of Motions Scaled by Maximum Incremental Velocity

The peak acceleration of the matched time histories are compared in Figure 2-25 also showing the peak accelerations of the original motions. The scattered character of Maximum Acceleration values were preserved after scaling.
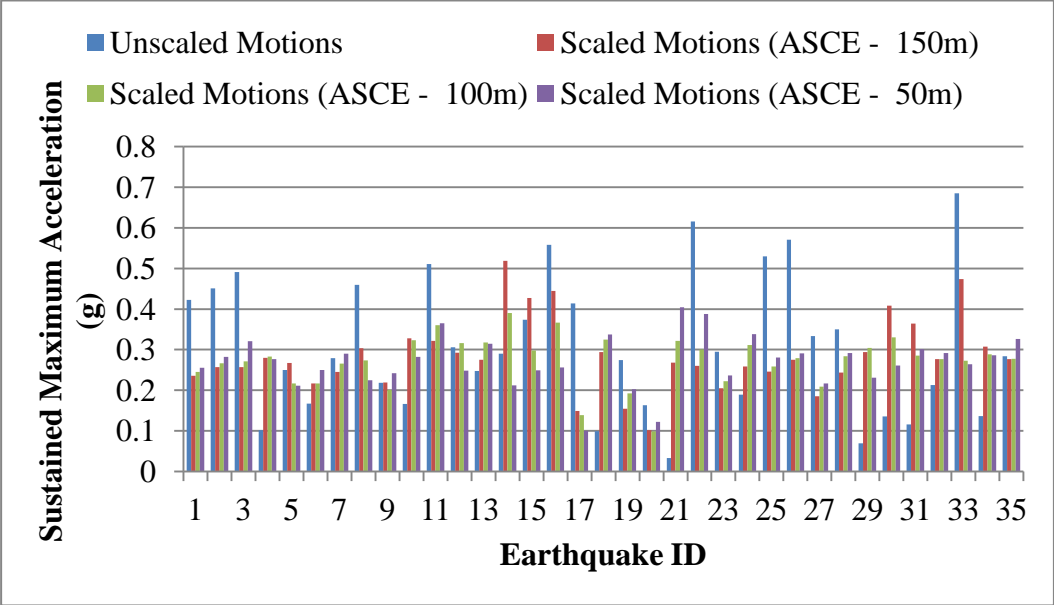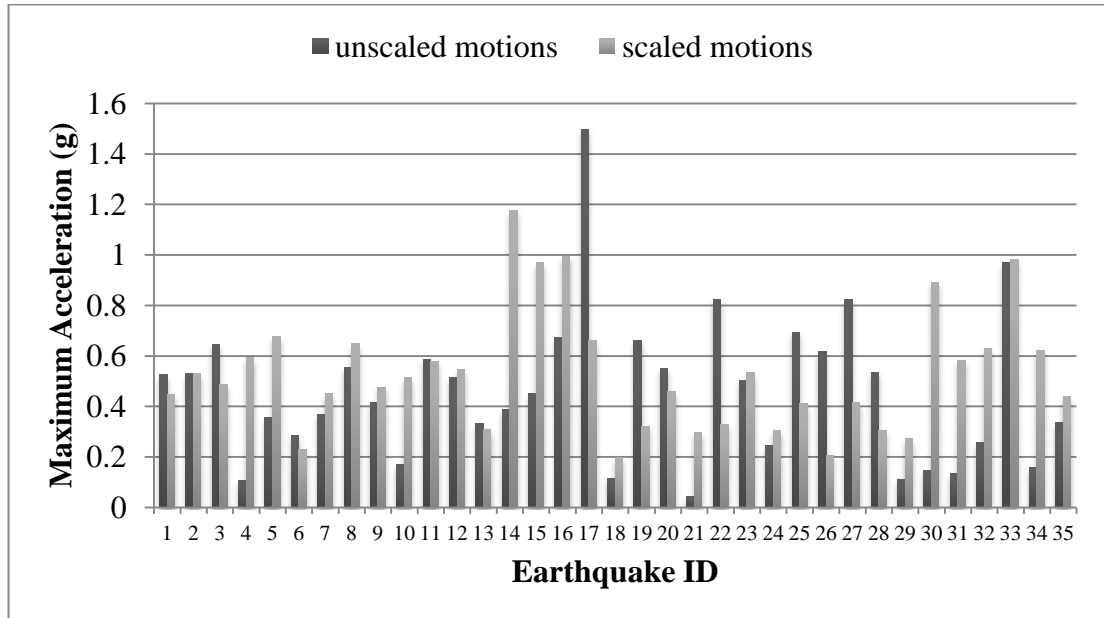

Figure 2-25   Maximum Accelerations of the Scaled Motions (MIV)

The maximum velocities of the matched time histories are compared in Figure 2-26 also showing the maximum velocity of the original motions.
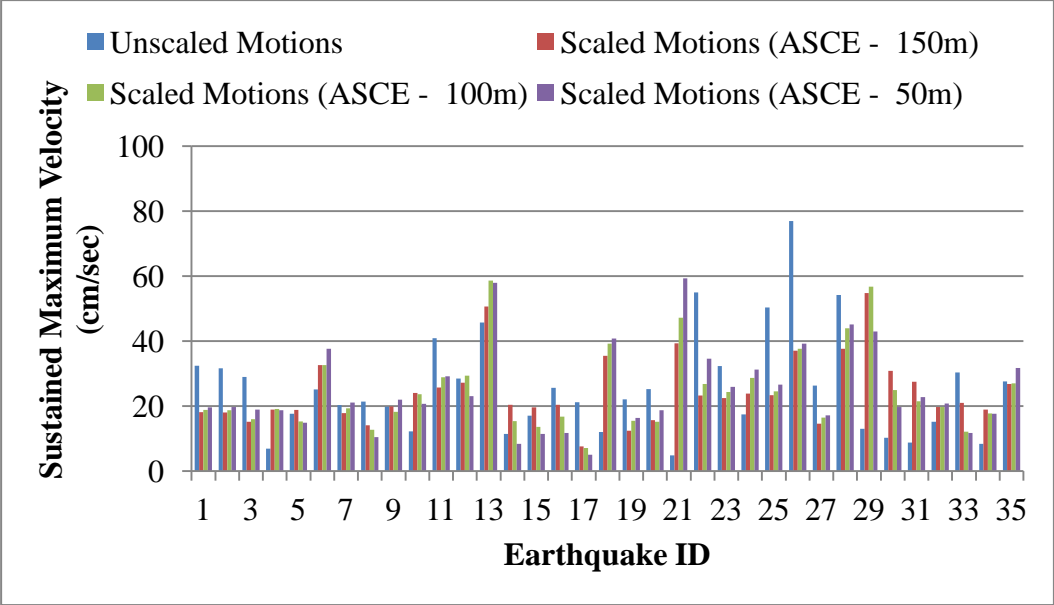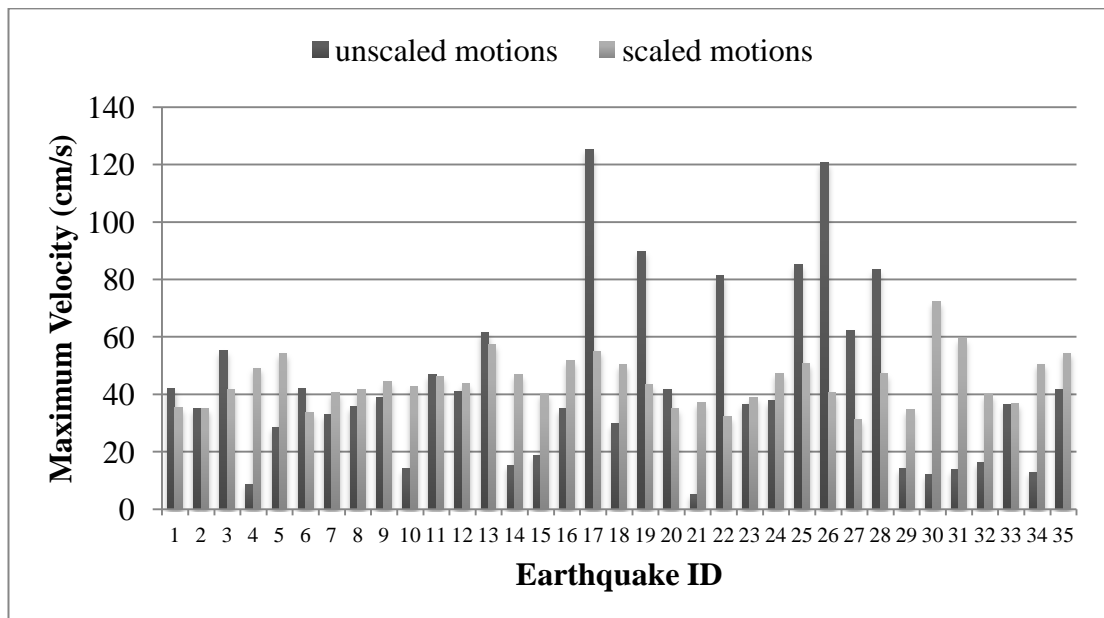

Figure 2-26 Maximum Velocities of the Scaled Motions (MIV)

The sustained maximum accelerations of the matched time histories are compared in Figure 2-27 also showing the sustained maximum accelerations of the original motions.
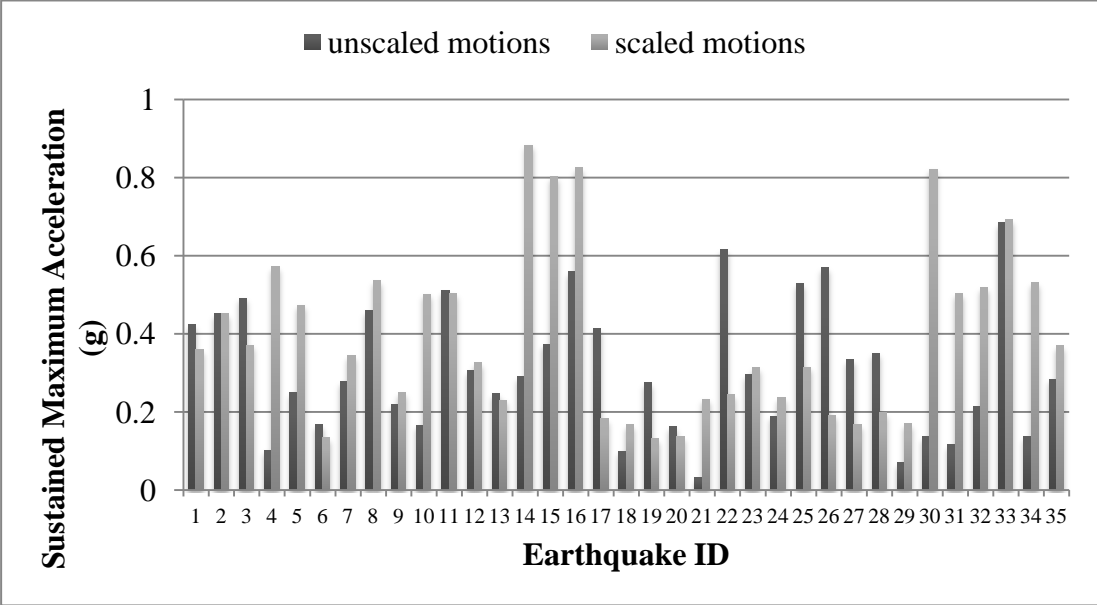
Figure 2-27 Sustained Maximum Accelerations of the Scaled Motions (MIV)

The sustained maximum velocities of the matched time histories are compared in Figure 2-28 also showing the sustained maximum velocities of the original motions.
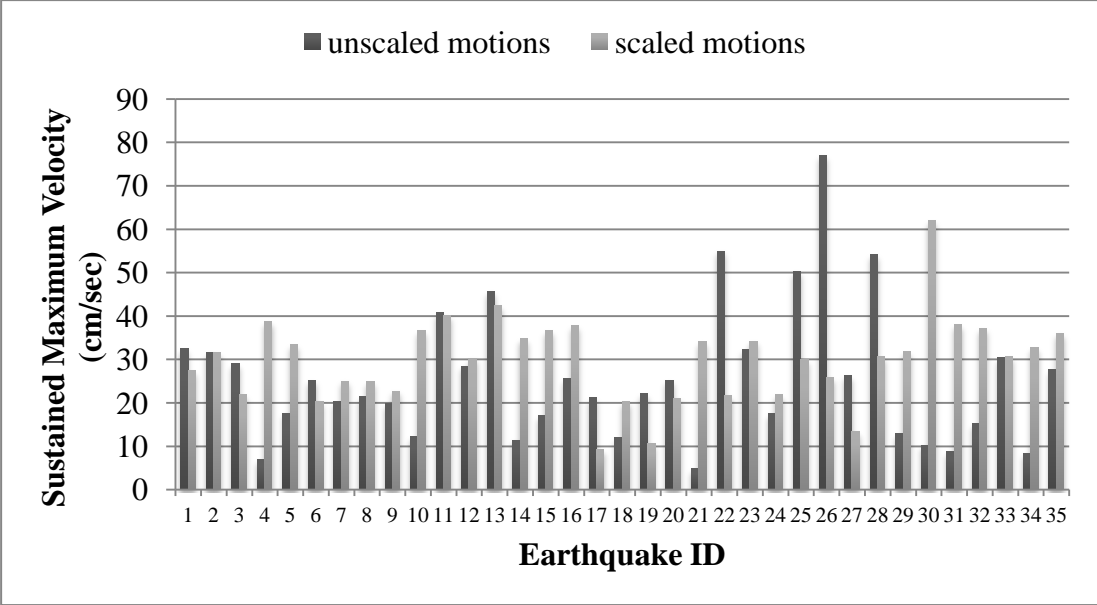
Figure 2-28 Sustained Maximum Velocities of the Scaled Motions (MIV)

2.4.4 MODAL - PUSHOVER BASED GROUND MOTION SCALING

Modal pushover based scaling is comprised of scaling of the ground motions to the inelastic displacements obtained using an idealized SDOF system obtained using the the push-over behavior of the full scale system. For this purpose, pushover analysis was performed for the chosen systems and the resulting force displacement relations were idealized to a SDOF system. The load-relationships for the 50, 100 and 150m tall monoliths are presented in Figure 2-29 .

(a) 50m R=2	(b) 50m R=1.5
(c) 100m R=2	(d) 100m R=1.5
(e) 150m R=2	(f) 150m R=1.5
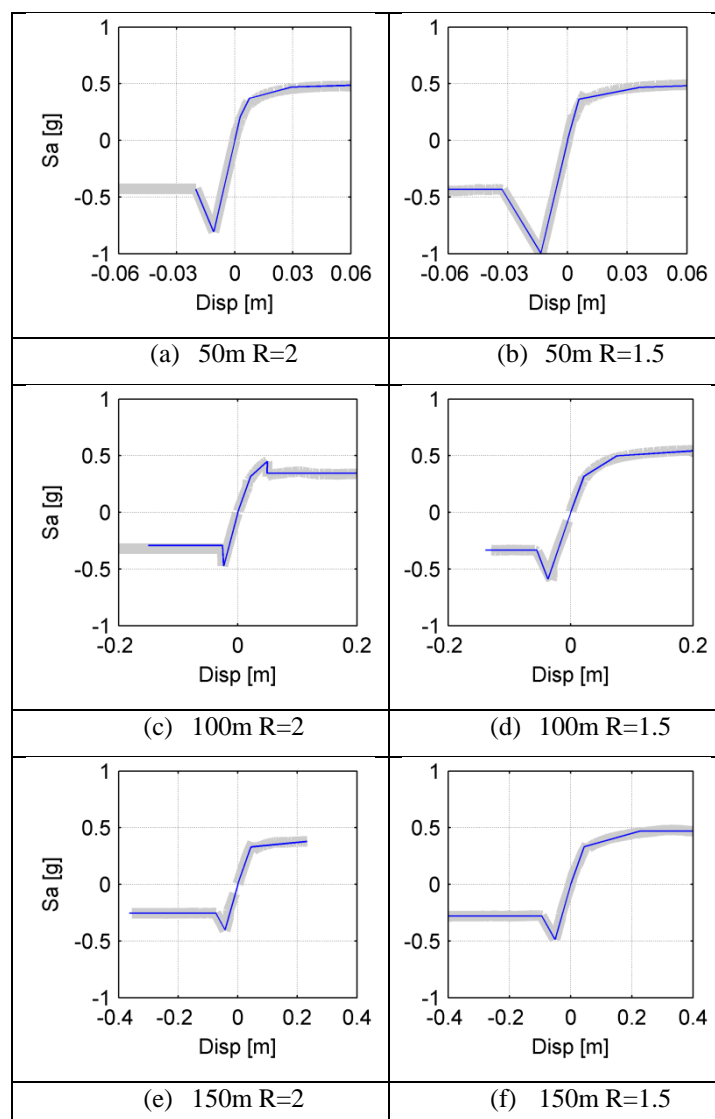
Figure 2-29 Push-Over Curves and Idealizations

The pushover curves were obtained using monotonic loading proportional to the first mode shape after the hydrostatic loading is applied to these systems. Both the curves and the idealizations shown in Figure 2-29 exclude the hydrostatic load-displacement curve obtained before the first-mode based pushover loading. Cyclic load displacement is obtained using the hysteretic material model in Opensees. Unloading stiffness is modeled in a degrading fashion based on ductility. As given in Figure 2-30, the idealized loading behavior was assumed differently in the two directions of loading, the upstream and downstream directions, in accordance with the results obtained from the push over analysis for the six different cases.

| (a) Cyclic Load History | (b) Load Displacement Relation for Cyclic Load |
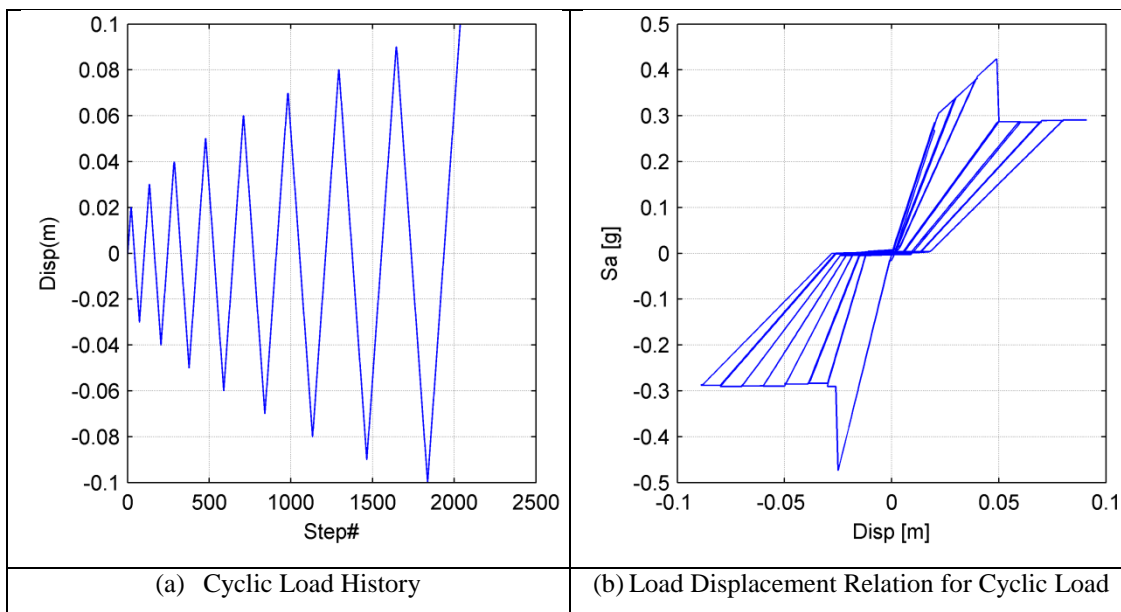
Figure 2-30 The Idealized Loading Behavior

The load-displacement curves as given above were transformed to the idealized SDOF system by dividing the displacements by $\Gamma_1 \phi_{r1}$ where $\Gamma_1 = (\phi_1^T M \iota)/(\phi_1^T M \phi_1)$ and the ϕ_{r1} represents the displacement at the crest of the monolith for the first mode. The vector ϕ_1 and the matrix M represent the first mode shape and the mass matrix of the monolith. The force quantity given in Figure 2-30 represents the base shear already normalized by the effective modal mass of the system for the first mode, M^*. The displacements obtained from the pushover curves were divided by a normalization factor of 2.01, 2.05 and 2.12 for the 50,100 and 150m monolith cases, respectively, in order to obtain the idealized single mode push-over relationships.

44

The next step in the procedure involves determining the target displacement $\bar{D}_1^I$ for each structure so that the motions can be scaled in a transient analyses with idealized relathionships to reach that goal. For this purpose, an estimate can be used such as the result due to a nonlinear transient analysis due to a large number of unscaled motions used. The median value of the peak displacement from these analyses can be used as the target displacement $\bar{D}_1^I$ of the scaling procedure. Another alternative for the computation of the target displacement involves the use of empirical formulas as developed by Chopra and Chintanapakdee (2004). In these equations, the inelastic deformation ratio to the elastic deformation for the spectra is obtained by a function of the elastic period and the yield strength reduction factor R_y . These equations are obtained using regression analysis for a range of systems in the acceleration, velocity and displacement sensitive parts of a response spectrum. This approach was not used in this study.

The target displacements for the 6 different cases are provided below. The procedure from Kalkan and Chopra (2011) was modified to some extent due to the bi-directional response of the dam monoliths at hand. Therefore, target displacements were determined in two different directions separately.

Table 2-3 Target Displacements in US/DS Cases for the Monoliths

	50m-R=1.5	50m-R=2	100m-R=1.5	100m-R=2	150m-R=1.5	150m-R=2
U-S	0.0337	0.0323	0.0479	0.0626	0.0707	0.0708
D-S	0.0338	0.0352	0.0812	0.0657	0.1093	0.1052

A series of nonlinear transient analysis were then conducted in order to obtain the scale factor that would yield the target displacement from the idealized SDOF models for the 35 different ground motions. The tolerance with which the target displacement was assumed to be reached was kept at 2%. In other words, the scale factor for a given motion was obtained when the peak displacement for the scaled motion was within ±2% of the target displacement. It should also be noted that both the Upstream (U-S) and Downstream (D-S) target displacements were used in the study. Whichever is obtained first for a lower scale of the ground motion was kept as the final scaling factor for that ground motion. The list of the final scaling factors for the different cases is presented in Table 2-4.

Table 2-4 Final Scaling Factors for Different Cases

	50m-R=1.5	50m-R=2	100m-R=1.5	100m-R=2	150m-R=1.5	150m-R=2
1	0.810	0.660	0.690	0.770	0.57	0.96
2	0.670	0.688	0.610	0.720	0.69	0.615
3	0.790	0.800	0.630	0.870	0.82	0.8
4	1.800	3.235	3.690	3.168	4.39	3.95
5	1.310	1.160	1.600	2.485	3.24	2.86
6	1.770	1.600	1.520	1.330	1.78	1.56
7	1.090	1.120	1.630	0.920	1.08	0.96
8	0.980	0.990	1.350	0.920	1.06	1.34
9	1.030	1.290	0.750	1.100	0.9	1.43
10	1.660	2.453	3.180	2.640	2.4	2.46
11	0.940	0.970	0.630	0.650	0.78	0.64
12	1.270	1.530	1.440	1.330	1.18	1.345
13	1.428	1.340	1.250	0.950	1.04	0.98
14	1.300	2.533	3.400	2.690	2.678	2.765
15	0.730	1.490	2.230	1.940	1.9	2
16	0.990	1.120	1.180	0.890	0.84	0.78
17	0.590	0.510	0.780	0.640	0.64	0.64
18	2.710	3.533	3.150	2.843	2.14	2.36
19	0.970	0.960	1.280	0.580	0.56	0.56
20	0.760	0.730	0.590	0.760	0.7	1.3
21	8.680	8.035	6.300	5.100	4.735	4.23
22	0.565	0.520	0.370	0.390	0.419	0.395
23	0.875	0.820	0.750	1.090	0.94	0.84
24	1.700	1.650	1.600	1.230	0.96	0.9
25	0.725	0.725	0.720	0.750	0.645	0.575
26	0.535	0.520	0.570	0.433	0.514	0.405
27	0.955	0.880	0.563	0.520	0.58	0.6
28	0.970	1.040	0.840	0.725	0.6875	0.62
29	6.200	5.565	6.783	5.510	5.26	5.24
30	2.100	4.103	4.525	4.353	5.44	4.97
31	1.830	3.228	3.090	4.608	4.01	4.26
32	1.110	1.500	1.970	2.210	1.64	2.606
33	0.320	0.570	1.270	0.930	1.82	2.14
34	1.690	2.093	3.470	3.193	4.28	4.21
35	1.030	1.020	1.380	1.080	1.002	0.94

The scale factors for each ground motion are presented for different cases in Figure 2-31.
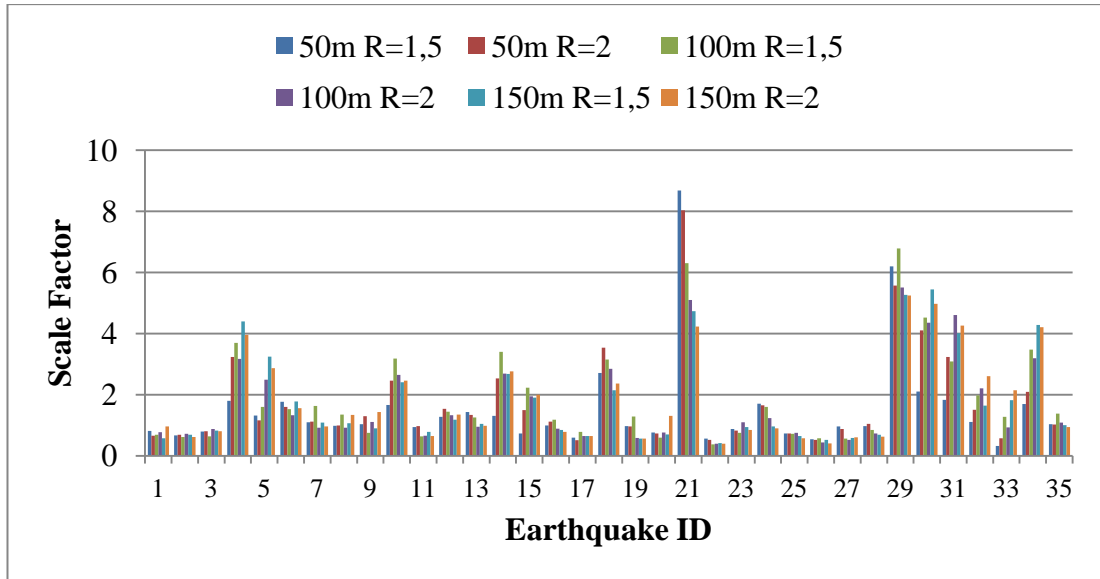
Figure 2-31 Scale Factors of the Ground Motions for MPS Method

The pseudo-velocities, the accelerograms and the response spectra of the scaled motions are shown in Figure 2-32, Figure 2-33 and Figure 2-34, respectively.
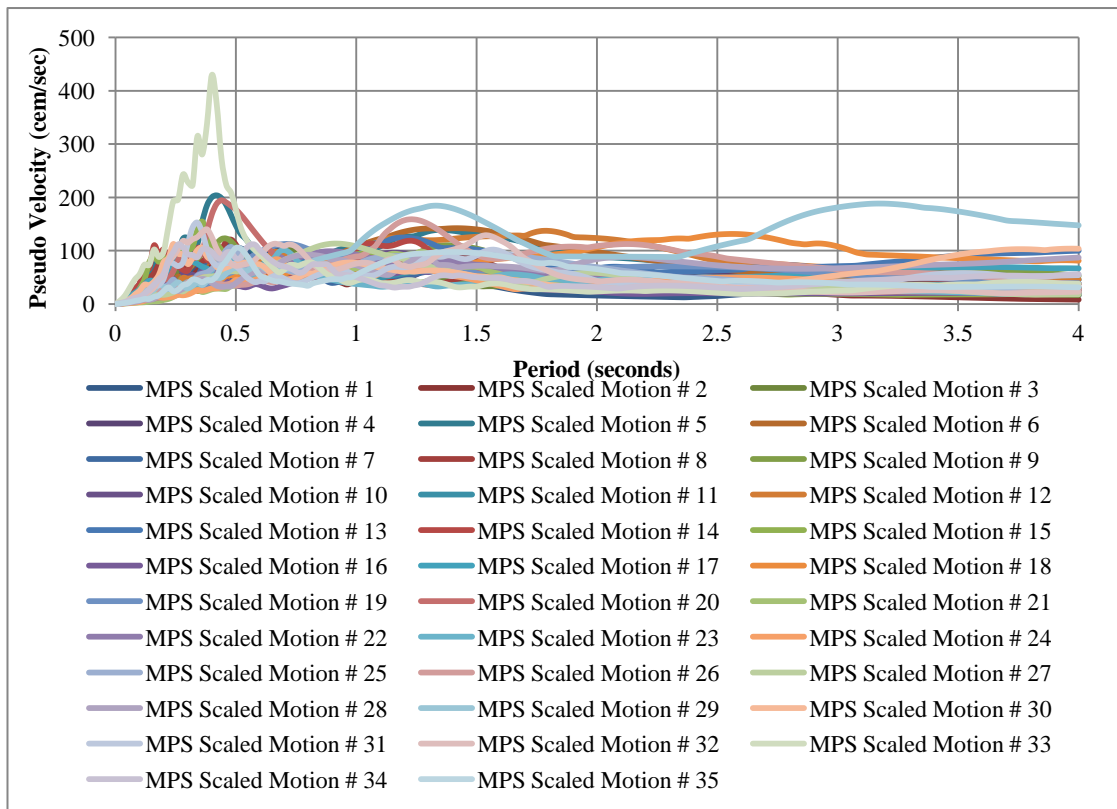
Figure 2-32 Pseudo Velocities of Motions Scaled by MPS (Model 3 - R=2)
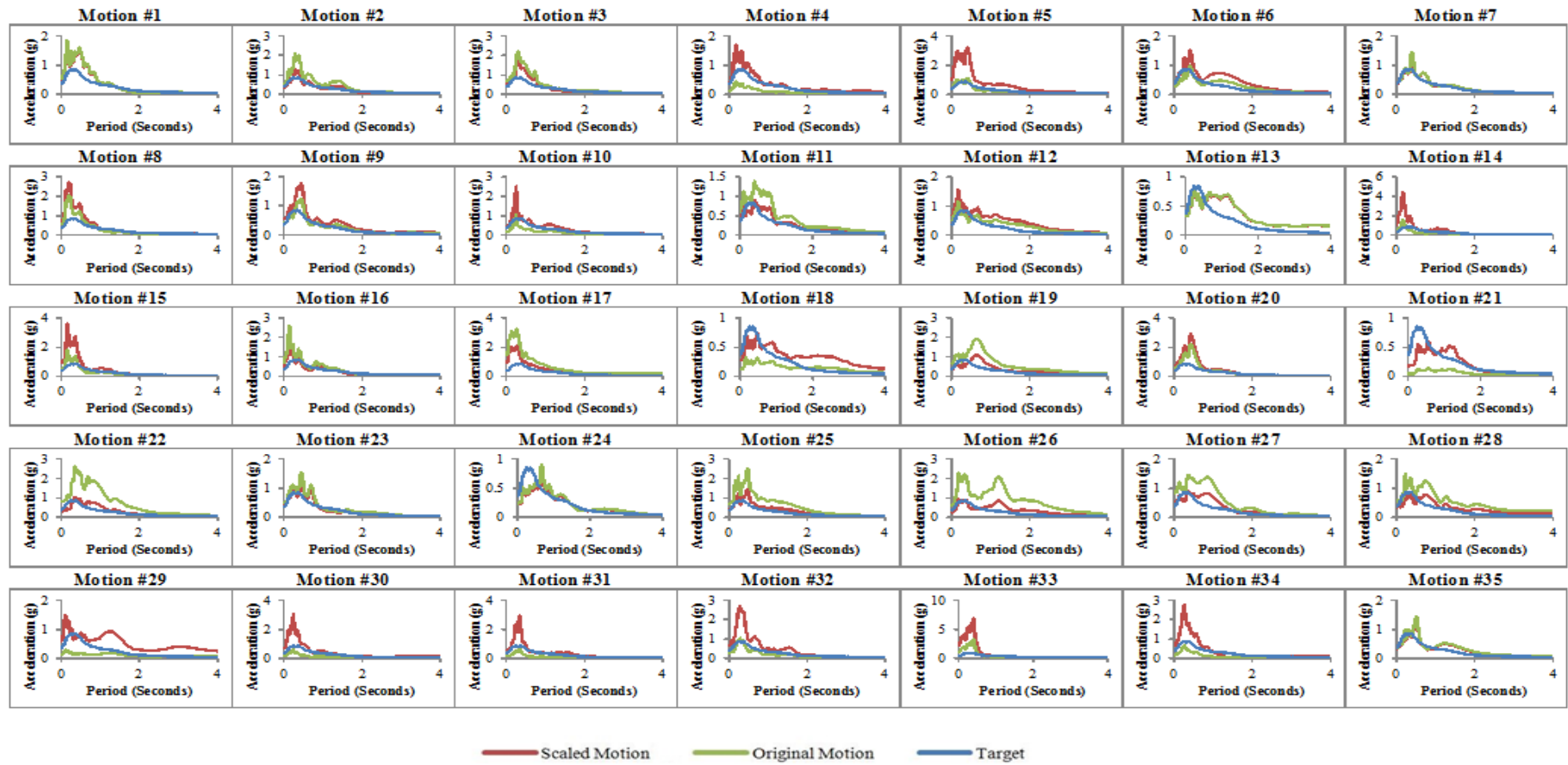
Figure 2-33   Response Spectra of Motions Scaled by MPS (Model 3 - R=2)
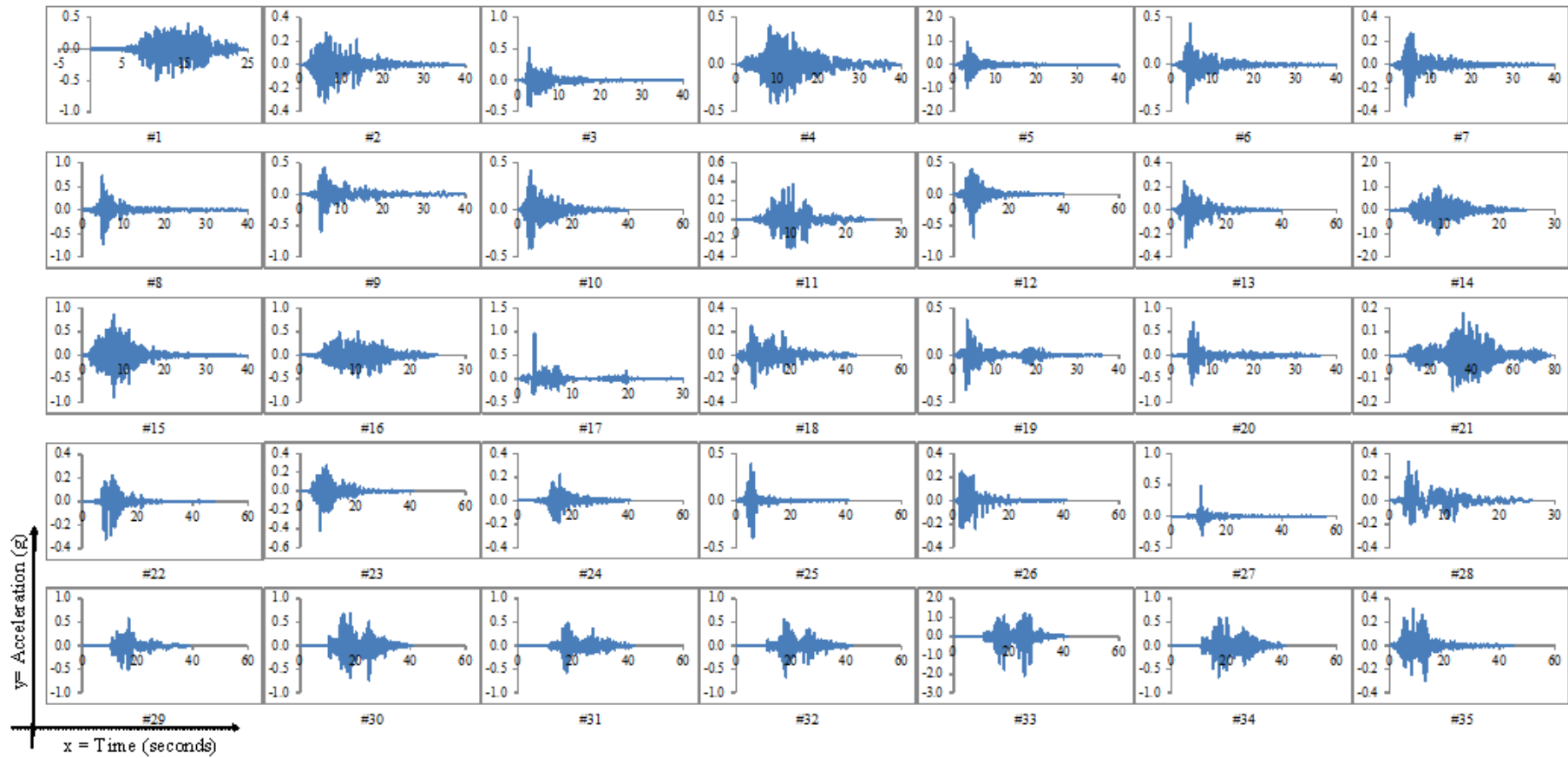
Figure 2-34 Acceleration Time Histories of Motions Scaled by MPS (Model 3 - R=2)

y= Acceleration (g)

x = Time (seconds)

49

The peak acceleration of the matched time histories are compared in Figure 2-35 also showing the peak accelerations of the original motions.
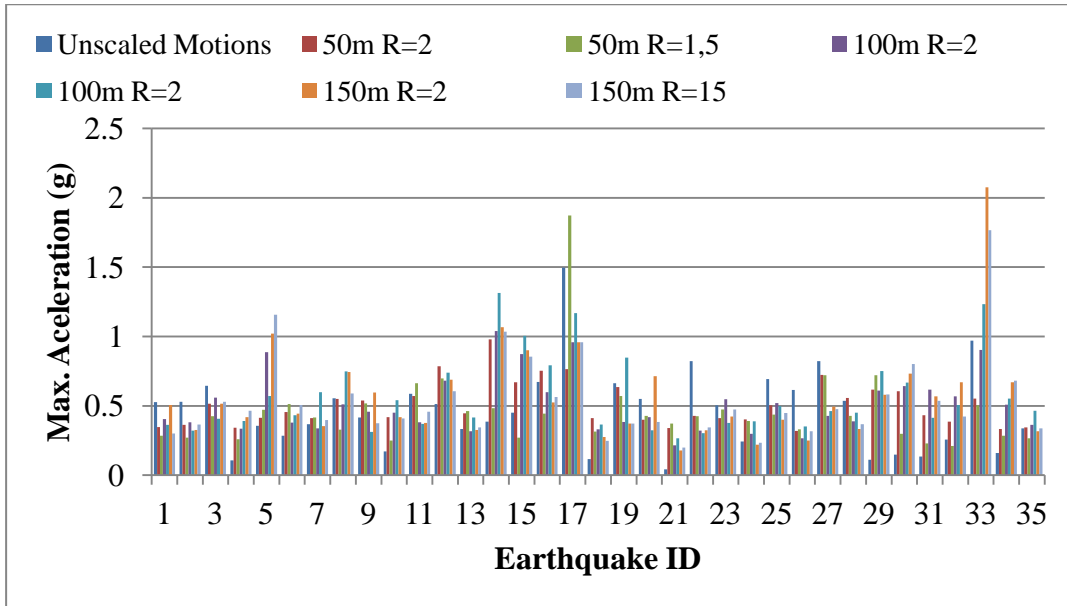
Figure 2-35   Maximum Accelerations of the Scaled Motions (MPS)

The maximum velocities of the matched time histories are compared in Figure 2-36 also showing the maximum velocity of the original motions.
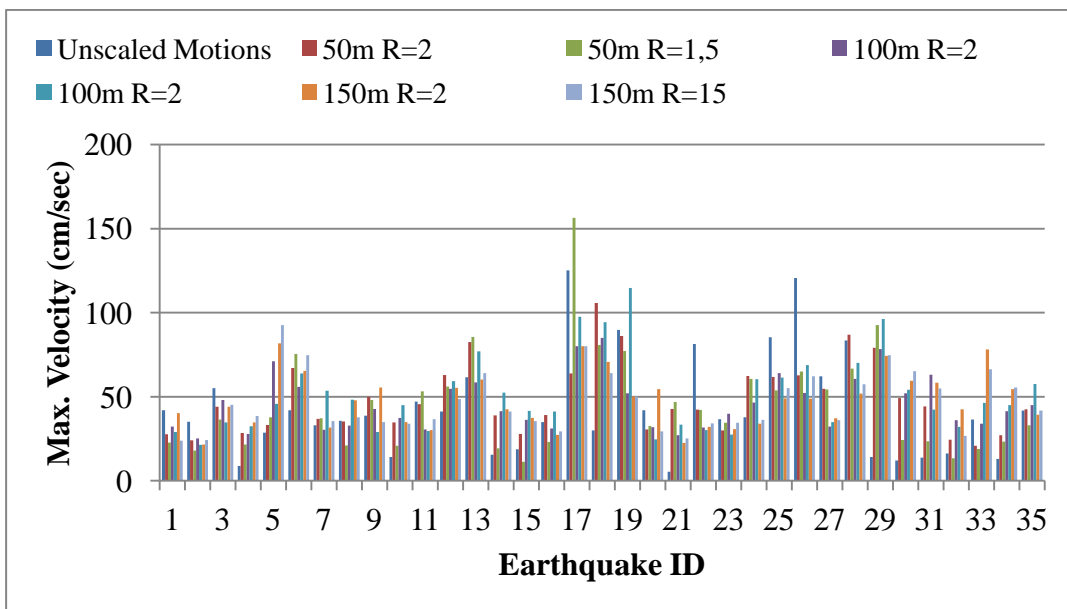
Figure 2-36 Maximum Velocities of the Scaled Motions (MPS)

The sustained maximum accelerations of the matched time histories are compared in Figure 2-37 also showing the sustained maximum accelerations of the original motions.

Figure 2-37 Sustained Maximum Accelerations of the Scaled Motions (MPS)

The sustained maximum velocities of the matched time histories are compared in Figure 2-38 also showing the sustained maximum velocities of the original motions.

Figure 2-38 Sustained Maximum Velocities of the Scaled Motions (MPS)

Table 2-5 Scaling Factors for Different Scaling Procedures.

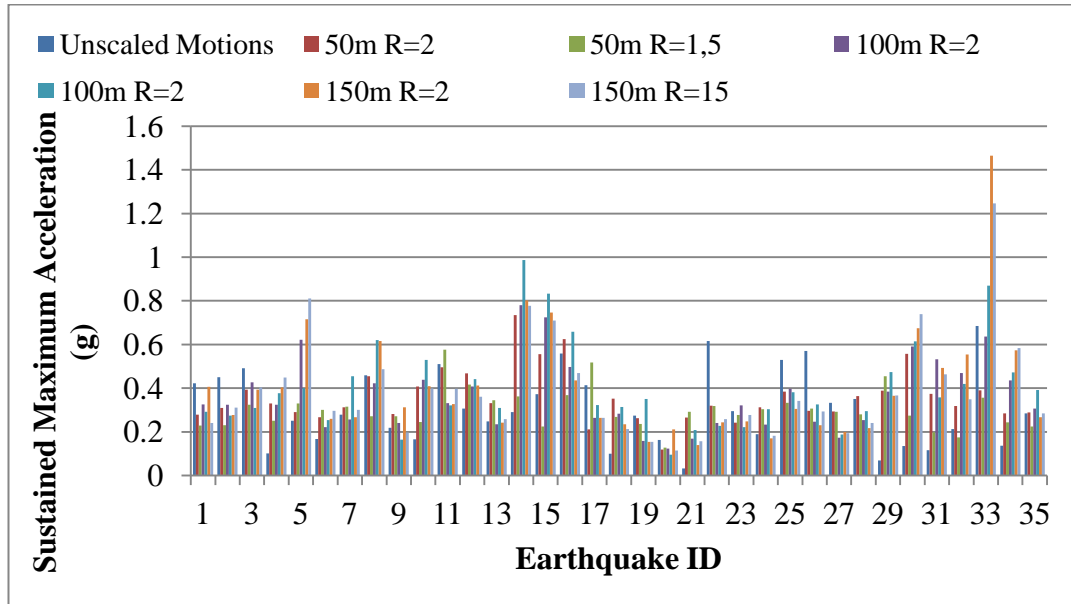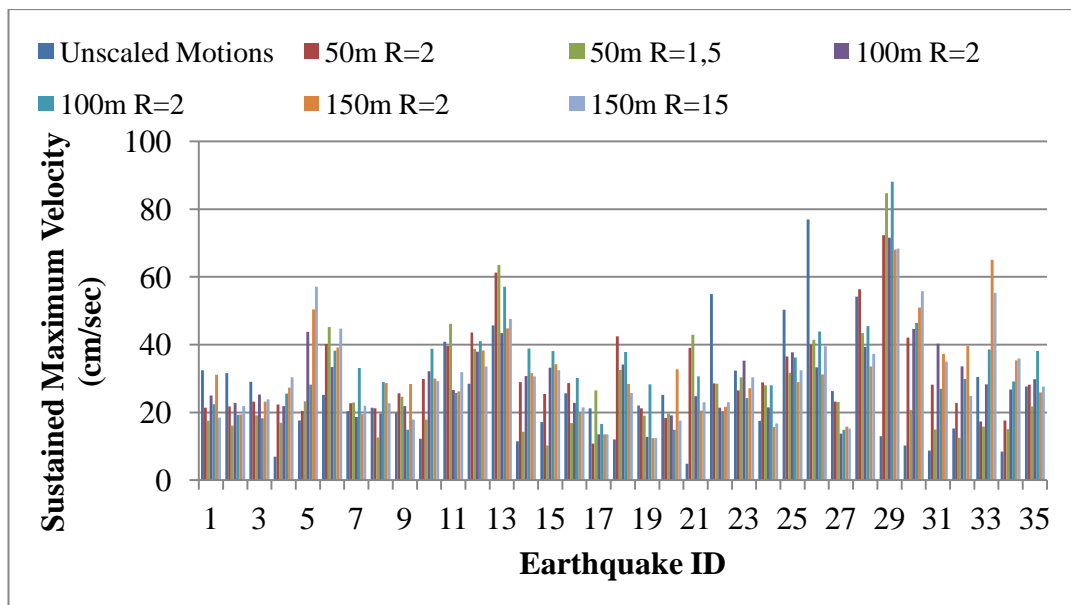| Motion	MPS 50m R=2	MPS 50m R=15	MPS 100m R=2	MPS 100m R=15	MPS 150m R=2	MPS 150m R=15	ASCE 50m	ASCE 100m	ASCE 150m	MIV
1	0.660	0.810	0.770	0.690	0.960	0.570	0.604	0.579	0.558	0.848
2	0.688	0.670	0.720	0.610	0.615	0.690	0.625	0.591	0.570	1.001
3	0.800	0.790	0.870	0.630	0.800	0.820	0.653	0.552	0.524	0.755
4	3.235	1.800	3.168	3.690	3.950	4.390	2.710	2.768	2.741	5.608
5	1.160	1.310	2.485	1.600	2.860	3.240	0.846	0.868	1.066	1.891
6	1.600	1.770	1.330	1.520	1.560	1.780	1.499	1.300	1.301	0.805
7	1.120	1.090	0.920	1.630	0.960	1.080	1.042	0.953	0.880	1.232
8	0.990	0.980	0.920	1.350	1.340	1.060	0.490	0.595	0.661	1.166
9	1.290	1.030	1.100	0.750	1.430	0.900	1.107	0.919	1.001	1.144
10	2.453	1.660	2.640	3.180	2.460	2.400	1.699	1.942	1.971	3.013
11	0.970	0.940	0.650	0.630	0.640	0.780	0.715	0.706	0.630	0.983
12	1.530	1.270	1.330	1.440	1.345	1.180	0.811	1.032	0.955	1.064
13	1.340	1.428	0.950	1.250	0.980	1.040	1.269	1.283	1.109	0.930
14	2.533	1.300	2.690	3.400	2.765	2.678	0.731	1.345	1.786	3.042
15	1.490	0.730	1.940	2.230	2.000	1.900	0.668	0.798	1.146	2.150
16	1.120	0.990	0.890	1.180	0.780	0.840	0.459	0.657	0.797	1.479
17	0.510	0.590	0.640	0.780	0.640	0.640	0.242	0.335	0.360	0.440
18	3.533	2.710	2.843	3.150	2.360	2.140	3.385	3.265	2.951	1.688
19	0.960	0.970	0.580	1.280	0.560	0.560	0.738	0.700	0.565	0.484
20	0.730	0.760	0.760	0.590	1.300	0.700	0.748	0.604	0.622	0.838
21	8.035	8.680	5.100	6.300	4.230	4.735	12.208	9.710	8.096	7.020
22	0.520	0.565	0.390	0.370	0.395	0.419	0.630	0.488	0.423	0.397
23	0.820	0.875	1.090	0.750	0.840	0.940	0.802	0.753	0.694	1.059
24	1.650	1.700	1.230	1.600	0.900	0.960	1.786	1.645	1.366	1.249
25	0.725	0.725	0.750	0.720	0.575	0.645	0.530	0.488	0.465	0.594
26	0.520	0.535	0.433	0.570	0.405	0.514	0.510	0.490	0.482	0.336
27	0.880	0.955	0.520	0.563	0.600	0.580	0.651	0.627	0.556	0.505
28	1.040	0.970	0.725	0.840	0.620	0.688	0.833	0.810	0.694	0.565
29	5.565	6.200	5.510	6.783	5.240	5.260	3.309	4.367	4.217	2.446
30	4.103	2.100	4.353	4.525	4.970	5.440	1.924	2.433	3.007	6.051
31	3.228	1.830	4.608	3.090	4.260	4.010	2.606	2.464	3.146	4.351
32	1.500	1.110	2.210	1.970	2.606	1.640	1.370	1.300	1.301	2.440
33	0.570	0.320	0.930	1.270	2.140	1.820	0.386	0.399	0.691	1.010
34	2.093	1.690	3.193	3.470	4.210	4.280	2.101	2.115	2.254	3.904
35	1.020	1.030	1.080	1.380	0.940	1.002	1.150	0.977	0.973	1.303
Average	**1.742**	**1.511**	**1.723**	**1.879**	**1.807**	**1.781**	**1.481**	**1.453**	**1.444**	**1.823**
St. Dev.	**1.589**	**1.593**	**1.415**	**1.591**	**1.427**	**1.507**	**2.036**	**1.702**	**1.493**	**1.685**

CHAPTER 3

NONLINEAR TIME HISTORY ANALYSES

3.1 INTRODUCTION

Nonlinear transient analyses of three different dam monoliths were performed for 35 different ground motions at two different strength levels at this section. The ground motions were scaled in accordance with the aforementioned four scaling procedures. The results were classified in terms of engineering demand parameters chosen as the base shear, the maximum crest acceleration, displacement and the ratio of the cracked area of the given monolith to the total area of the system. The results presented in this section are limited to the selected motion suite and dam geometries, thus are only valid under the circumstances defined for this study.
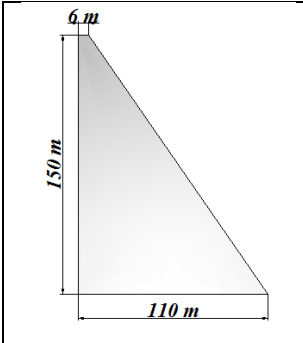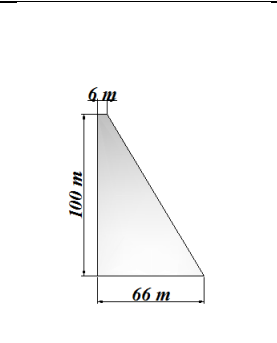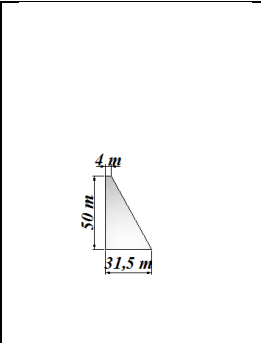
3.2 CONCRETE GRAVITY DAM MODEL

In this study, the general purpose finite element program DIANA was used for the structural analyses of concrete gravity dam models (DIANA, 2010). The analyses were made for monoliths of three different heights. Two different material properties are assigned to each of the models in order to represent the effect of the use of different concrete strengths for a given system. Rotating crack model was used in the study to model the cracking of the concrete with exponential post-peak softening behavior. The different capacity conditions, defined as (R=1,5 and R=2) are summarized in Table 3-1. The geometric properties of the structural models are shown in Table 3-2.

Table 3-1 Material Properties Assigned to the Models

Material Property	Models with R=1,5	Models with R=2
Young's Modulus	31 GPa	31 GPa
Poisson's ratio	0.2	0.2
Density	2400 kg/m^3	2400 kg/m^3
Tensile Strength	2.6 MPa	1.95 MPa
Compressive Strength	25 MPa	14 MPa
G_c (Compressive Fracture Energy)	60000 N/m	34000 N/m
G_f (Tensile Fracture Energy)	200 N/m	150 N/m

Table 3-2 Geometric Properties of Structural Models

	Model 1	Model 2	Model 3
Height (m)	150	100	50
Area (m^2)	8700	3600	887.5
# of Nodes	31703	13170	3356
# of Elements	11097	4742	1294

An equivalent damping was determined for each of the models using the simplified approach given in USACE (1995). The effective damping factors were converted to Rayleigh damping coefficients for each of the six different structural models. In order to simplify and reduce the size of the computational models to be used in the analyses, a fixed base assumption was made, which is applicable for a significant number of systems resting on hard rock foundations. The rigorous consideration of the soil-structure relationship is not included within the scope of this study.

In order to account for the hydrodynamic forces that occur during an earthquake on a dam, Westergaard's added mass approach was used (Westergaard, 1933). The reservoir elevations were assumed to be at the maximum levels and their hydrodynamic forces were calculated accordingly.

The smeared crack with a rotating crack assumption was used as the nonlinear constitutive relation for concrete in this study (Rashid, 1968, Rots et. al., 1985, Yamaguchi et. al., 2008). This robust material model is widely utilized in the literature for the prediction and evaluation of the performance of monolithic concrete structures (Bhattacharjee and Leger, 1992 ; Kumar and Nayak, 1994 ; Cervera et al., 1995 ; Leger and Bhattacharjee, 1995 ; Bazant , 1996 ; Valliappan et al., 1996 ; Plizzari, 1997 ; Lee and Fenves, 1998; Ghaemian and Ghobarah, 1999 ; Guanglun, et al., 2000 ; Espandar et al. 2003 ; Calayir and Karaton, 2005). The smeared crack model maintains the continuum of the cracked solid in contrast to the discrete crack models. The uncracked concrete behaves isotropically; after the occurrence of cracking, the material obeys the orthotropic law and the Poissons' effect. The tensile (f_t) and compressive strengths (f_c) and the shape of the post-peak response are the key characteristics of the stress-strain models. The mesh dependence of such models has been addressed by using the fracture energy (G_f). Secant unloading is applied during cyclic loading (Rots, 1988)

3.2.1 BENCHMARK SET (UNSCALED SUITE)

The dynamic analyses were performed for the time history records of the unscaled motion set in order to determine the base EDP values for the time histories used. The target spectrum was assumed as the mean (geometric) of these ground motions and the mean values from these analyses with unscaled ground motions were defined as the benchmark values in this study. Comprised of a large set of possible ground motions that can be observed at a near field site, these motions are assumed to form a representative set containing the possible variety in the frequency, duration and pulse content fitting the target spectrum.

3.2.2 DYNAMIC ANALYSES with SCALED MOTIONS

The dynamic analyses were performed for the time history records of the scaled motion sets which were obtained by using four different scaling approaches defined in Chapter 2. One unscaled and four scaled motions sets, each consisting of 35 different motions, were used for the dynamic analyses of the six different dam models. The results from different sets are presented and compared in the next section. As mentioned above, the results from the suite of analyses with unscaled

ground motions are denoted as "benchmark" in the next section, while the acronyms for the scaling methods "ASCE", "RSPM", "MIV" and "MPS" are used as the shorthand notations while presenting the results.

3.3   RESULTS OF THE ANALYSES

In order to conduct non-linear dynamic analyses of six different concrete gravity dam models for five different ground motion suites each consisting of thirty five different acceleration time histories, 1050 different analyses had to be conducted. The main goal of these analyses are to obtain the cracking schemes (as an index of performance) as well as the maximum acceleration, displacement and the base shear. A significant quantity of output was obtained for each analysis which had to be summarized in terms of these EDP's for comparison purposes.

As a simple mean to assess the performance level of a monolith, the ratio of the cracked area to the total cross sectional areas of the dams were used. The propagation of cracking on each of the dam monoliths obtained after each analyses are given in the Appendices section. The choices of the maximum base shear, maximum acceleration and the maximum displacement at the top of the dam structures as EDPs are self-explanatory. These EDPs were chosen as they are very commonly used as indices for the performance of the structure and are easy to interpret, whether as an equivalent amplification (crest acceleration), a displacement capacity or a base shear capacity.

The comparison of the results was made by comparing the mean and the coefficient of variation values of the EDPs obtained for each scaling procedure to the benchmark result for each dam model. For each set of dynamic analyses, the average value of maximum acceleration, displacement, base shear and the cracked area were calculated and compared with the corresponding benchmark value and the results obtained from the other sets of analyses.

The mean value of the results obtained from each motion suite represents the overall performance of the methods. Similarly, coefficient of variation values represents the dispersion of the results obtained by using these methods. Arguably, the mean is

more important in showing the performance of the procedure: however, an accurate mean with a large coefficient of variation would imply a significant number of ground motions are required for the procedure to be effective. The results for the mean values of the maximum acceleration at the top of the structures indicate that the average results obtained from RSPM (μ=18.271m/s² for R = 2 and μ=18.322m/s² for R = 1.5) and ASCE (μ=19.567 m/s² for R = 2 and μ=18.912 m/s²   for R = 1.5) methods are closer to the results obtained by using the original motion suite (μ=20.654m/s² for R = 2 and μ=20.385m/s² for R = 1.5). However, MIV method (μ=25.369m/s² for R = 2 and μ=24.139m/s² for R = 1.5) and MPS (μ=24.15m/s² for R = 2 and μ=22.421m/s² for R = 1.5) produces higher results than the original motion suite. (Table 3-3, Figure 3-1, Figure 3-2 and Figure 3-9.a)

Coefficient of variation of the results for the maximum acceleration at the top of the structures show that RSPM (Cv=0.175 for R = 2 and Cv=0.16 for R = 1.5) and ASCE (Cv=0.266 for R=2 and Cv=0.269 for R=1.5) methods produce far less dispersed results than the results obtained from original motion suite (Cv=0.553 for R = 2 and Cv=0.539 for R = 1.5). The results obtained from MIV (Cv=0.502 for R = 2 and Cv=0.499 for R = 1.5) and MPS(Cv=0.46 for R = 2 and Cv=0.465 for R = 1.5) methods have significantly larger dispersion compared to the other methods, although the dispersion is less than the benchmark counterpart. (Table 3-4, Figure 3-1, Figure 3-2 and Figure 3-10.a)

Additionally, increasing the strength of the structure (decreasing R=2 to R=1.5) improved the results of MPS method but did not considerably affect the results of the other methods. However, increasing the height of the structure leads to improved results for all of the scaling methods. Performance of the scaling methods are significantly better for increased period of the monolith in accordance with the change of the spectral demand from the acceleration sensitive to the velocity sensitive region of the spectrum (Table 3-3 and Table 3-4; Figure 3-1 and Figure 3-2).

Figure 3-1 Maximum acceleration values obtained from analyses of four different scaling methods for models having R=2

MAXIMUM ACCELERATION MEASURED AT THE TOP OF THE STRUCTURES (m/s^2) (R=1.5)
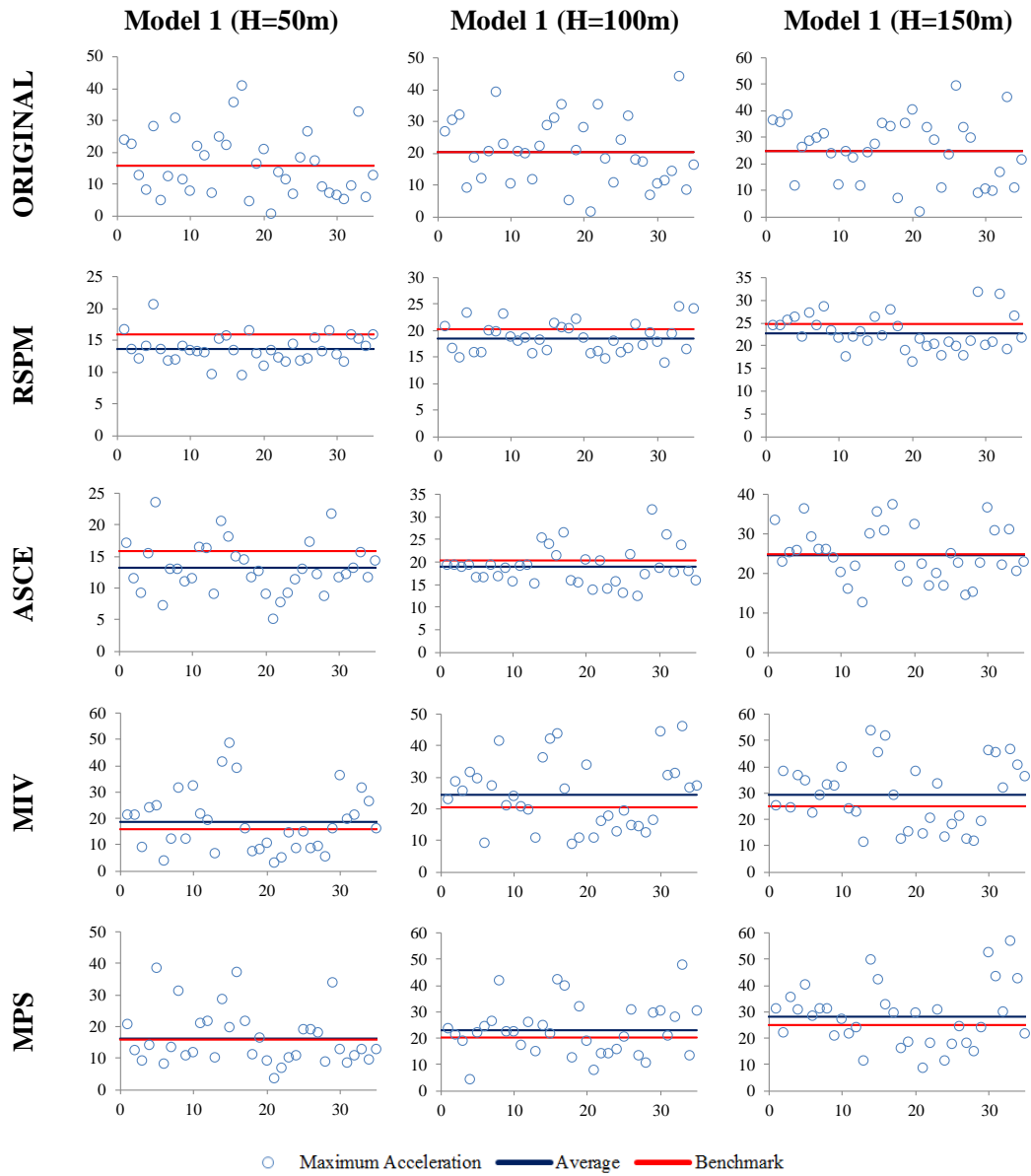
Figure 3-2 Maximum acceleration values obtained from analyses of four different scaling methods for models having R=1,5

Table 3-3 Mean Values of Maximum Acceleration Results

	R=2		R=1.5	
Model 1 (h=50m)				
Method	Mean (m/s²)	Difference From Benchmark	Mean (m/s²)	Difference From Benchmark
ORIGINAL	16.715	0.0%	15.926	0.0%
RSPM	13.368	-20.0%	13.616	-14.5%
ASCE	13.646	-18.4%	13.135	-17.5%
MIV	19.687	17.8%	18.507	16.2%
MPS	18.434	10.3%	16.085	1.0%
Model 2 (h=100m)				
Method	Mean (m/s²)	Difference From Benchmark	Mean (m/s²)	Difference From Benchmark
ORIGINAL	19.895	0.0%	20.337	0.0%
RSPM	18.483	-7.1%	18.557	-8.8%
ASCE	19.851	-0.2%	18.911	-7.0%
MIV	26.060	31.0%	24.415	20.0%
MPS	24.535	23.3%	22.925	12.7%
Model 3 (h=150m)				
Method	Mean (m/s²)	Difference From Benchmark	Mean (m/s²)	Difference From Benchmark
ORIGINAL	25.351	0.0%	24.892	0.0%
RSPM	22.963	-9.4%	22.794	-8.4%
ASCE	25.203	-0.6%	24.689	-0.8%
MIV	30.360	19.8%	29.497	18.5%
MPS	29.506	16.4%	28.253	13.5%
Mean Results				
Method	Mean (m/s²)	Difference From Benchmark	Mean (m/s²)	Difference From Benchmark
ORIGINAL	20.654	0.0%	20.385	0.0%
RSPM	18.271	-11.5%	18.322	-10.1%
ASCE	19.567	-5.3%	18.912	-7.2%
MIV	25.369	22.8%	24.139	18.4%
MPS	24.158	17.0%	22.421	10.0%

Table 3-4 Coefficient of Variation of Maximum Acceleration Results

Model 1 (h=50m)				
	R=2		R=1.5	
Method	Coefficient of Variation	Difference From Benchmark	Coefficient of Variation	Difference From Benchmark
ORIGINAL	0.656	0.0%	0.628	0.0%
RSPM	0.155	-76.4%	0.162	-74.3%
ASCE	0.294	-55.1%	0.313	-50.2%
MIV	0.637	-2.9%	0.632	0.6%
MPS	0.545	-16.9%	0.544	-13.4%
Model 2 (h=100m)				
	R=2		R=1.5	
Method	Coefficient of Variation	Difference From Benchmark	Coefficient of Variation	Difference From Benchmark
ORIGINAL	0.520	0.0%	0.511	0.0%
RSPM	0.163	-68.6%	0.152	-70.1%
ASCE	0.260	-50.1%	0.220	-56.9%
MIV	0.464	-10.9%	0.447	-12.5%
MPS	0.407	-21.8%	0.435	-14.9%
Model 3 (h=150m)				
	R=2		R=1.5	
Method	Coefficient of Variation	Difference From Benchmark	Coefficient of Variation	Difference From Benchmark
ORIGINAL	0.483	0.0%	0.477	0.0%
RSPM	0.207	-57.2%	0.166	-65.2%
ASCE	0.245	-49.4%	0.273	-42.7%
MIV	0.405	-16.2%	0.418	-12.4%
MPS	0.427	-11.6%	0.416	-12.8%
Mean Results				
	R=2		R=1.5	
Method	Coefficient of Variation	Difference From Benchmark	Coefficient of Variation	Difference From Benchmark
ORIGINAL	0.553	0.0%	0.539	0.0%
RSPM	0.175	-68.4%	0.160	-70.3%
ASCE	0.266	-51.9%	0.269	-50.1%
MIV	0.502	-9.3%	0.499	-7.4%
MPS	0.460	-16.9%	0.465	-13.7%

The results for the mean values of the maximum displacement at the top of the structures indicate that the mean results obtained from all methods - RSPM ($\mu=$ 0.046m for R=2 and $\mu=$ 0.045m for R=1.5), ASCE ($\mu=0.050$m for R=2 and $\mu=0.048$m for R=1.5), MIV ($\mu=0.067$m for R=2 and $\mu=0.062$m for R=1.5) and MPS ($\mu=0.065$m for R=2 and $\mu=0.061$m for R=1.5) methods are close to the results obtained by using the original motion suite ($\mu=0.080$m for R=2 and $\mu=0.068$ for R=1.5) (Table 3-5; Figure 3-3 Figure 3-4 and Figure 3-9.b).

Coefficient of variation of the results for the maximum displacement at the top of the structures show that RSPM (Cv=0.119 for R=2 and Cv=0.115 for R=1.5), ASCE (Cv=0.172 for both R=2 and R=1.5), MIV (Cv=0.483 for R=2 and Cv=0.435 for R=1.5) and MPS (Cv= 0.385 for R=2 and Cv=0.414 for R=1.5) methods produces far less dispersed results than the results obtained from original motion suite (Cv=1.111 for R=2 and Cv=0.806 for R = 1.5) (Table 3-6; Figure 3-3, Figure 3-4 and Figure 3-10.b).

Additionally, increasing the strength (decreasing R=2 to R=1.5) was improved the performance of MPS method and increasing the height of the structure (from 50m to 150m) did not considerably affect the mean results. The results indicate that the MPS and MIV methods provide a closer estimate to the mean compared to the other methods. However, the dispersions in the results obtained from these methods are far greater compared to RSPM or ASCE estimates which provide much smaller mean prediction values compared to the benchmark goal. (Table 3-5 and Table 3-6; Figure 3-3 and Figure 3-4).
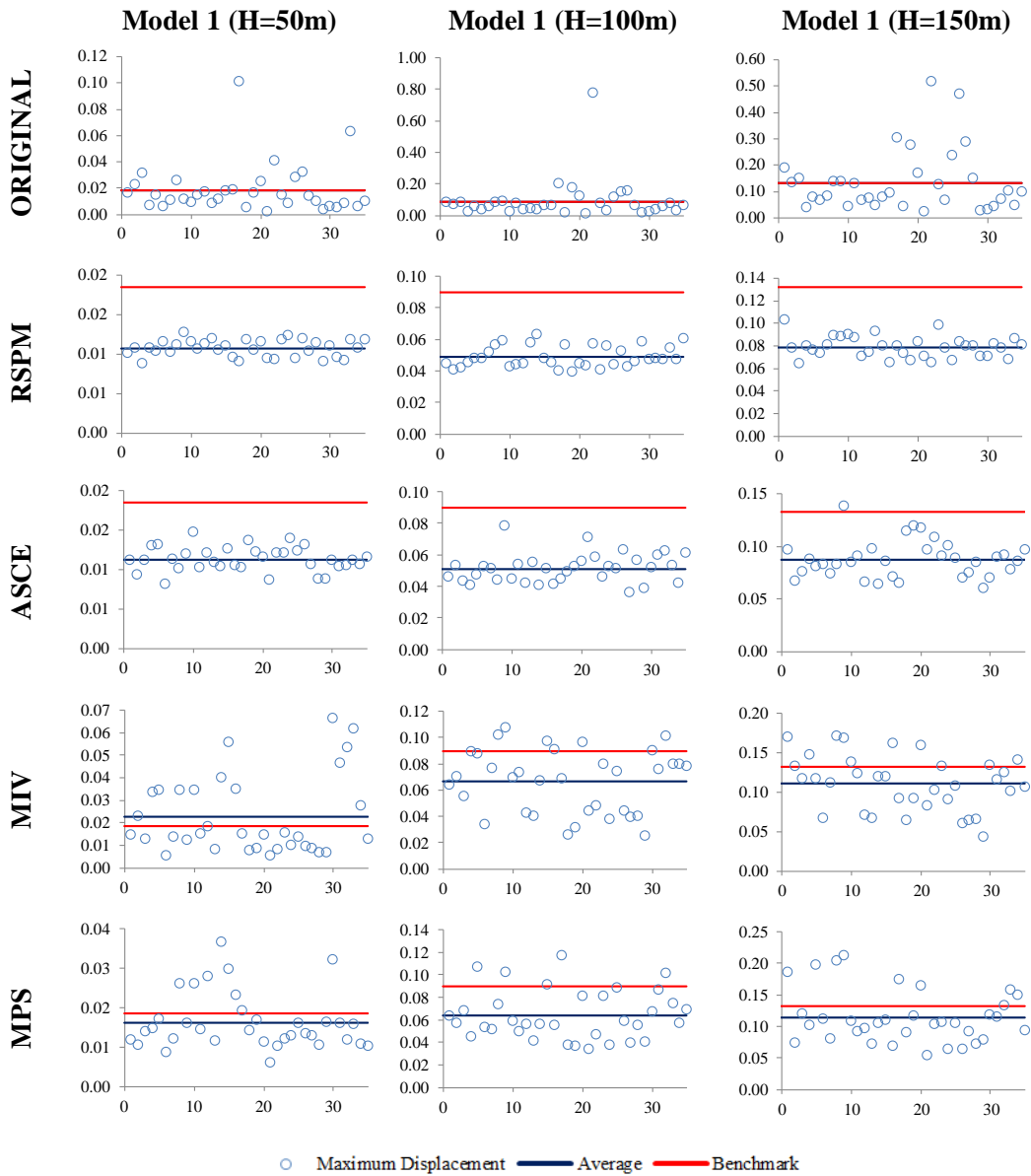
Figure 3-3 Maximum Displacement values obtained from analyses of four different scaling methods for models having R=2
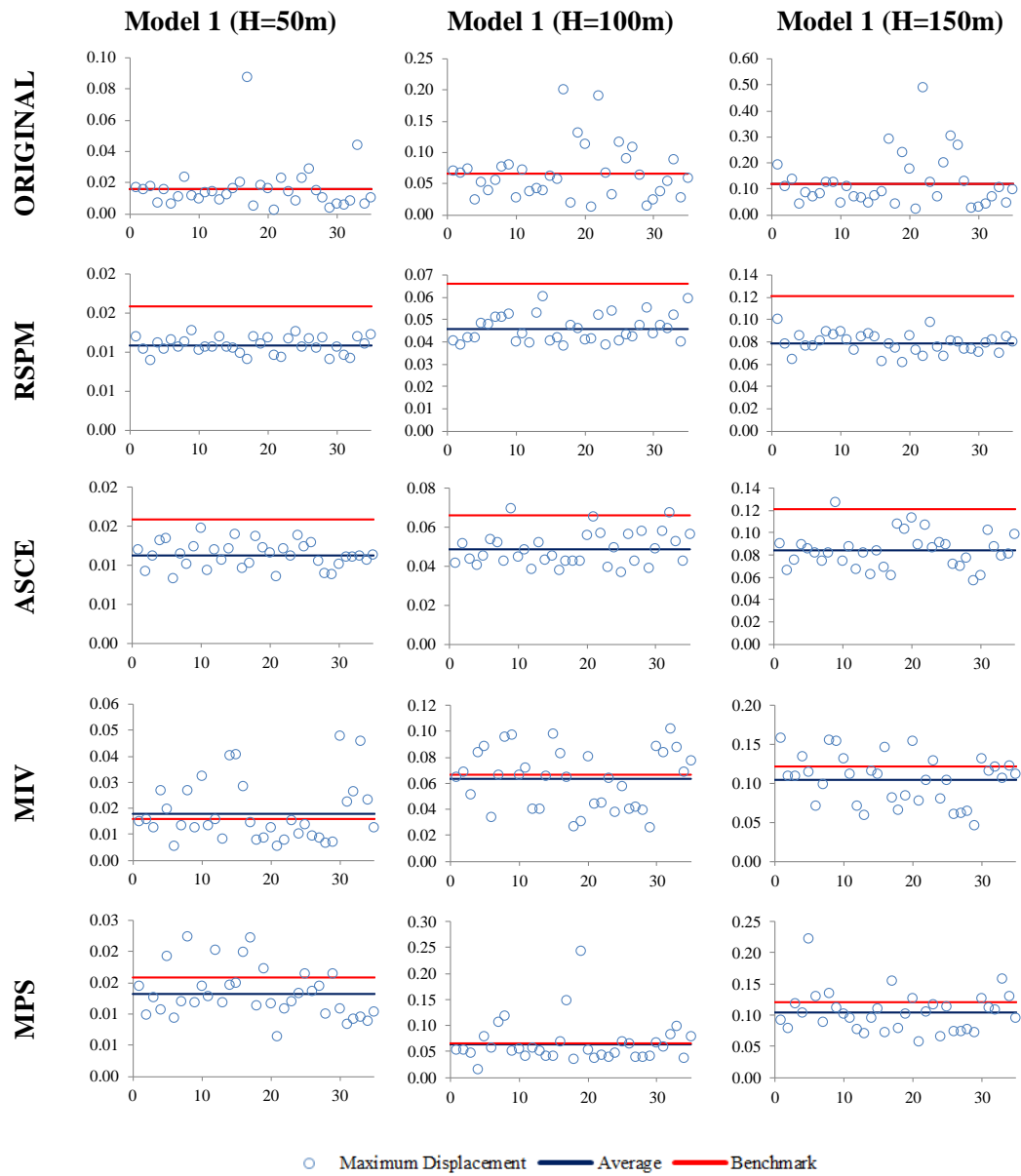
Figure 3-4 Maximum Displacement values obtained from analyses of four different scaling methods for models having R=1,5

Table 3-5 Mean Values of Maximum Displacement Results

Model 1 (50m)				
	R=2		R=1.5	
Method	Mean (m)	Difference From Benchmark	Mean (m)	Difference From Benchmark
ORIGINAL	0.018	0.0%	0.016	0.0%
RSPM	0.011	-42.0%	0.011	-31.8%
ASCE	0.011	-39.0%	0.011	-28.9%
MIV	0.023	22.2%	0.018	13.6%
MPS	0.016	-12.1%	0.013	-16.4%
Model 2 (h=100m)				
	R=2		R=1.5	
Method	Mean (m)	Difference From Benchmark	Mean (m)	Difference From Benchmark
ORIGINAL	0.090	0.0%	0.066	0.0%
RSPM	0.049	-45.5%	0.046	-30.7%
ASCE	0.051	-42.9%	0.049	-26.7%
MIV	0.066	-25.9%	0.063	-4.4%
MPS	0.064	-28.7%	0.064	-3.0%
Model 3 (h=150m)				
	R=2		R=1.5	
Method	Mean (m)	Difference From Benchmark	Mean (m)	Difference From Benchmark
ORIGINAL	0.132	0.0%	0.121	0.0%
RSPM	0.079	-40.4%	0.079	-35.0%
ASCE	0.087	-34.2%	0.084	-30.8%
MIV	0.111	-16.2%	0.105	-13.4%
MPS	0.114	-13.9%	0.104	-14.1%
Mean Results				
	R=2		R=1.5	
Method	Mean (m)	Difference From Benchmark	Mean (m)	Difference From Benchmark
ORIGINAL	0.080	0.0%	0.068	0.0%
RSPM	0.046	-42.4%	0.045	-33.3%
ASCE	0.050	-37.8%	0.048	-29.4%
MIV	0.067	-16.8%	0.062	-8.4%
MPS	0.065	-19.2%	0.061	-10.6%

Table 3-6 Coefficient of Variation of Maximum Displacement Results

Model 1 (50m)				
	R=2		R=1.5	
Method	Coefficient of Variation	Difference From Benchmark	Coefficient of Variation	Difference From Benchmark
ORIGINAL	1.019	0.0%	0.935	0.0%
RSPM	0.099	-90.3%	0.098	-89.5%
ASCE	0.137	-86.5%	0.147	-84.3%
MIV	0.772	-24.2%	0.650	-30.5%
MPS	0.440	-56.8%	0.301	-67.8%
Model 2 (h=100m)				
	R=2		R=1.5	
Method	Coefficient of Variation	Difference From Benchmark	Coefficient of Variation	Difference From Benchmark
ORIGINAL	1.431	0.0%	0.663	0.0%
RSPM	0.137	-90.4%	0.133	-80.0%
ASCE	0.179	-87.5%	0.177	-73.3%
MIV	0.362	-74.7%	0.357	-46.1%
MPS	0.345	-75.9%	0.634	-4.4%
Model 3 (h=150m)				
	R=2		R=1.5	
Method	Coefficient of Variation	Difference From Benchmark	Coefficient of Variation	Difference From Benchmark
ORIGINAL	0.883	0.0%	0.818	0.0%
RSPM	0.119	-86.5%	0.114	-86.1%
ASCE	0.201	-77.2%	0.191	-76.7%
MIV	0.316	-64.2%	0.298	-63.6%
MPS	0.371	-57.9%	0.309	-62.2%
Mean Results				
	R=2		R=1.5	
Method	Coefficient of Variation	Difference From Benchmark	Coefficient of Variation	Difference From Benchmark
ORIGINAL	1.111	0.0%	0.806	0.0%
RSPM	0.119	-89.3%	0.115	-85.7%
ASCE	0.172	-84.5%	0.172	-78.7%
MIV	0.483	-56.5%	0.435	-46.0%
MPS	0.385	-65.3%	0.414	-48.5%

For the maximum base shear, each result was divided to the total weight of the concrete gravity dam model to obtain unitless quantities (in terms of g). The results for the mean values of the maximum base shear indicate that the mean results obtained from RSPM ($\mu= 1.158$ for R=2 and $\mu= 1.173$ for R=1.5), ASCE ($\mu= 1.159$ for R=2 and $\mu= 1.181$ for R=1.5), MPS ($\mu= 1.283$ for R=2 and $\mu= 1.261$ for R=1.5) and MIV ($\mu= 1.281$ for R=2 and $\mu= 1.302$ for R=1.5) methods are very close to the results obtained by using the original motion suite ($\mu=1.188$ for R=2 and $\mu=1.218$ for R=1.5). These results suggest that all methods can very well represent the maximum base shear of the concrete gravity dams. (Table 3-7; Figure 3-5, Figure 3-6 and Figure 3-9.c)

Coefficient of variation of the results for the maximum base shear show that RSPM ($Cv=0.189$ for R=2 and $Cv=0.18$ for R=1.5), ASCE ($Cv=0.159$ for R=2 and $Cv=0.153$ for R=1.5), MPS ($Cv= 0.19$ for R=2 and $Cv= 0.176$ for R=1.5) and MIV ($Cv=0.20$ for R=2 and $Cv=0.198$ for R=1.5) methods produces less dispersed results than the results obtained from original motion suite ($Cv=0.271$ for R=2 and $Cv=0.274$ for R = 1.5). (Table 3-8; Figure 3-5, Figure 3-6 and Figure 3-10.c)

Additionally, increasing the strength (decreasing R=2 to R=1.5) of the structure improved the results for the MPS method. Increasing the height of the structure (from 50m to 150m) did not considerably affect the mean results. (Table 3-7 and Table 3-8; Figure 3-5 and Figure 3-6)
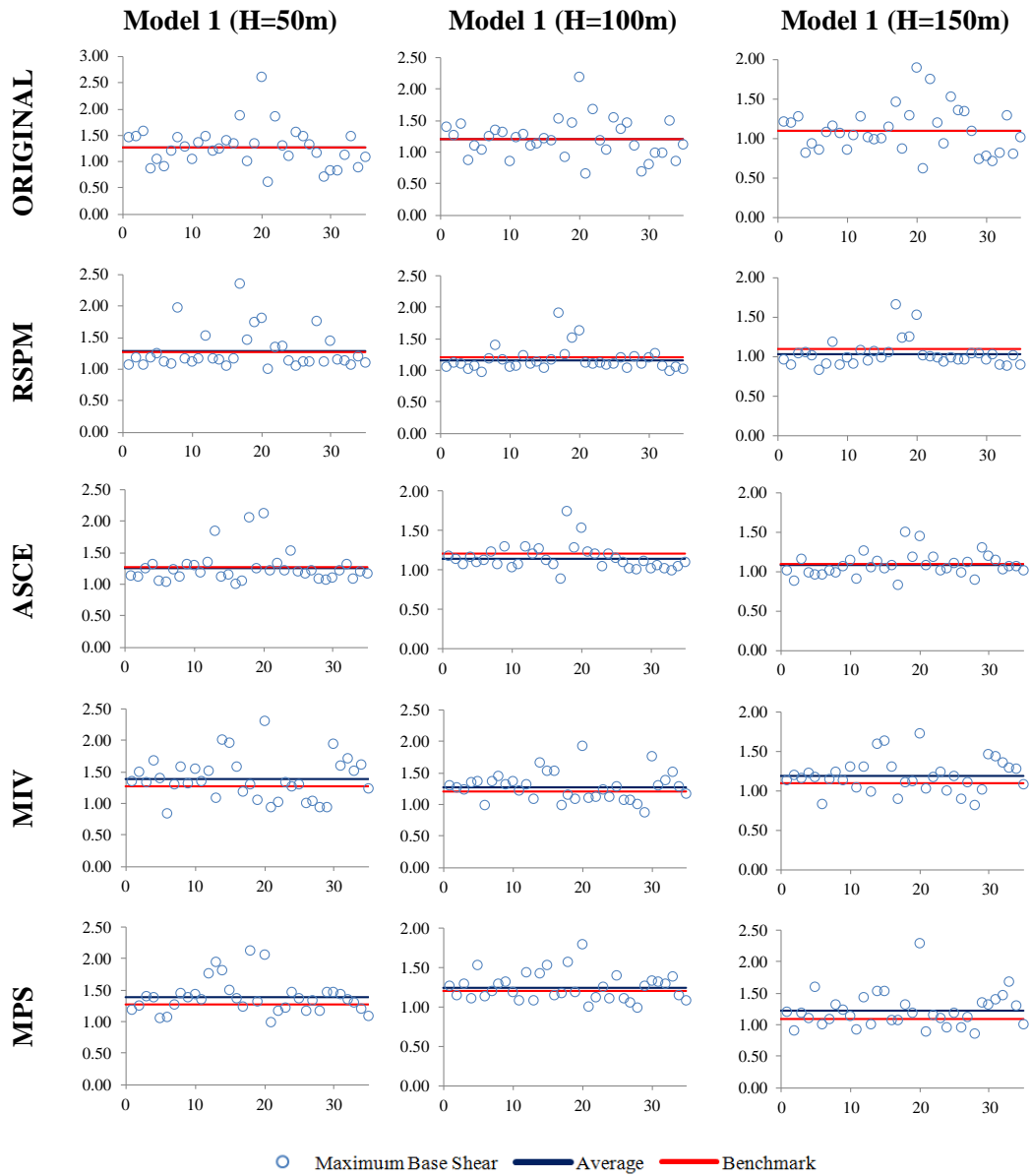
Figure 3-5 Maximum Base shear values obtained from analyses of four different scaling methods for models having R=2
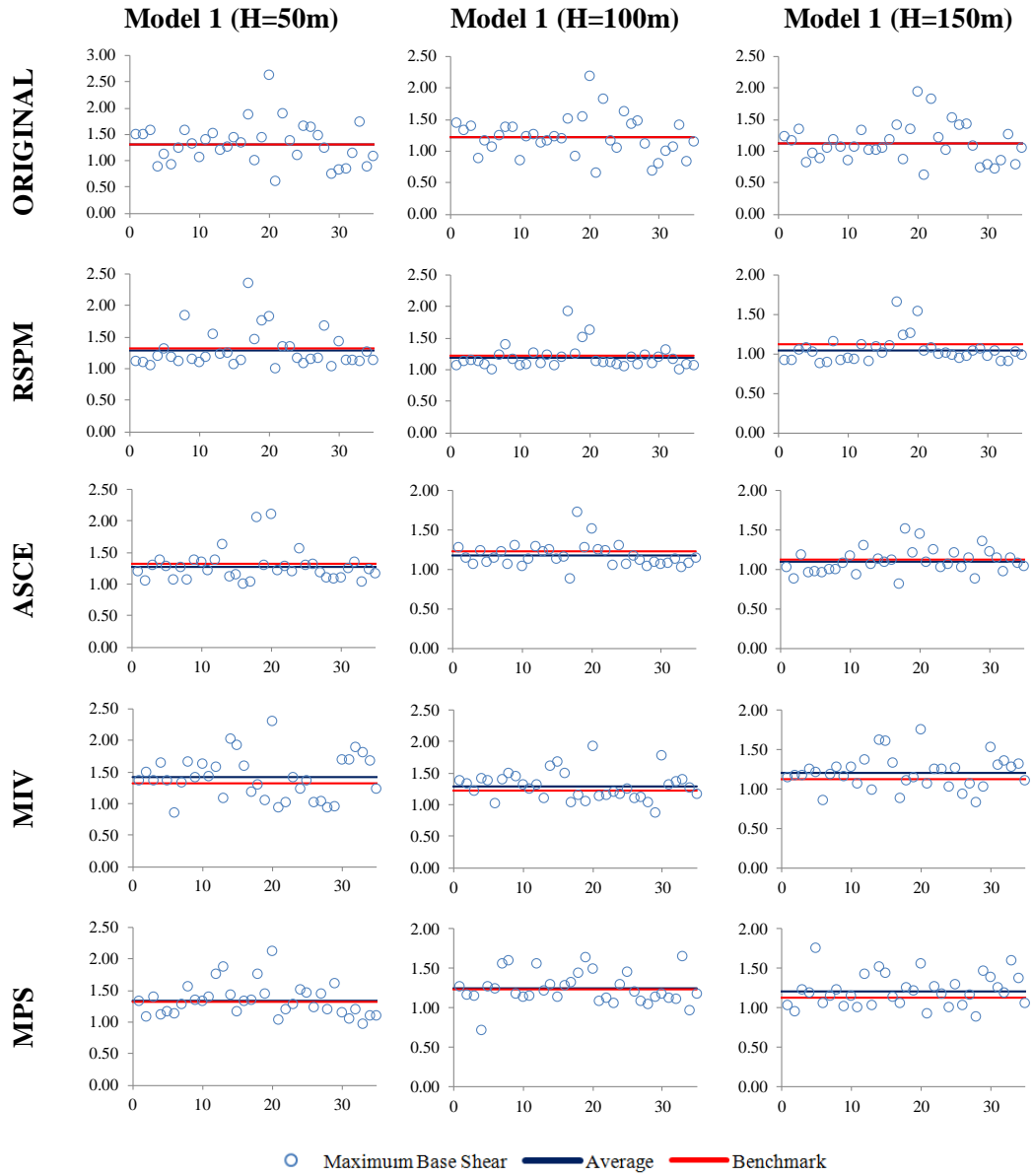
Figure 3-6 Maximum Base shear values obtained from analyses of four different scaling methods for models having R=1,5

Table 3-7 Mean Values of Maximum Base Shear Results

Model 1 (50m)				
	R=2		R=1.5	
Method	Mean	Difference From Benchmark	Mean	Difference From Benchmark
ORIGINAL	1.268	0.0%	1.315	0.0%
RSPM	1.281	1.1%	1.289	-2.0%
ASCE	1.257	-0.8%	1.275	-3.1%
MIV	1.384	9.2%	1.412	7.4%
MPS	1.382	9.1%	1.339	1.8%
Model 2 (h=100m)				
	R=2		R=1.5	
Method	Mean	Difference From Benchmark	Mean	Difference From Benchmark
ORIGINAL	1.200	0.0%	1.223	0.0%
RSPM	1.164	-3.0%	1.186	-3.0%
ASCE	1.140	-5.0%	1.170	-4.4%
MIV	1.275	6.3%	1.292	5.6%
MPS	1.247	4.0%	1.236	1.0%
Model 3 (h=150m)				
	R=2		R=1.5	
Method	Mean	Difference From Benchmark	Mean	Difference From Benchmark
ORIGINAL	1.097	0.0%	1.116	0.0%
RSPM	1.029	-6.2%	1.045	-6.4%
ASCE	1.079	-1.6%	1.098	-1.6%
MIV	1.185	8.0%	1.202	7.7%
MPS	1.221	11.3%	1.207	8.1%
Mean Results				
	R=2		R=1.5	
Method	Mean	Difference From Benchmark	Mean	Difference From Benchmark
ORIGINAL	1.188	0.0%	1.218	0.0%
RSPM	1.158	-2.5%	1.173	-3.7%
ASCE	1.159	-2.5%	1.181	-3.1%
MIV	1.281	7.9%	1.302	6.9%
MPS	1.283	8.0%	1.261	3.5%

Table 3-8 Coefficient of Variation of Maximum Base Shear Results

Model 1 (50m)				
	R=2		R=1.5	
Method	Coefficient of Variation	Difference From Benchmark	Coefficient of Variation	Difference From Benchmark
ORIGINAL	0.296	0.0%	0.299	0.0%
RSPM	0.238	-19.6%	0.225	-24.7%
ASCE	0.207	-30.2%	0.192	-35.6%
MIV	0.246	-17.1%	0.245	-17.9%
MPS	0.195	-34.2%	0.191	-36.1%
Model 2 (h=100m)				
	R=2		R=1.5	
Method	Coefficient of Variation	Difference From Benchmark	Coefficient of Variation	Difference From Benchmark
ORIGINAL	0.254	0.0%	0.258	0.0%
RSPM	0.163	-35.9%	0.155	-39.6%
ASCE	0.138	-45.8%	0.127	-50.5%
MIV	0.178	-30.1%	0.175	-32.2%
MPS	0.142	-44.0%	0.164	-36.1%
Model 3 (h=150m)				
	R=2		R=1.5	
Method	Coefficient of Variation	Difference From Benchmark	Coefficient of Variation	Difference From Benchmark
ORIGINAL	0.263	0.0%	0.266	0.0%
RSPM	0.165	-37.2%	0.160	-40.0%
ASCE	0.133	-49.3%	0.139	-47.8%
MIV	0.178	-32.4%	0.174	-34.8%
MPS	0.231	-12.0%	0.172	-35.5%
Mean Results				
	R=2		R=1.5	
Method	Coefficient of Variation	Difference From Benchmark	Coefficient of Variation	Difference From Benchmark
ORIGINAL	0.271	0.0%	0.274	0.0%
RSPM	0.189	-30.4%	0.180	-34.3%
ASCE	0.159	-41.2%	0.153	-44.2%
MIV	0.200	-26.1%	0.198	-27.8%
MPS	0.190	-30.0%	0.176	-35.9%

For the total cracked area, each result were divided to the total cross sectional area of the concrete gravity dam model to obtain the percentage of the cracked area on the monolith. The results for the mean values of the cracked areas indicate that the mean results obtained from MPS (μ= 24.2% for R=2 and μ= 13.9% for R=1.5) and MIV (μ=25.3% for R=2 and μ= 16.2% for R=1.5) methods are very close to the results obtained by using the original motion suite (μ= 22.4% for R=2 and μ=14.6%for R=1.5). The results of RSPM (μ= 14% for R=2 and μ= 7.6% for R=1.5) and ASCE (μ= 16.2% for R=2 and μ=9.1% for R=1.5) methods are less than the results obtained by using the original motion suite. (Table 3-9; Figure 3-7, Figure 3-8 and Figure 3-9.d)

Coefficient of variation of the results for the maximum base shear show that RSPM (Cv=0.31 for R=2 and Cv=0.328 for R=1.5) and ASCE (Cv=0.376 for R=2 and Cv=0.404 for R=1.5) methods produces less dispersed results than the results obtained from original motion suite (Cv=0.987 for R=2 and Cv=1.187 for R = 1.5). However, MPS (Cv= 0.726 for R=2 and Cv= 0.980 for R=1.5) and MIV (Cv=0.717 for R=2 and Cv=0.831 for R=1.5) methods produce dispersions similar to the original motion suite (Table 3-10).

Increasing the strength (decreasing R=2 to R=1.5) reduces the cracked area for all motions. Similarly, increasing the height of the structure (from 50m to 150m) considerably increases the mean results. Taken together, the results indicate that ASCE and RSPM methods performed adequately for predicting the cracked areas of concrete gravity dam models. The mean results of MPS and MIV methods were better but the results were more dispersed than the other methods. (Table 3-9 and Table 3-10; Figure 3-7 and Figure 3-8)
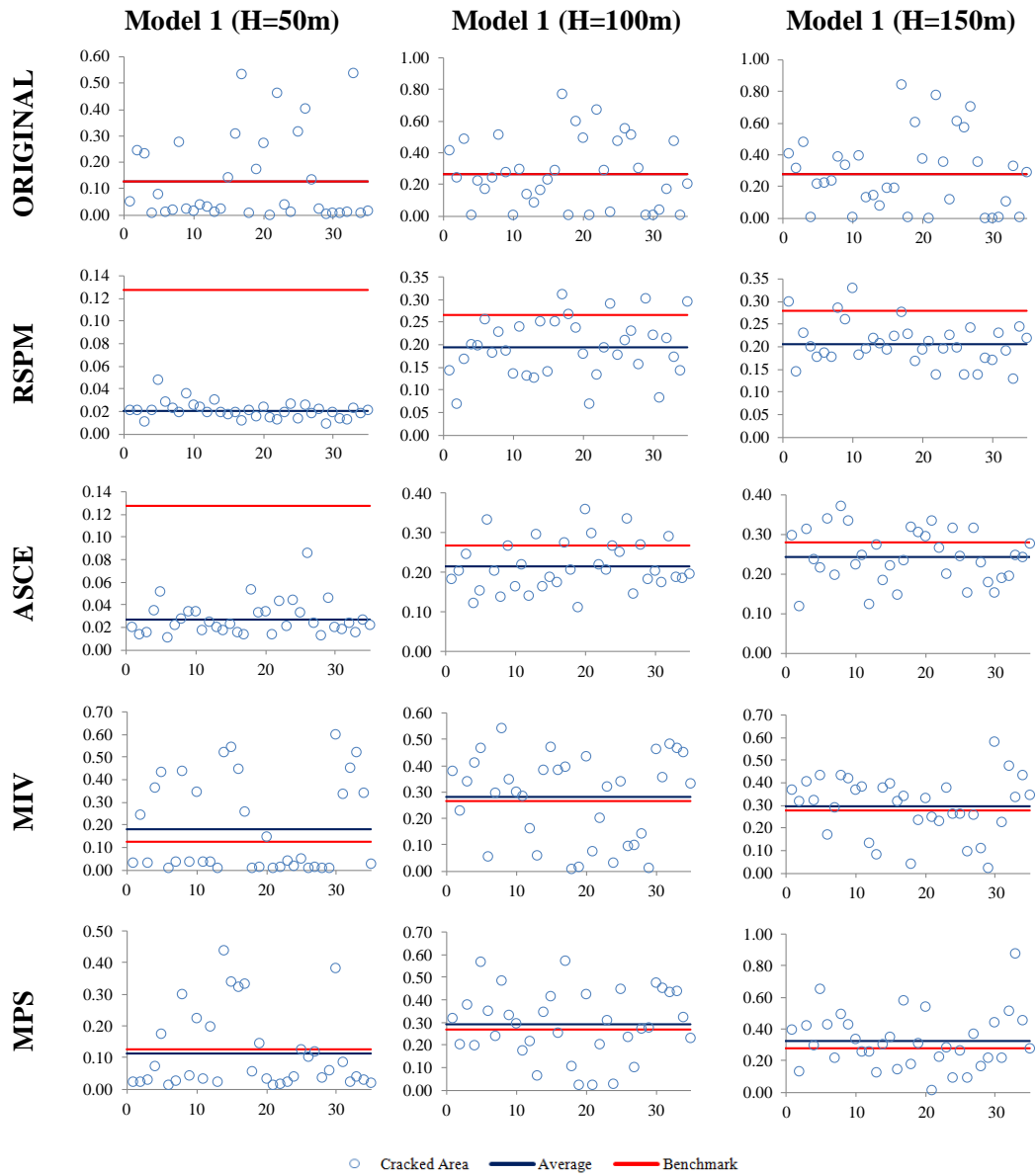
Figure 3-7 Percentage of cracked area to total area values obtained from analyses of four different scaling methods for models having R=2

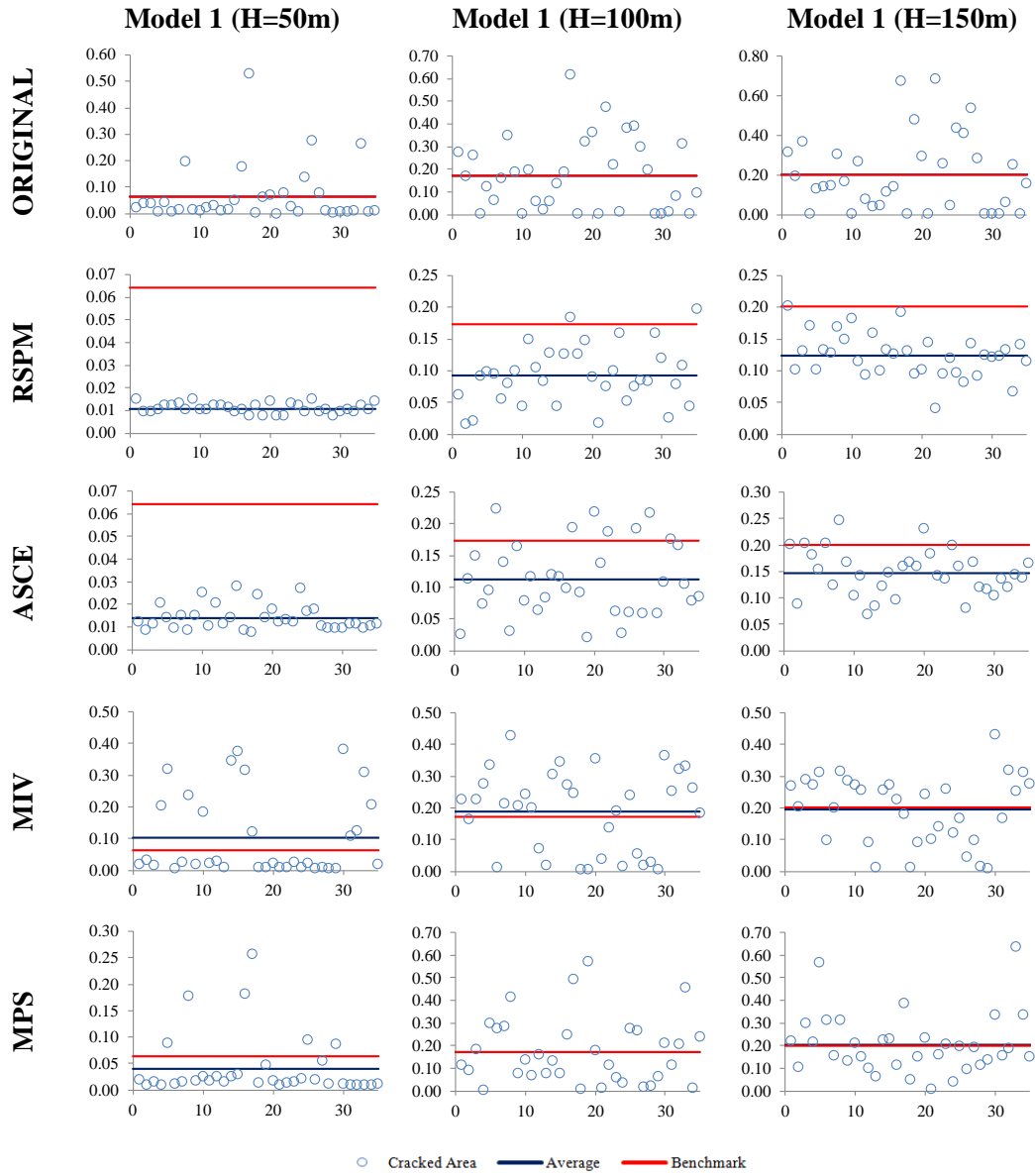CRACKED AREA OF TOTAL DAM SECTION (%) (R=1.5)

Figure 3-8 Percentage of cracked area to total area values obtained from analyses of four different scaling methods for models having R=1,5

**Table 3-9 Mean Values of Total Cracked Area Results**

Model 1 (50m)				
	R=2		R=1.5	
Method	Mean	Difference From Benchmark	Mean	Difference From Benchmark
ORIGINAL	12.7%	0.0%	6.4%	0.0%
RSPM	2.0%	-84.0%	1.1%	-83.1%
ASCE	2.7%	-78.6%	1.4%	-78.4%
MIV	18.3%	43.7%	10.2%	57.5%
MPS	11.2%	-11.8%	4.0%	-38.4%

Model 2 (h=100m)				
	R=2		R=1.5	
Method	Mean	Difference From Benchmark	Mean	Difference From Benchmark
ORIGINAL	26.6%	0.0%	17.3%	0.0%
RSPM	19.4%	-27.3%	9.2%	-46.6%
ASCE	21.5%	-19.4%	11.2%	-34.8%
MIV	28.0%	5.1%	18.8%	9.1%
MPS	29.1%	9.2%	17.1%	-1.0%

Model 3 (h=150m)				
	R=2		R=1.5	
Method	Mean	Difference From Benchmark	Mean	Difference From Benchmark
ORIGINAL	27.9%	0.0%	20.1%	0.0%
RSPM	20.6%	-26.2%	12.4%	-38.0%
ASCE	24.4%	-12.8%	14.7%	-26.5%
MIV	29.7%	6.1%	19.6%	-2.1%
MPS	32.2%	15.4%	20.5%	2.2%

Mean Results				
	R=2		R=1.5	
Method	Mean	Difference From Benchmark	Mean	Difference From Benchmark
ORIGINAL	22.4%	0.0%	14.6%	0.0%
RSPM	14.0%	-37.6%	7.6%	-48.0%
ASCE	16.2%	-27.8%	9.1%	-37.4%
MIV	25.3%	12.8%	16.2%	11.1%
MPS	24.2%	7.8%	13.9%	-5.0%

Table 3-10 Coefficient of Variation of Total Cracked Area Results

| Model 1 (50m)				
	R=2		R=1.5	
Method	Coefficient of Variation	Difference From Benchmark	Coefficient of Variation	Difference From Benchmark
ORIGINAL	1.294	0.0%	1.679	0.0%
RSPM	0.373	-71.2%	0.205	-87.8%
ASCE	0.562	-56.6%	0.404	-75.9%
MIV	1.127	-12.9%	1.268	-24.4%
MPS	1.110	-14.2%	1.436	-14.5%
Model 2 (h=100m)				
	R=2		R=1.5	
Method	Coefficient of Variation	Difference From Benchmark	Coefficient of Variation	Difference From Benchmark
ORIGINAL	0.818	0.0%	0.919	0.0%
RSPM	0.331	-59.6%	0.501	-45.5%
ASCE	0.294	-64.1%	0.517	-43.8%
MIV	0.587	-28.3%	0.677	-26.3%
MPS	0.514	-37.1%	0.856	-6.8%
Model 3 (h=150m)				
	R=2		R=1.5	
Method	Coefficient of Variation	Difference From Benchmark	Coefficient of Variation	Difference From Benchmark
ORIGINAL	0.850	0.0%	0.963	0.0%
RSPM	0.228	-73.2%	0.277	-71.2%
ASCE	0.273	-67.9%	0.291	-69.8%
MIV	0.437	-48.6%	0.547	-43.2%
MPS	0.555	-34.8%	0.649	-32.7%
Mean Results				
	R=2		R=1.5	
Method	Coefficient of Variation	Difference From Benchmark	Coefficient of Variation	Difference From Benchmark
ORIGINAL	0.987	0.0%	1.187	0.0%
RSPM	0.310	-68.6%	0.328	-72.4%
ASCE	0.376	-61.9%	0.404	-66.0%
MIV	0.717	-27.4%	0.831	-30.0%
MPS	0.726	-26.4%	0.980	-17.4%
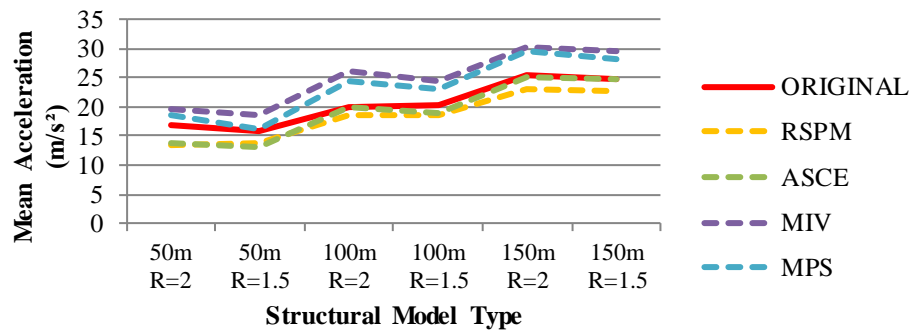
(a)
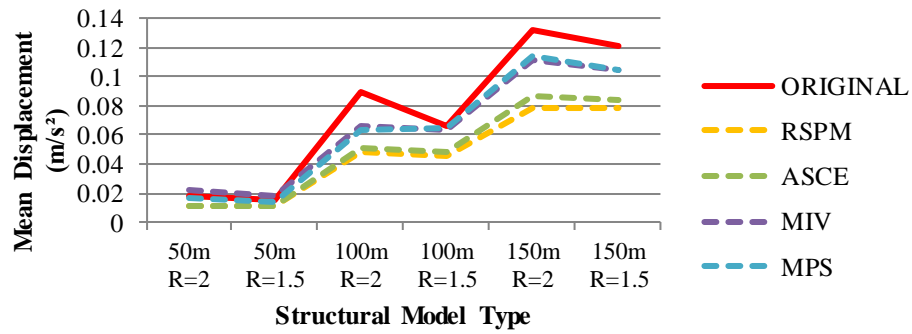
(b)
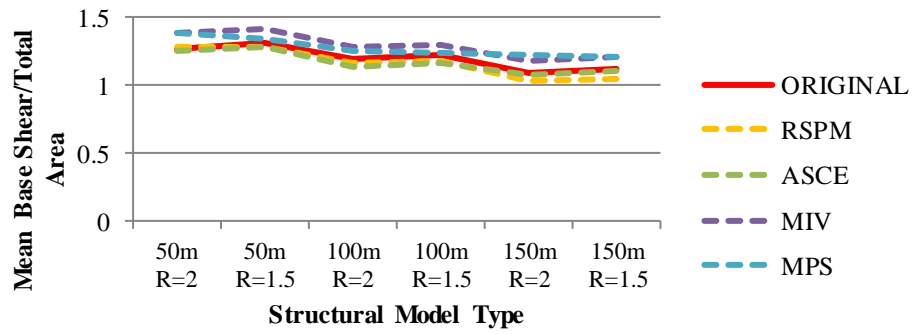
(c)
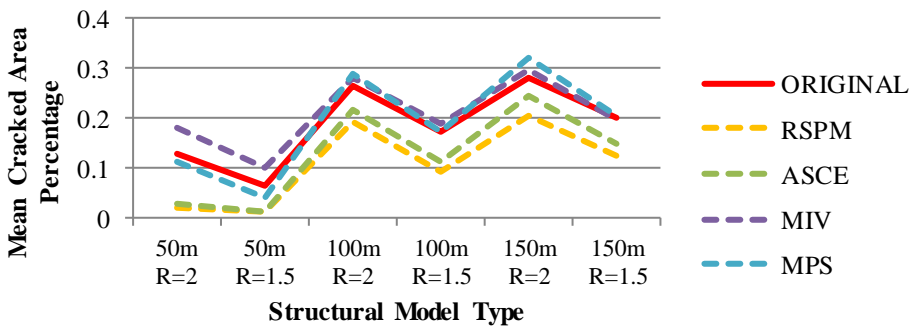
(d)

Figure 3-9 Comparison of Ground Motion Scaling Procedures (Mean Results)
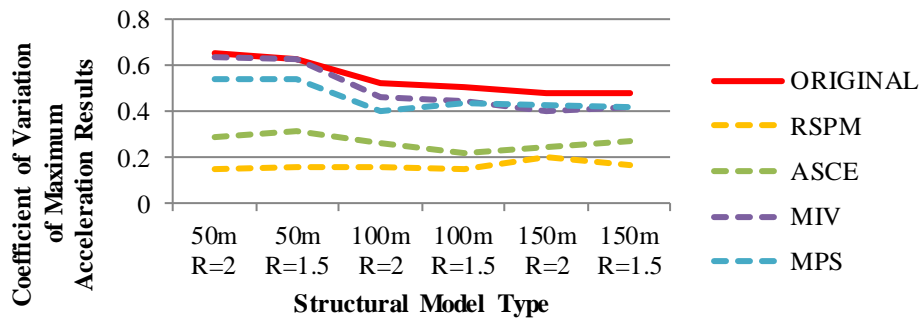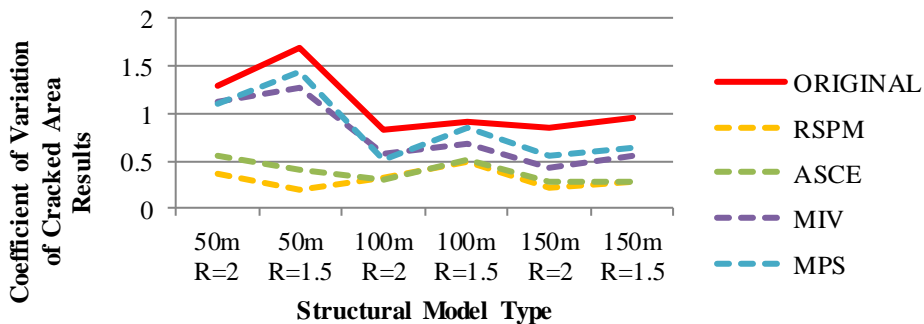
(a)
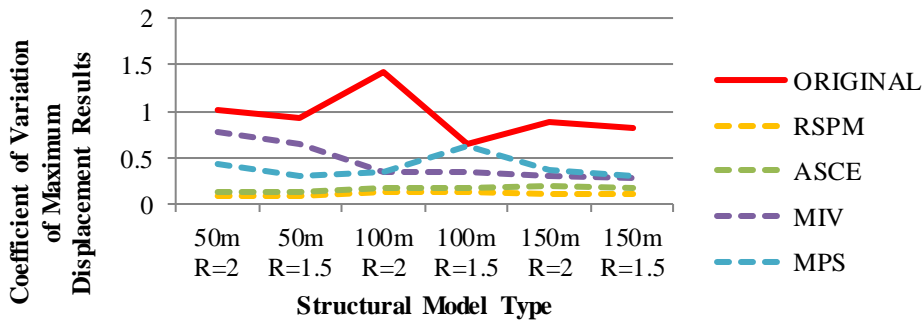
(b)
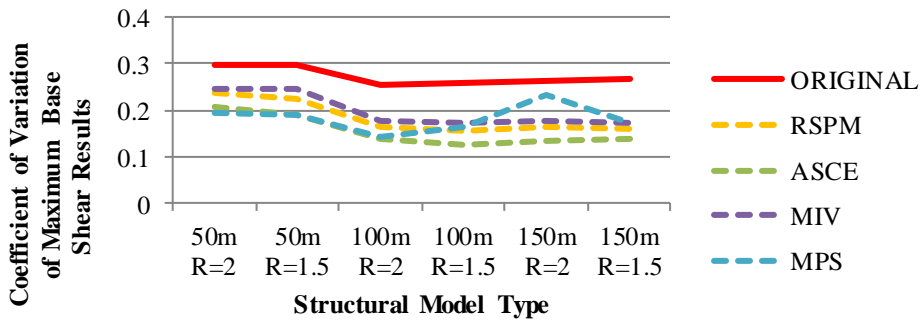
(c)

(d)

Figure 3-10 Comparison of Ground Motion Scaling Procedures (Coefficient of Variations)

CHAPTER 4

EVALUATION OF THE ANALYSIS RESULTS

The results of a significant number of nonlinear time history analyses were presented in the previous chapter. These results form a significant number of data points which can be investigated from the point of ground motion selection: however, they also offer an opportunity to investigate the behavior of concrete monoliths during earthquake.

4.1   GROUND MOTION SELECTION

In this study, four different ground motion scaling methods (RSPM, ASCE 07, MIV, MPS) were investigated by nonlinear dynamic structural analyses of six different concrete gravity dam models and different acceleration time histories for each scaling method. 35 different analyses were conducted for 6 different monoliths for each method in order to ascertain the prediction of the mean response from each model as well as the dispersion. This significant trove of analysis offers an opportunity to compare the methods of ground motion scaling, however, it should not be forgotten that in the design or evaluation of such concrete dams, 35 different motions could hardly be used. Therefore, the amount of reduction in the number of motions is a significant issue. The minimum number of motions which can be used to predict the mean response reasonably well in a given method should be determined.

The ASCE7-10 provides the well-known suggestions to this end: If 3 different ground motions are used, the maximum of the response quantities from each different motion can be used as a design quantity, whereas for 7 or more motions, the mean value of the response from the different analyses may be utilized. There are numerous engineering demand parameters that could be interpreted and used for

design purposes. The drift ratio at different floors is the generally chosen response quantity for buildings which is often linked to some performance criteria. For the dam monoliths, the cracked area ratio and the top displacement are assumed as the engineering demand parameters for this study as these parameters were observed to yield a closer correlation with a performance interpretation of the system. The base shear quantity was obtained with small dispersion for almost all analysis cases, indicating that the capacity of the system is well-set, and as expected, does not yield an indicator of the system behavior once the elastic limits are exceeded.

The number of ground motions for adequate prediction of the mean could be established by treating the 35 analyses for the base cases as the populations and using sampling from each population by n number of ground motions in order to obtain the sample cases. The mean of each sample is tested for closeness to the population mean in order to ascertain the distribution of the predicted mean and its effectiveness. This procedure is conducted using the student t-distribution, which produces the distribution of a mean estimate for population parameters when the sample size is small. The use of the t-distribution requires the following conditions: The mean value of the dispersion from the 35 different ground motions were assumed to be normally distributed, the sample size collected was greater than 40, the distribution of the error for the sampled analyses (with respect to population mean) is assumed to be symmetric and without outliers.

The t-distribution is used for each of the four scaling methods in order to test the number of ground motions that should be selected such that the mean of the sample is smaller than or equal to 90% of the population mean. The probability of this preposition, obtained for each method and different monolith cases, is presented in Figure 4-1. The figure can be interpreted in a number of ways. For example, in order to predict the population means reasonably, 5 and 7 ground motions, respectively, should be used for a 50m monolith using the RSPM ground motion selection.
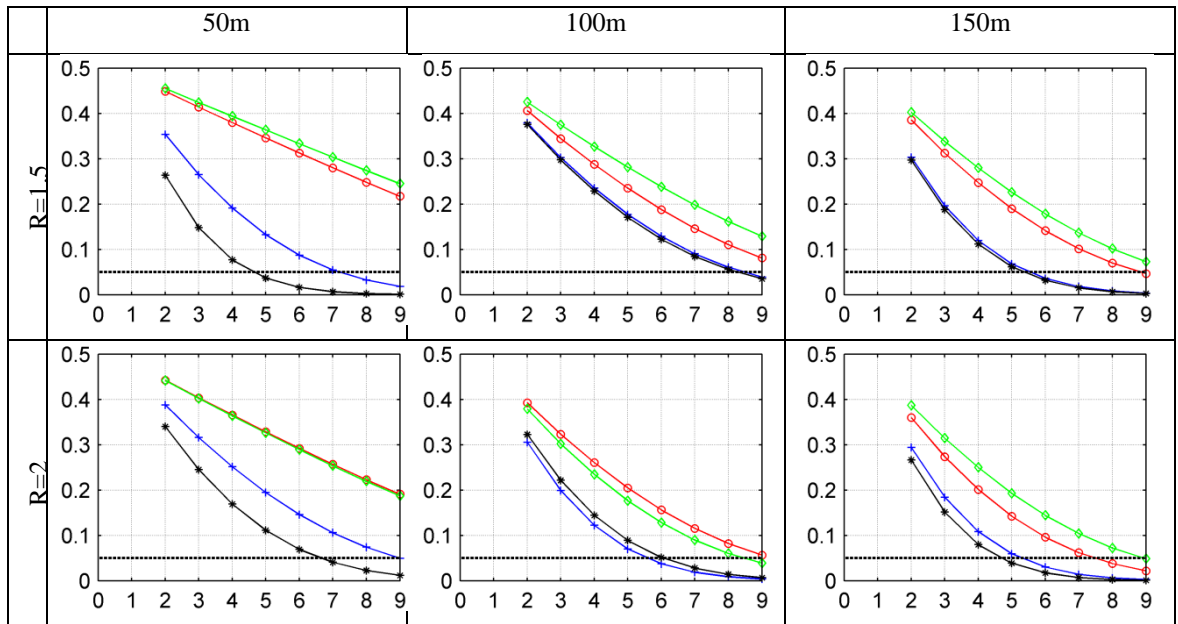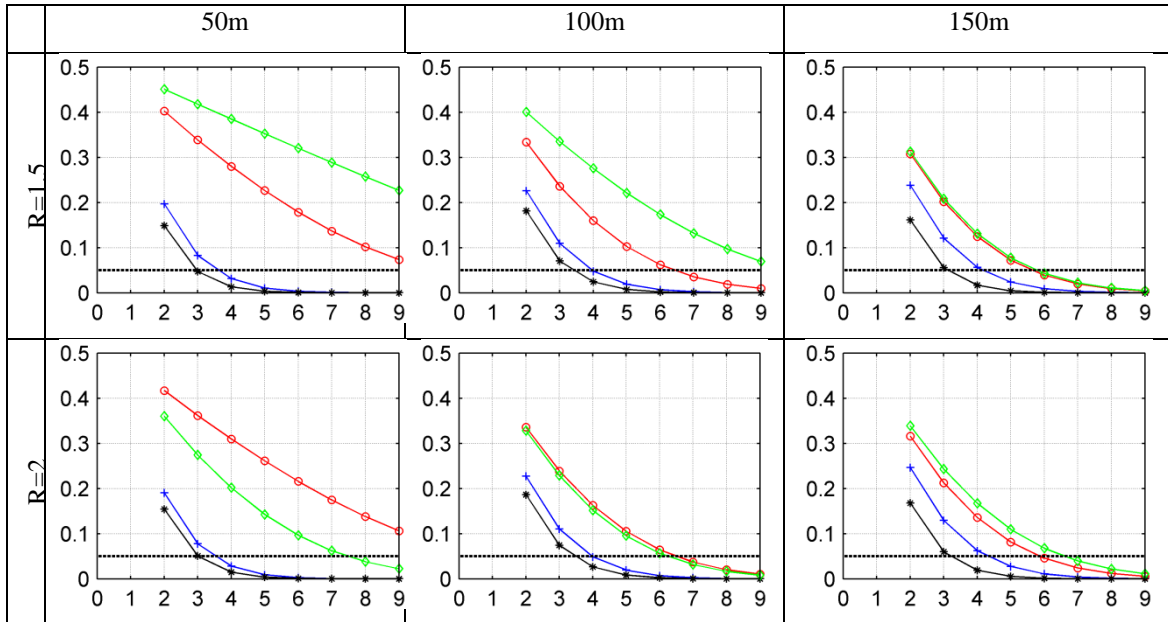
Figure 4-1 The Probability of Sample Mean of Cracked Area Ratio≤PopulationMeanx0.9 (Black-RSPM, Blue-ASCE, Red-MIV, Green-MPS)

The lower dispersion in the ASCE scaling results can also be observed in Figure 4-1. of the mean for the ASCE and RSPM scaling is very similar. On the other hand, modal push-over based scaling appears to require a considerably higher number of motions for a satisfactory prediction of the target mean. For the 50m cases, the number of motions required is very high. For the 100 and 150m cases, the use of 9-10 motions appears to be required for the MPS based scaling to accurately predict the mean response from the population.

A similar trend is observed if the probability for approaching the population mean of the crest displacement is presented, as given in Figure 4-2. However, the number of motions required to predict the population mean is reduced. The selection of 4 motions with ASCE and RSPM scaling methodologies appear to be satisfactory for predicting the population mean for this EDP.

The number of analysis that need to be conducted for predicting the mean of the population accurately changes significantly if the maximum of the EDP from the sampled population is used. As given in Figure 4-3, the analyses of the motions with 3 motions is adequate for the 50m monolith if the ground motion selection is conducted using the RSPM methodology. For the 100m monolith, the use of 4 motions is satisfactory for the RSPM, ASCE and MIV methods for the R=1.5

condition. For the other case, the use of 4 motions appears satisfactory for all ground motion scaling techniques. For the 150m motion, the use of 4 motions again yields satisfactory results to predict the mean of the population.

Figure 4-2 The Probability of Sample Mean of Crest Displacement Ratio≤PopulationMeanx0.9 (Black-RSPM, Blue-ASCE, Red-MIV, Green-MPS)
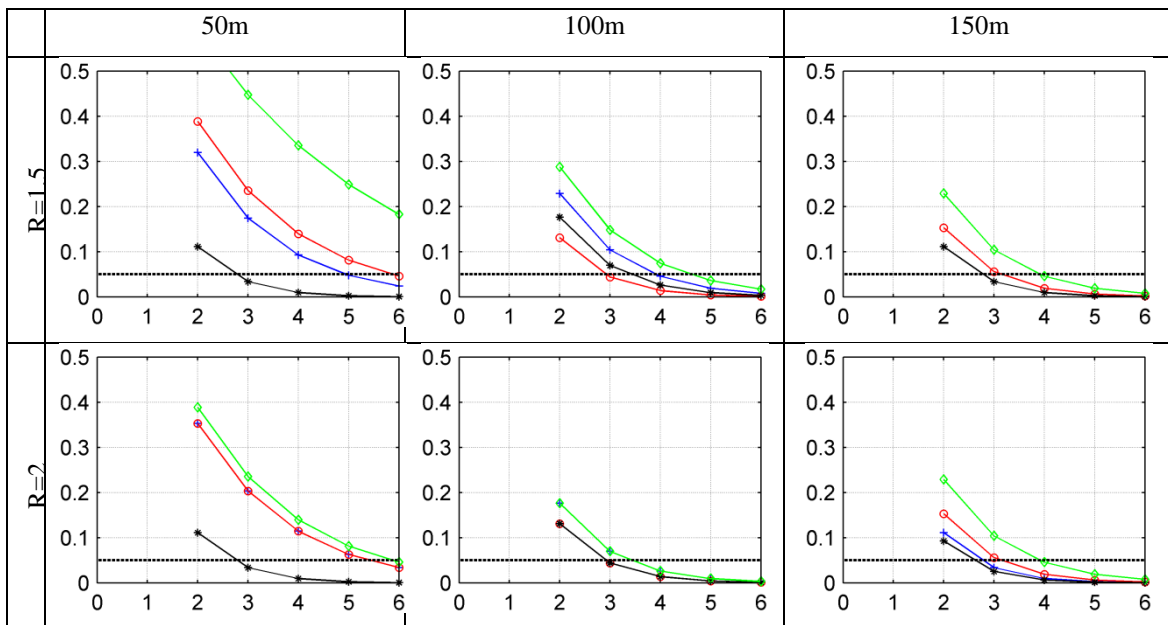
Figure 4-3 Probability of Maximum Cracked Area Ratio of Sample≤PopulationMeanx0.9 (Black-RSPM, Blue-ASCE, Red-MIV, Green-MPS)

	50m	100m	150m
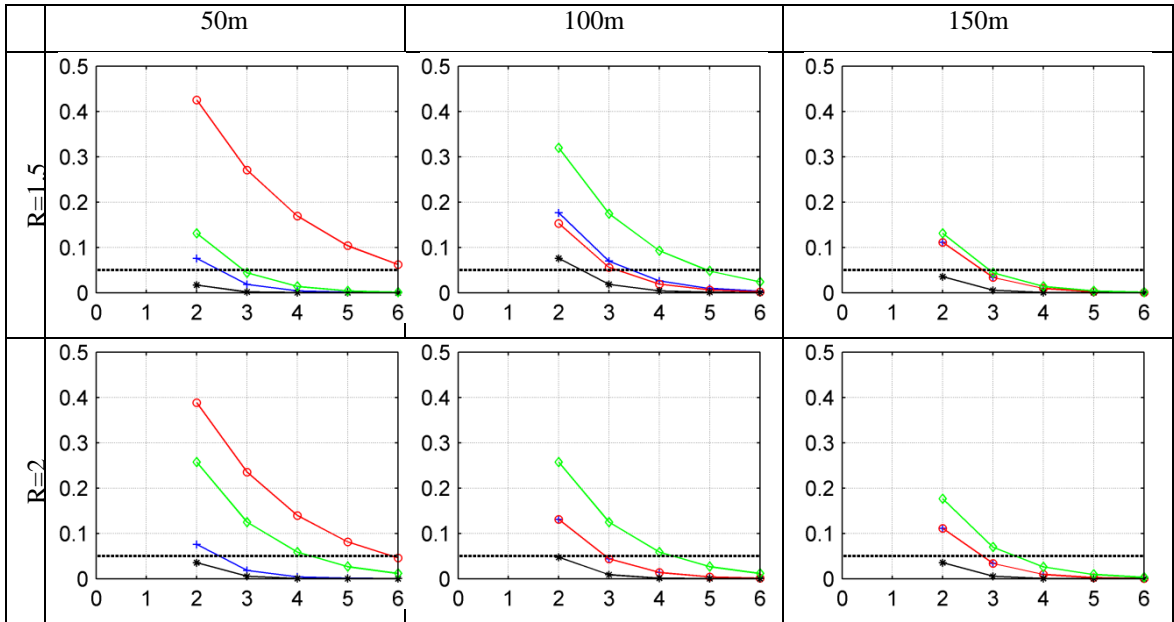
Figure 4-4 The Probability of Maximum Displacement of Sample<=PopulationMeanx0.9 (Black-RSPM, Blue-ASCE, Red-MIV, Green-MPS)

For each of the scaling procedures given above, an independent scaling factor exists for each motion, related to the motion's match to the target spectrum (RSPM), target MIV value (MIV), target displacement value (MPS) and for the target spectrum (ASCE07). However, the ASCE07 methodology also involves a second scaling factor which is used in case the mean of the spectrum for the used time histories falls below the target spectrum. Therefore, a ground motion's scaling factor may depend on the ground motion bin it is chosen from in contrast to the other scaling methods. This factor was ignored for convenience in the computations provided above.

Given the need for different scaling factors for a given ground motion for each selected bin, a further study was conducted on ASCE-07 methodology scaling for 15 randomly selected samples below in order to test the methodology's prediction of the mean response.

4.2   SELECTED ASCE MOTION SETS

For the motion suites obtained by utilizing the scaling procedures (RSPM, MIV and MPS) the effectiveness of selecting different motion sets was analyzed. For this purpose, each possible motion set which consists of 7 different motions was investigated and average values of the EDP's were analyzed for each one of them (6.742.520 different sets for each motion suite). For these motions, being in different

motion sets would not alter the results obtained because of the scaling procedure. However, for ASCE, the scaling procedure usually forces the analyst to utilize different scaling factors for a unique motion present in different motion sets. It is due to the fact that in ASCE-07, after scaling of motions to a pre-determined target spectrum, it is required that the minimums of the obtained spectrum must be compared to the target spectrum once more and a new scale factor (SF_2) is defined to cover the maximum difference between the average and target spectra. In this thesis, SF_2 was equal to one since the mean values of the scaled motions were not smaller than the geometric means of the unscaled motions (Target Spectrum) for any period. It is obviously possible to select motion sets having lower mean than the target spectrum for some periods and consequently having SF_2 higher than one. In view of the fact that selection of a given set for ASCE method can change the pre-scaled ground motions, to conduct this analysis for this method, millions of new structural analyses may be required. For this reason, 15 different sets of motions were randomly selected for ASCE method in order to verify the efficacy of the ASCE scaling methodology,. Ten of the selected fifteen sets had SF_2 greater than one while for the remaining five sets SF_2 was equal to one. Therefore, the structural nonlinear analyses were re-performed for the first 10 sets corresponding to analyses for a total 70 different motions (for the 100 m Model having R=1.5).

The selected motion sets are given in Table 4-1. The results obtained for these motion sets are given in Figure 4-5. along with the mean from the benchmark results and the mean of the ASCE scaling results for the 35 ground motions. Most of the sets produced results close to the mean values of the whole motion suite analyses. It can also be seen in these results that only two sets fell below the 90 % of the mean results for cracked areas and maximum displacement which provides a crosscheck for Figure 4-1. Similar to the results from Figure 4-1, if seven motions were used in a set, there is approximately 10 % chance of falling below the population mean (for the 100 m Model having R=1.5). The scale factor SF2 did not appear to have a significant effect on the mean for the randomly selected 15 ground motion sets.

Table 4-1 Selected Motion Sets for ASCE

Set 1	Motion #5	Motion #6	Motion #19	Motion #25	Motion #26	Motion #30	Motion #33
Set 2	Motion #5	Motion #16	Motion #18	Motion #23	Motion #26	Motion #29	Motion #30
Set 3	Motion #14	Motion #15	Motion #20	Motion #23	Motion #26	Motion #31	Motion #34
Set 4	Motion #10	Motion #15	Motion #20	Motion #25	Motion #26	Motion #28	Motion #35
Set 5	Motion #4	Motion #15	Motion #19	Motion #23	Motion #24	Motion #29	Motion #30
Set 6	Motion #4	Motion #16	Motion #18	Motion #23	Motion #26	Motion #30	Motion #35
Set 7	Motion #6	Motion #10	Motion #20	Motion #23	Motion #25	Motion #31	Motion #32
Set 8	Motion #11	Motion #15	Motion #20	Motion #25	Motion #26	Motion #33	Motion #35
Set 9	Motion #3	Motion #7	Motion #17	Motion #22	Motion #25	Motion #33	Motion #34
Set 10	Motion #1	Motion #2	Motion #18	Motion #21	Motion #25	Motion #30	Motion #31
Set 11	Motion #7	Motion #9	Motion #19	Motion #25	Motion #26	Motion #28	Motion #32
Set 12	Motion #12	Motion #14	Motion #18	Motion #21	Motion #23	Motion #27	Motion #31
Set 13	Motion #3	Motion #16	Motion #19	Motion #22	Motion #23	Motion #28	Motion #29
Set 14	Motion #4	Motion #5	Motion #17	Motion #24	Motion #26	Motion #28	Motion #29
Set 15	Motion #2	Motion #16	Motion #19	Motion #21	Motion #23	Motion #29	Motion #34
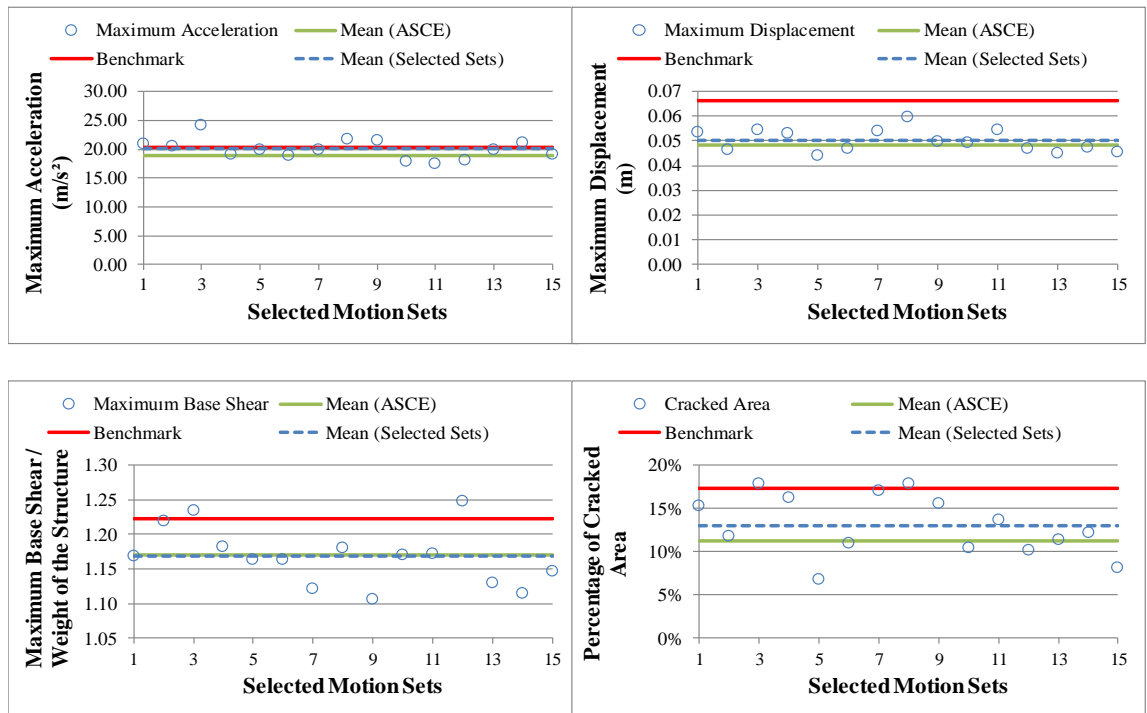
Figure 4-5 Motion Set Results (ASCE)

CHAPTER 5

CONCLUSION AND OUTLOOK

5.1 CONCLUSION

In this study, the use of four different ground motion scaling methods (RSPM, ASCE 07, MIV, MPS) for the nonlinear dynamic structural analyses of dams were investigated using a range of concrete gravity dam models and a set of acceleration time histories. A ground motion suite comprised near field ground motions were used in the analyses. The set of 35 motions, used in many other studies (Kurama and Farrow, 2003; O'Donnell et al., 2013), is comprised of a set of carefully selected motions with near field properties. These motions were scaled by using four different scaling methods in order to conduct the nonlinear transient analysis of the gravity dam models.

Six different computer models were generated for the analyses and each scaled motion was used for the incremental dynamic analyses of each model. In total, 1050 non-linear structural analyses were conducted for 6 models and 35 motions, 4 different scaling methods and one original motion suite. The models were investigated for damage development and crack patterns occurring on the structures as well as the maximum base shear, displacement and acceleration.

Analyses of the results indicate two counter trends. The MPS and MIV scaling yielded very close estimates to the mean of the benchmark set while the RSPM and ASCE methods underestimated the mean values. On the other hand, the dispersion on the results for the RSPM and ASCE scaling was significantly lower than their counterparts obtained from MIV and MPS scaling. Since the target earthquake spectrum for ASCE and RSPM methods were defined for the geometric mean of the

original motion suite rather than the arithmetic mean, it was also expected that the results of these methods to be a bit lower than the original motions in most of the cases. The higher dispersion produced by the MIV and the MPS scaling indicate a larger number of analyses are required in order to estimate the response quantities with acceptable confidence levels using these methods compared to the RSPM and ASCE techniques.

5.2 OUTLOOK

Based on the findings of this study, some possible avenues of future research are given below.

- ❖ The efficacy of the ground motion scaling methods should also be investigated for different target earthquake spectra given the effect of the performance level on the dispersion quantities.
- ❖ In this study, a total number of 1050 analyses were conducted to assess the effectiveness of ground motion scaling methods. This amount of non-linear dynamic analyses requires at least three months of run-time by using a decent computer. In order to compare different scaling methods for practical uses, a statistical method can be developed to reduce the amount of the analyses and the run-time.
- ❖ Scaling factors were obtained unreasonably high for some cases which were also reflected in the predicted performance of the dam systems. Further studies on limiting the scaling factors based on expected performance are required in order to reduce the dispersion in the resulting EDP's.

REFERENCES

Abrahamson, N. A. (1992). Non-stationary spectral matching. *Seismological research letters, Vol. 63,* pp. 30.

Alavi, B. & Krawinkler, H. (2000). Consideration of near-fault ground motion effects in seismic design. *12th World Conference on Earthquake Engineering.*

Alavi, B. & Krawinkler, H. (2004). Behavior of moment-resisting frame structures subjected to near-fault ground motions. *Earthquake Engineering and Structural Dynamics, Vol.33,* pp. 687-706.

Alembagheri, M. & Ghaemian, M. (2012). Seismic Assessment of Concrete Gravity Dams Using Capacity Estimation and Damage Indexes. *Earthquake Engineering and Structural Dynamics, Vol. 42*, pp. 123-144.

Ali, M. H., Alam, M. R., Haque, M. N. & Alam, M. J. (2012). Comparison of Design and Analysis of Concrete Gravity Dam. *Natural Resources, Vol. 3,* pp. 18-28.

Araujo, J. M. & Awruch, A. M. (1998). Probabilistic Finite Element Analysis of Concrete Gravity Dams. *Advances in Engineering Software, Vol. 29*, pp. 97-104.

ASCE - American Society of Civil Engineers (2010). Minimum Design Loads for Buildings and Other Structures, ASCE/SEI 7-10,.

Asteris, P. G. & Tzamtzis, A. D. (2003). Nonlinear Seismic Response Analysis of Realistic Gravity Dam-Reservoir Systems. *International Journal of Nonlinear Sciences and Numerical Simulation, Vol. 4*, pp. 329-338.

ATC - Applied Technology Council (2011). Seismic Performance Assessment of Buildings, ATC-58-1.

Bahar, O., M. Shahrouzi, and M. Sazjini (2012) "Seismic Responses of RC Frames under Wavelet-Based Matched Accelerograms and Real Records." *Proceedings of the 15th World Conference on Earthquake Engineering,* Lizbon

Baker, J. (2007). Quantitative classification of near-fault ground motions using wavelet analysis. *Bulletin of the Seismological Society of America, Vol. 97*, pp. 1486–1501.

Baker, J. W. & Cornell, C. A. (2006). Which spectral acceleration are you using. *Earthquake Spectra, Vol. 22*, pp. 293–312.

Bhattacharjee, S. S. & Leger, P. (1992). Concrete Constitutive Models for Nonlinear Seismic Analysis of Gravity Dams State of the Art. *Canadian Journal of Civil Engineering, Vol. 19*, pp. 492-509.

Bazant, Z. (1996). Is No-Tension Design of Concrete or Rock Structures Always Safe? –Fracture Analysis. *Journal of Structural Engineering, Vol. 122*, pp. 2-10.

Bazzurro, P. (1998). Probabilistic Seismic Demand Analysis: *Ph.D. thesis, Dept. Of Civil and Env. Eng., Stanford University, California*

Beyer, K. & Bommer, J. J. (2007). Selection and Scaling of Real Accelerograms for Bi-Directional Loading: A Review of Current Practice and Code Provisions. *Journal of Earthquake Engineering, Vol. 11,* pp. 13-45.

Bommer, J. J. & Acevedo, A. B. (2004). The Use of Real Earthquake Accelerograms as Input to Dynamic Analysis. *Journal of Earthquake Engineering, Vol. 8,* pp. 43-91.

Bommer, J. J., Scott, S. G. & Sarma, S. K. (2000). Hazard-consistent earthquake scenarios. *Soil Dynamics and Earthquake Engineering, Vol. 19*, pp.219–231.

Bray, J. & Rodriguez-Marek, A. (2004). Characterization of forward-directivity ground motions in the nearfault region. *Soil Dynamics and Earthquake Engineering, Vol. 24,* pp. 815–828.

Calayir, Y. & Karaton, M. (2005). Seismic Fracture Analysis of Concrete Gravity Dams Including Dam-Reservoir Interaction. *Computers and Structures, Vol. 83*, pp. 1595-1606.

Cervera, M., Oliver, J. & Faria, R. (1995). Seismic Evaluation of Concrete Dams via Continuum Damage Models. *Earthquake Engineering and Structural Dynamics, Vol. 24*, pp. 1225-1245.

Chopra, A. & Chintapakdee, C. (2004). Seismic response of vertically irregular frames: response history and modal pushover analyses. *Journal of Structural Engineering*, pp.1177-1185, 130:8.

DBYBHY (2007). Deprem Bölgelerinde Yapılacak Binalar Hakkında Yönetmelik. *Official Gazette, 3 May, Issue 26454.*

Espandar, R., Lotfi, V. & Razaqpur, G. (2003). Influence of Effective Parameters of Non-Orthogonal Smeared Crack Approach in Seismic Response of Concrete Arch Dams. *Canadian Journal of Civil Engineering, Vol. 30*, pp. 890-901.

Fahjan, Y. M. (2008). Selection and Scaling of Real Earthquake Accelerograms to Fit the Turkish Design Spectra. *Teknik Dergi, Vol: 19,* pp. 4423-4444.

Fu, Q. & Menun, C. (2004). Seismic-environment-based simulation of near-fault ground motions. *13th World Conference on Earthquake Engineering.*

Ghaemian, M. & Ghobarah, A. (1999). Nonlinear Response of Concrete Dams with Dam-Reservoir Interaction. *Journal of Engineering Structures, Vol. 21*, pp. 306-315.

Guanglun, W., Pekau, O. A., Chuhan, Z., & Shaomin, W. (2000). Seismic Fracture Analysis of Concrete Gravity Dams Based on Nonlinear Fracture Mechanics. *Engineering Fracture Mechanics*, *Vol. 65*, pp. 67-87.

Haselton, C. B. (2009). Evaluation of Ground Motion Selection and Modification Methods: Predicting Median Interstory Drift Response of Buildings, *PEER Report 2009/01,*

ICC - International Code Council (2006). International Building Code.

Iervolino, I. & Cornell, C. A. (2005). Record selection for nonlinear seismic analysis of structures. *Earthquake Spectra, Vol. 21*, pp. 685-713.

Kalkan, E. & Chopra, A. (2010). Practical Guidelines to Select and Scale Earthquake Records for Nonlinear Response History Analysis of Structures, *US Geological Survey Open-File Report, 2010, 1068.2010: 126.*

Kalkan, E. & Chopra, A. (2011). Modal-Pushover based Ground Motion Scaling Procedure. *Journal of Structural Engineering, Vol. 137*, pp. 298:310

Kappos, A. J. & Kyriakakis, P. (2000). A re-evaluation of scaling techniques for natural records. *Soil Dynamics & Earthquake Engineering, Vol. 20*, pp. 111-123.

Kennedy, R. P., Short, S. A., Merz, K. L., Tokarz, F. J., Idriss, I. M., Power, M. S., & Sadigh, K. (1984). Engineering characterization of ground motion-task 1: Effects of characteristics of free-field motion on structural response, Structural Mechanics Associates, Inc., Newport Beach, CA (USA).

Kumar, R. & Nayak, G. C. (1994). Numerical Modeling of Tensile Crack Propagation in Concrete Dams. *Journal of Structural Engineering, Vol. 120*, pp. 1053-1074.

Kurama, Y. & Farrow, K. (2003). Ground motion scaling methods for different site conditions and structure characteristics. *Earthquake Engineering and Structural Dynamics, Vol. 32*, pp. 2425-2450.

Lee, J. & Fenves, G. L. (1998). A Plastic-Damage Concrete Model for Earthquake Analysis of Dams. *Earthquake Engineering and Structural Dynamics, Vol. 27*, pp. 937-956.

Leger, P. & Bhattacharjee, S. S. (1995). Seismic Fracture Analysis of Concrete Gravity Dams. *Canadian Journal of Civil Engineering, Vol. 22*, pp. 196-201.

Lilhanand, K. & Tseng, W. S. (1988). Development and application of realistic earthquake time histories compatible with multiple-damping design spectra. *Ninth World Conference on Earthquake Engineering, Vol. 2,* pp. 7-8.

Malhotra, P. K. (2003). Strong-motion records for site specific analysis. *Earthquake Spectra, Vol. 19,* pp. 557- 578.

Martinez-Rueda, J. E. (1998). Scaling procedure for natural accelerograms based on a system of spectrum intensity scales. *Earthquake Spectra, Vol.14*, pp. 135-152.

Mavroeidis, G. & Papageorgiou, A. (2003). A mathematical representation of near-fault ground motions. *Bulletin of the Seismological Society of America, Vol. 93,* p. 1099–1131.

Mehanny, S. (1999). Modeling and assessment of seismic performance of composite frames with reinforced concrete columns and steel beams,: *Ph.D. thesis, Dept. of Civil and Env. Eng., Stanford University, California.*

Miranda, E. (1993). Evaluation of site-dependent inelastic seismic design spectra. *Journal of Structural Engineering, Vol.119*, pp. 1319-1338.

Naeim, F., Alimoradi, A. & Pezeshk, S. (2004). Selection and scaling of ground motion time histories for structural design using genetic algorithms. *Earthquake Spectra, Vol. 20*, pp. 413-426.

Naeim, F. & Kelly, J. M. (1999). Design of Seismic Isolated Structures: From Theory to Practice. : *John Wiley & Sons*.

Nau, J. & Hall, W. (1984). Scaling methods for earthquake response spectra. *SCE Journal of Structural Engineering, Vol. 110*, pp. 91-109.

NEHRP Consultants Joint Venture (2011). Selecting and Scaling Earthquake Ground Motions for Performing Response-History Analyses, *Technical Reports of National Institute of Standards and Technology*, NIST GCR 11-917-15.

Nikolaou, A. S. (1998). A GIS Platform for Earthquake Risk Analysis, *Ph.D. Dissertation, State University of New York at Buffalo, New York.*

Nuss, L.K., Matsumoto, N, Hansen, K.D (2012) "Shaken, But Not Stirred - Earthquake Performance of Concrete Dams", *United States Society on Dams*.

O'Donnell, A. P., Beltsar, O. A., Kurama, Y. C., Kalkan, E., & Taflanidis, A. A. (2011). Evaluation of ground motion scaling methods for analysis of structural systems. *ASCE Structures Congress.*

O'Donnell, A., Kurama, Y., Kalkan, E. & Taflanidis, A. (2013). Experimental evaluation of ground motion scaling methods for nonlinear analysis of structural systems. *ASCE Structures Congress, Bridging Your Passion with Your Profession*, pp. 2180-2191.

Özdemir, Z. & Fahjan, Y. M. (2007). Comparison of time and frequency domain scaling of real accelerograms to match earthquake design spectra, *6th National Conference on Earthquake Engineering.*

PEER (1998). PEER NGA database. [Online] Available at: http://peer.berkeley.edu/peer_ground_motion_database [Accessed 17 December 2013].

Plizzari, G. A. (1997). LEFM Applications to Concrete Gravity Dams. *Journal of Structural Engineering, Vol. 123*, pp. 808-815.

Rashid, Y. R. (1968). Analysis of Prestressed Concrete Pressure Vessels. *Nuclear Engineering and Design, Vol. 7*, pp. 334-344.

Reiter, L. (1990) Earthquake Hazard Analysis: Issues and Insights. *Columbia University Press.*

Reyes, J.C. & Kalkan, E. (2012). How many records should be used in an ASCE/SEI-7 ground motion scaling procedure? *Earthquake Spectra, Vol. 28* , pp. 1223-1242.

Rots, J. G. Computational Modeling of Concrete Fracture. Ph.D. Dissertation, Delft University of Technology, Delft, 1988.

Rots J.G., Nauta P., Kusters G.M.A., Blaauwendraad J. (1985), Smeared crack approach and fracture localization in concrete, *HERON*, Vol. 30(1), pp. 1-48

Shahi, S. K. & Baker, J. W. (2011). An empirically calibrated framework for including the effects of near-fault directivity in probabilistic seismic hazard analysis. *Bulletin of the Seismological Society of America*, Vol.101, pp. 742–755.

Shome, N. & Cornell, A. C. (1998). Normalization and scaling accelerograms for nonlinear structural analysis. *Earthquake Engineering Research Institute, 6th U.S. National Conference on Earthquake Engineering.*

Shome, N. & Cornell, C. (1999). Probabilistic seismic demand analysis of nonlinear structures, *Department of Civil and Environmental Engineering, Stanford University, Reliability of Marine Structures Program Report No. RMS-35.*

Shome, N., Cornell, C. A., Bazzurro, P. & J. E. Carballo (1998). Earthquakes, records and nonlinear responses, *Earthquake Spectra, Vol. 14,* pp. 469-500.

Somerville, P., Collins, N., Graves, R. & Pitarka, A. (2004). An engineering ground motion model of basin generated surface waves, *13th World Conference on Earthquake Engineering.*

Stewart, J. P., Chiou, S. J., Bray, J. D., Graves, R. W., Somerville, P. G., & Abrahamson, N. A. (2001). Ground Motion Evaluation Procedures for Performance-Based Design, *Soil dynamics and earthquake engineering, Vol. 22,* pp. 765-772.

TNO DIANA (2010). *User's Manual*, R. 9.4.3,

US Army Corps of Engineers. (1995). *Seismic Design Provisions for Roller Compacted Concrete Dams.* Washington, D. C: Engineering and Design, EP 110-2-12.

Valliappan, S., Yazdchi, M. & Khalili, N. (1996). Earthquake Analysis of Gravity Dams Based on Damage Mechanics Concept. *International Journal for Numerical and Analytical Methods in Geomechanics, Vol. 20*, pp. 725-752.

Vidic, T., Fajfar, P. & Fischinger, M. (1994). Consistent inelastic design spectra: strength and displacement, *Earthquake Engineering & Structural Dynamics, Vol. 23*, pp. 507-521.

Watson-Lamprey, J. & Abrahamson, N. (2006). Selection of Ground Motion Time Series and Limits on Scaling, *Soil Dynamics and Earthquake Engineering, Vol. 26,* pp. 477-482.

Westergaard, H. M., (1933) Water Pressures on Dams during Earthquakes. *American Society of Civil Engineers, Vol. 98,* pp. 418-433.

Yamaguchi, Y., Sasaki, T., Iwashita, T., Sasaki, S., & Kurahashi, H. (2008). *Evaluation of Tensile Cracks in Concrete Gravity Dams by Shaking Table Tests and Non-linear FEM Analyses with Smeared Crack Model.*

Youngs, R., Power, M., Wang, G., Makdisi, F., & Chin, C. C. (2007). Design ground motion library (DGML) – tool for selecting time history records for specific engineering applications, *SMIP07 Seminar on Utilization of Strong-Motion Data*, pp. 109-110

APPENDICES
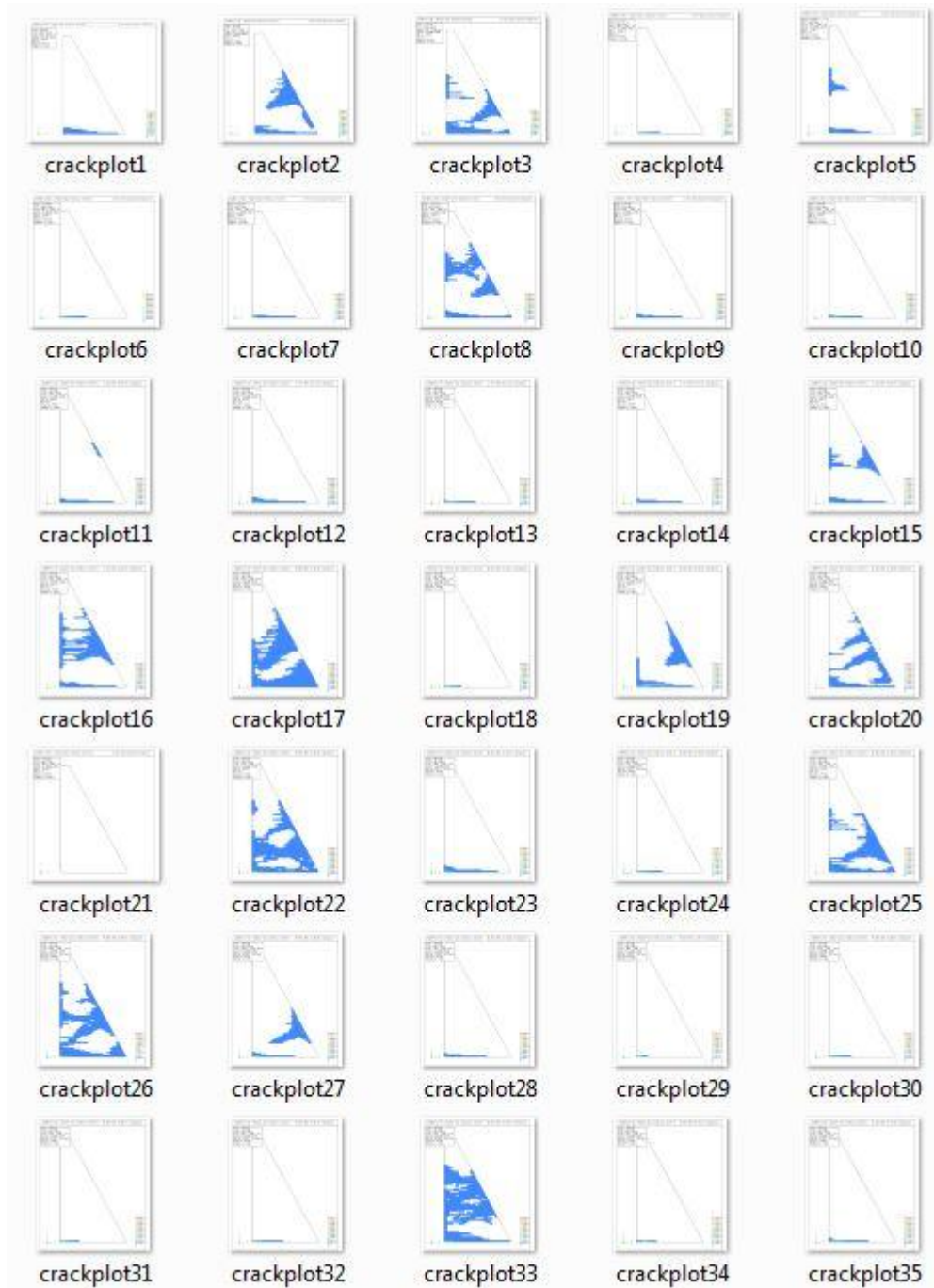
Figure A-1 Cracked Area Plots for Unscaled Analyses (h=50m , R=2)

crackplot1 crackplot2 crackplot3 crackplot4 crackplot5

crackplot6 crackplot7 crackplot8 crackplot9 crackplot10

crackplot11 crackplot12 crackplot13 crackplot14 crackplot15

crackplot16 crackplot17 crackplot18 crackplot19 crackplot20

crackplot21 crackplot22 crackplot23 crackplot24 crackplot25

crackplot26 crackplot27 crackplot28 crackplot29 crackplot30

crackplot31 crackplot32 crackplot33 crackplot34 crackplot35

Figure A-2 Cracked Area Plots for Unscaled Analyses (h=50m , R=1.5)
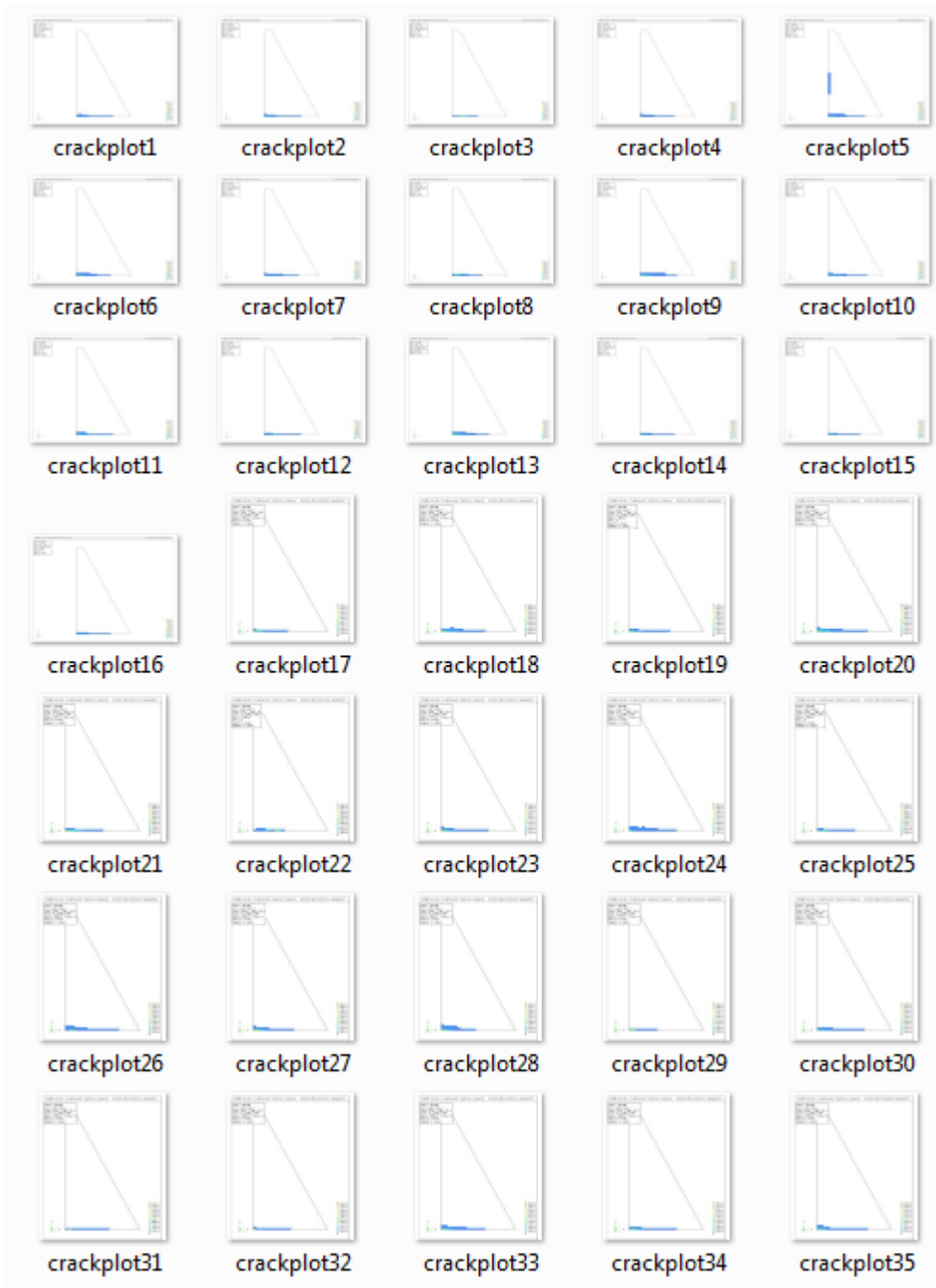
Figure A-3 Cracked Area Plots for RSPM Analyses (h=50m , R=2)
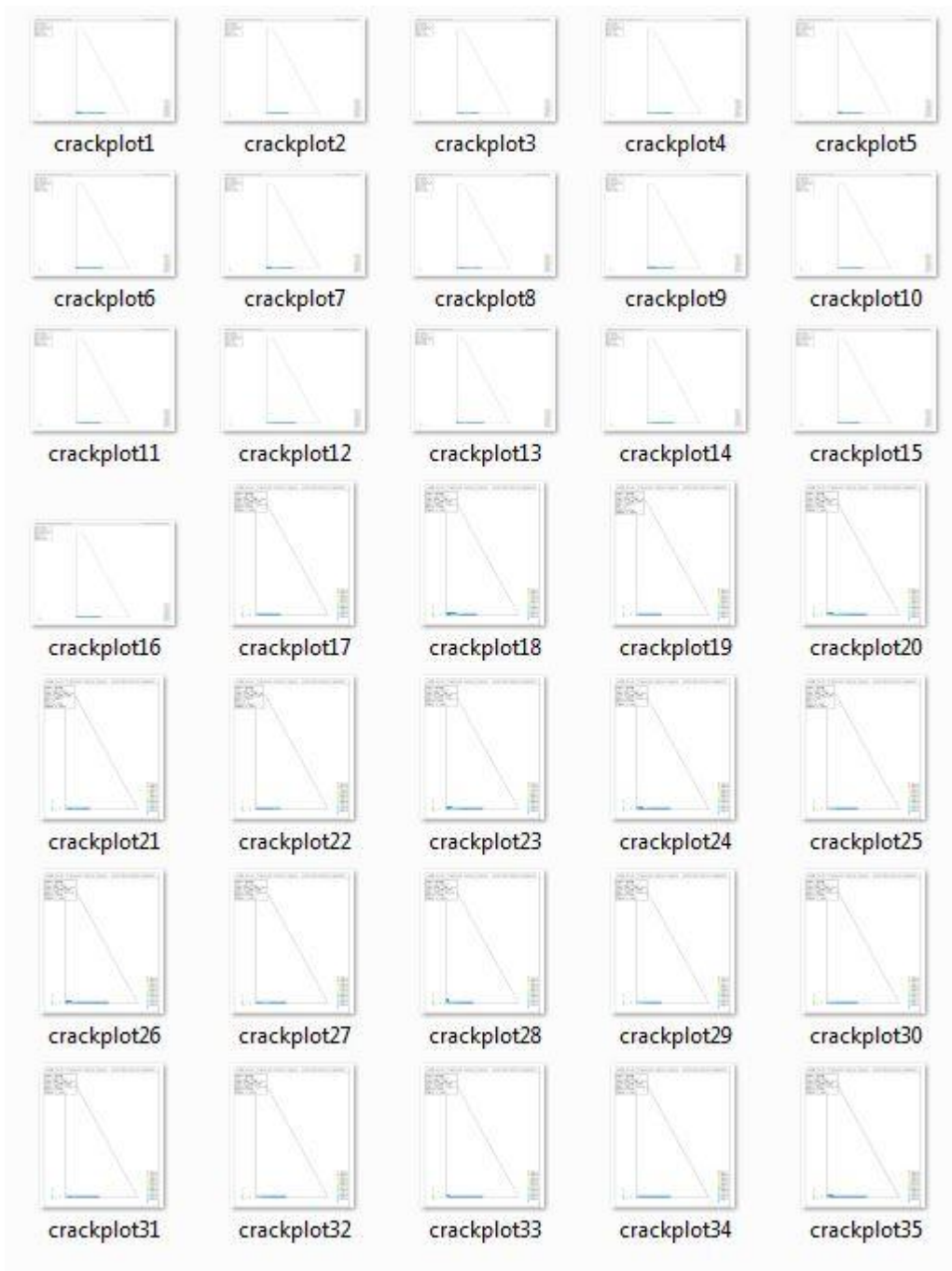
Figure A-4 Cracked Area Plots for RSPM Analyses (h=50m , R=1.5)
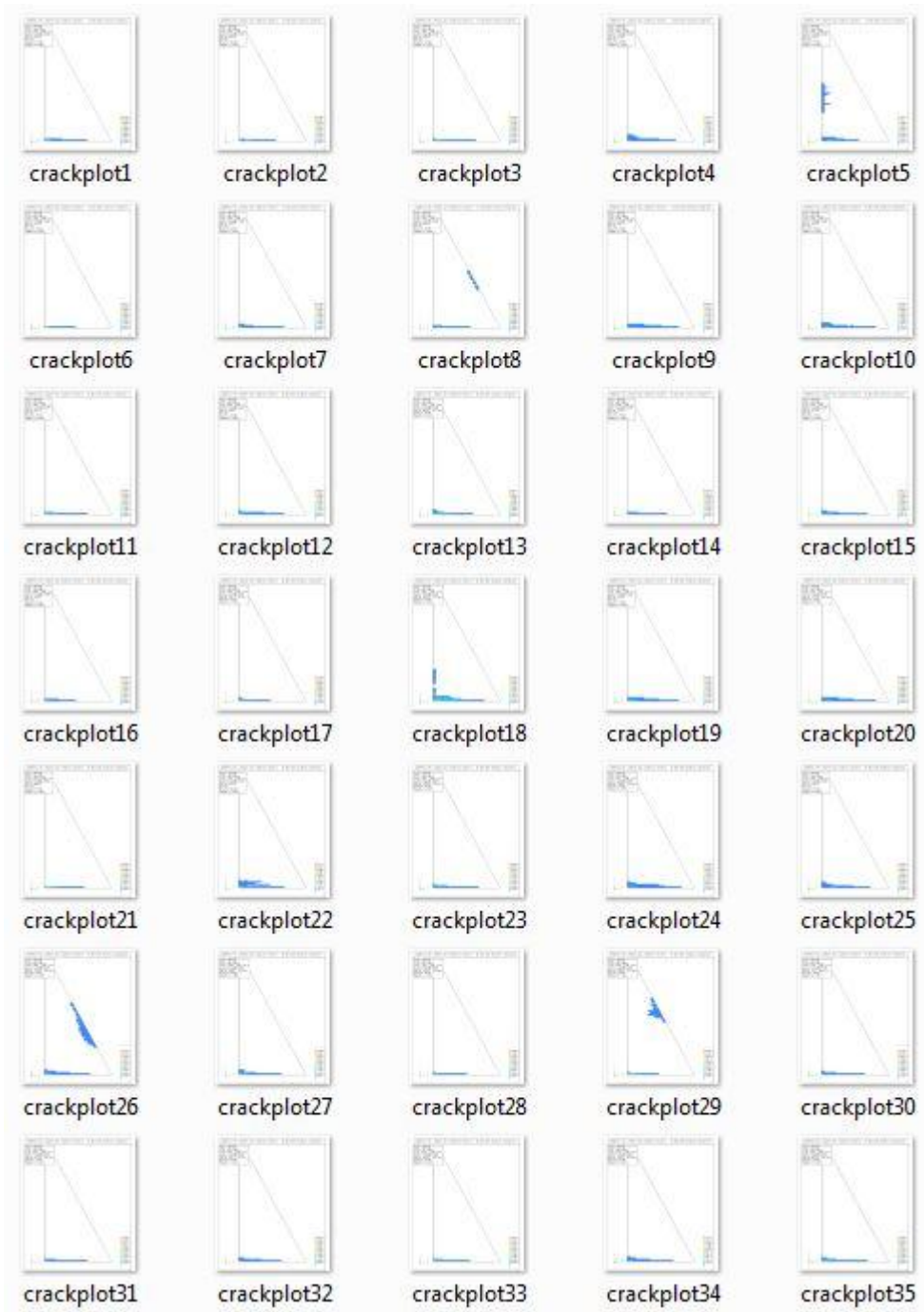
Figure A-5 Cracked Area Plots for ASCE Analyses (h=50m , R=2)
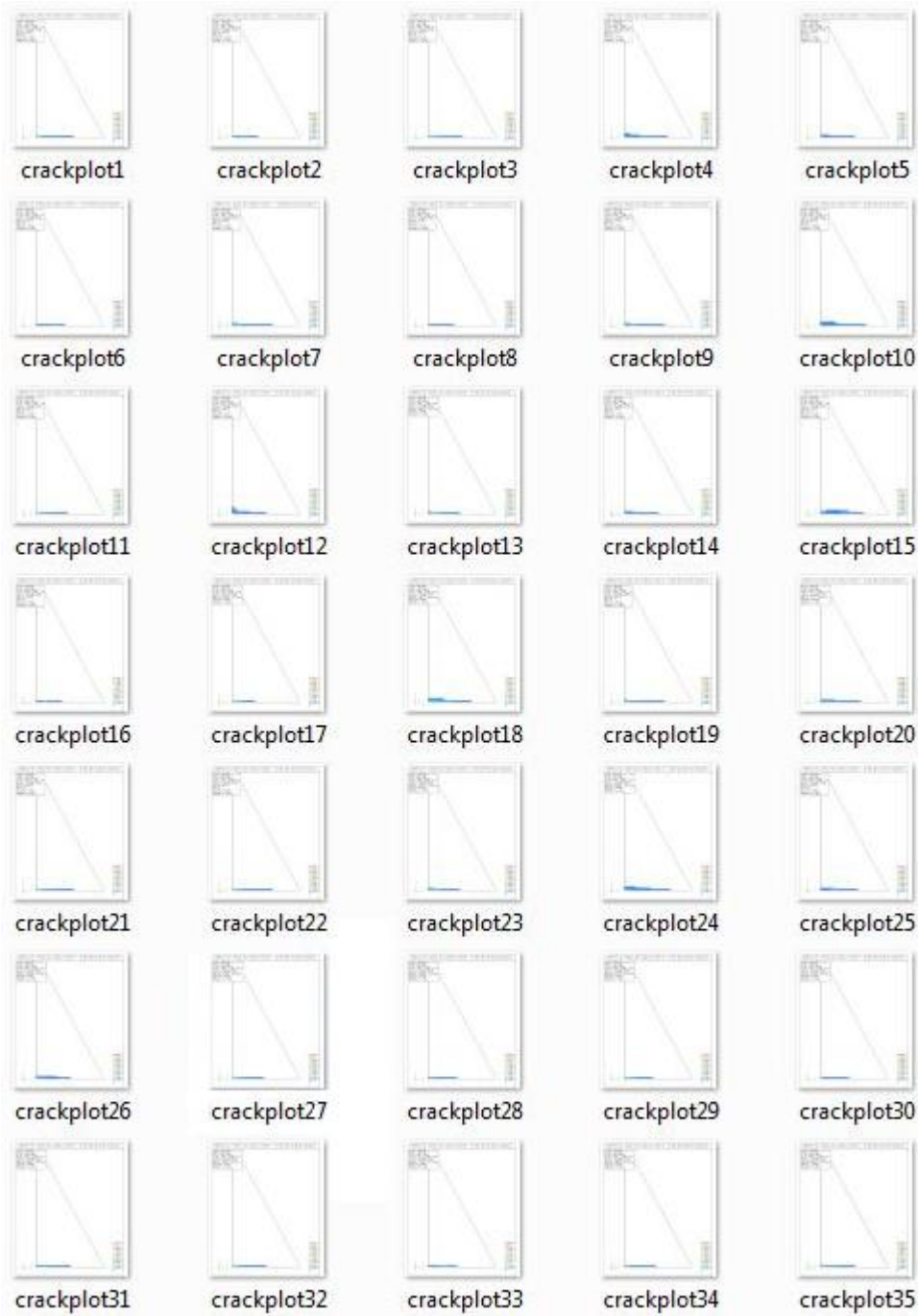
Figure A-6 Cracked Area Plots for ASCE Analyses (h=50m , R=1.5)

100
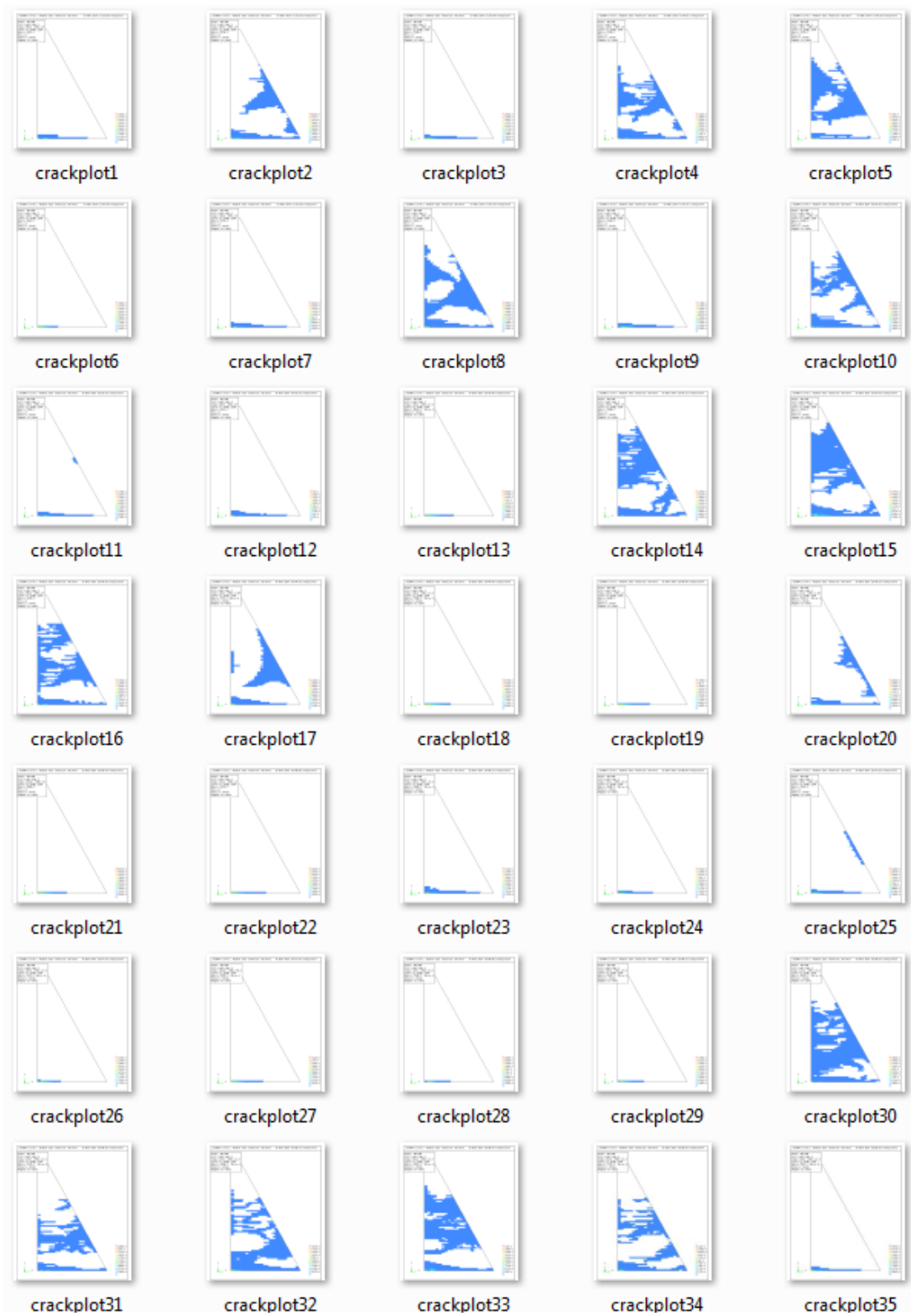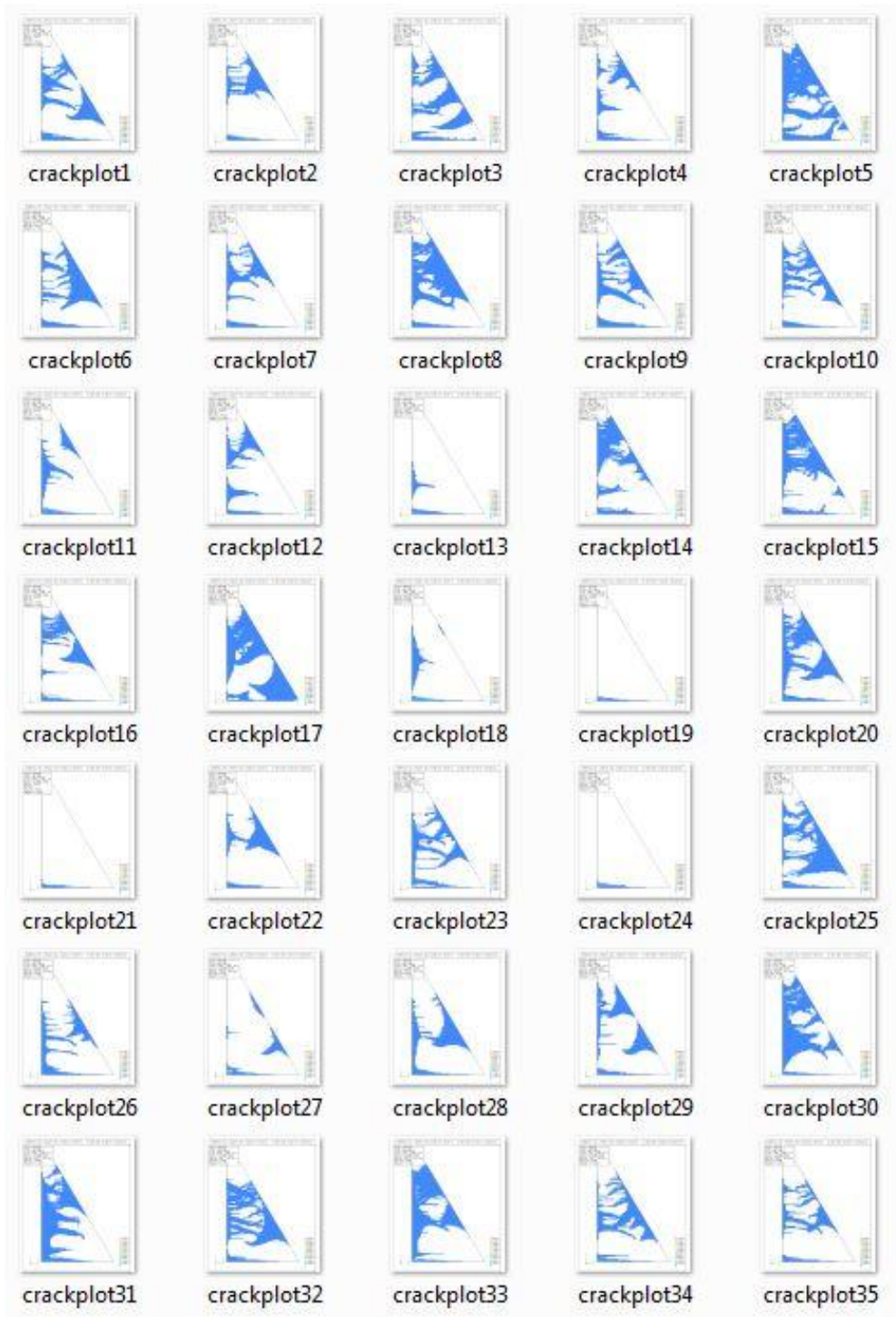
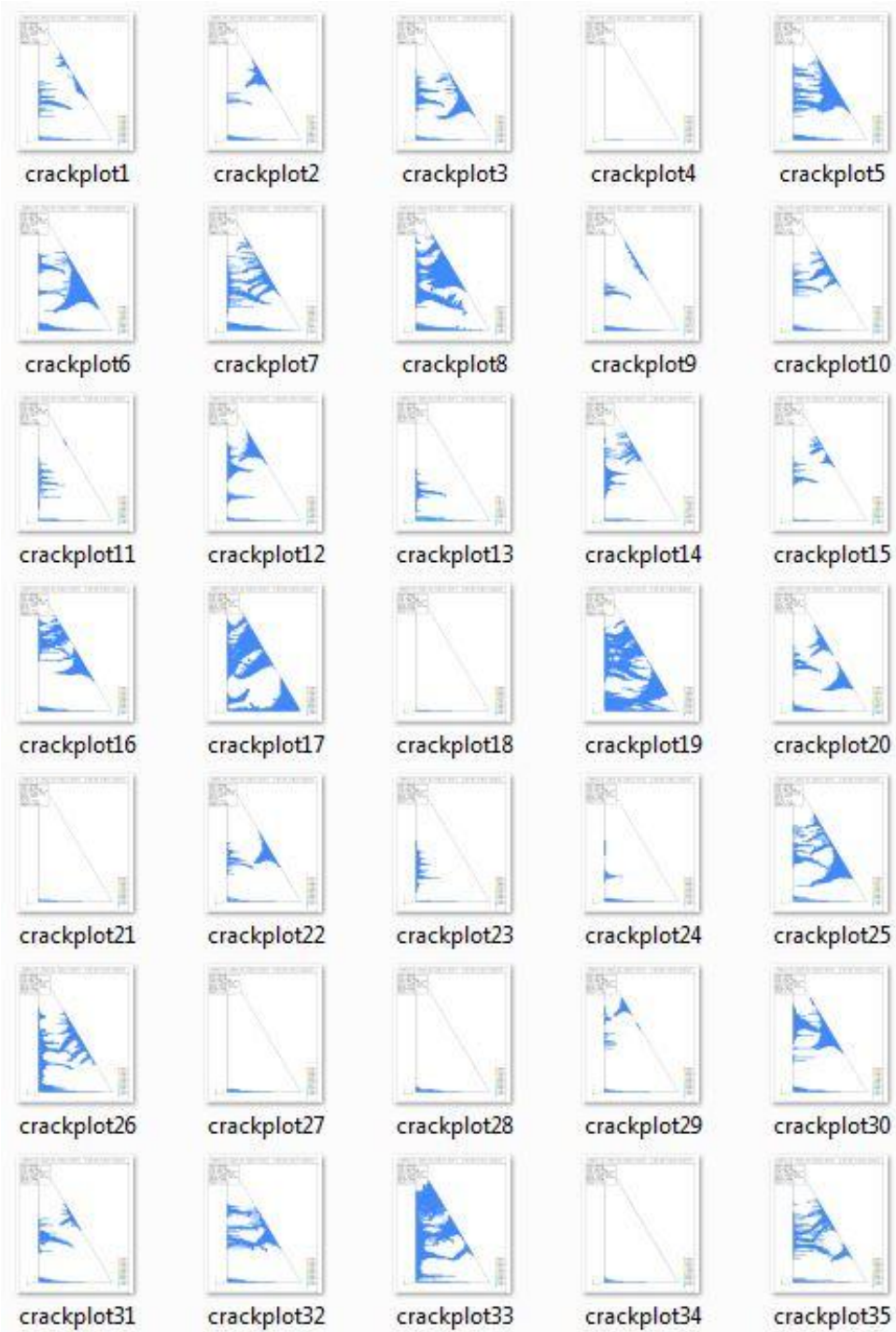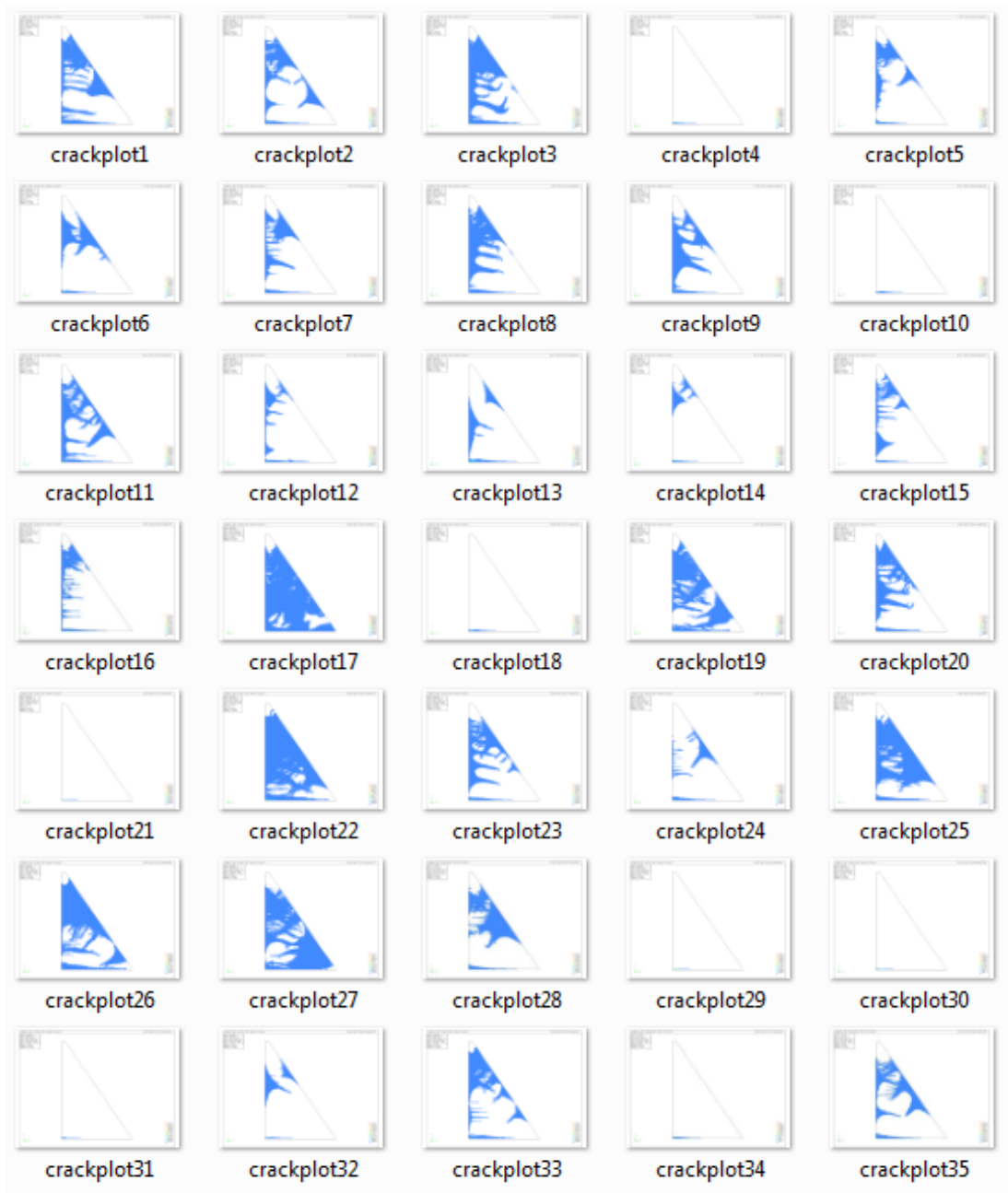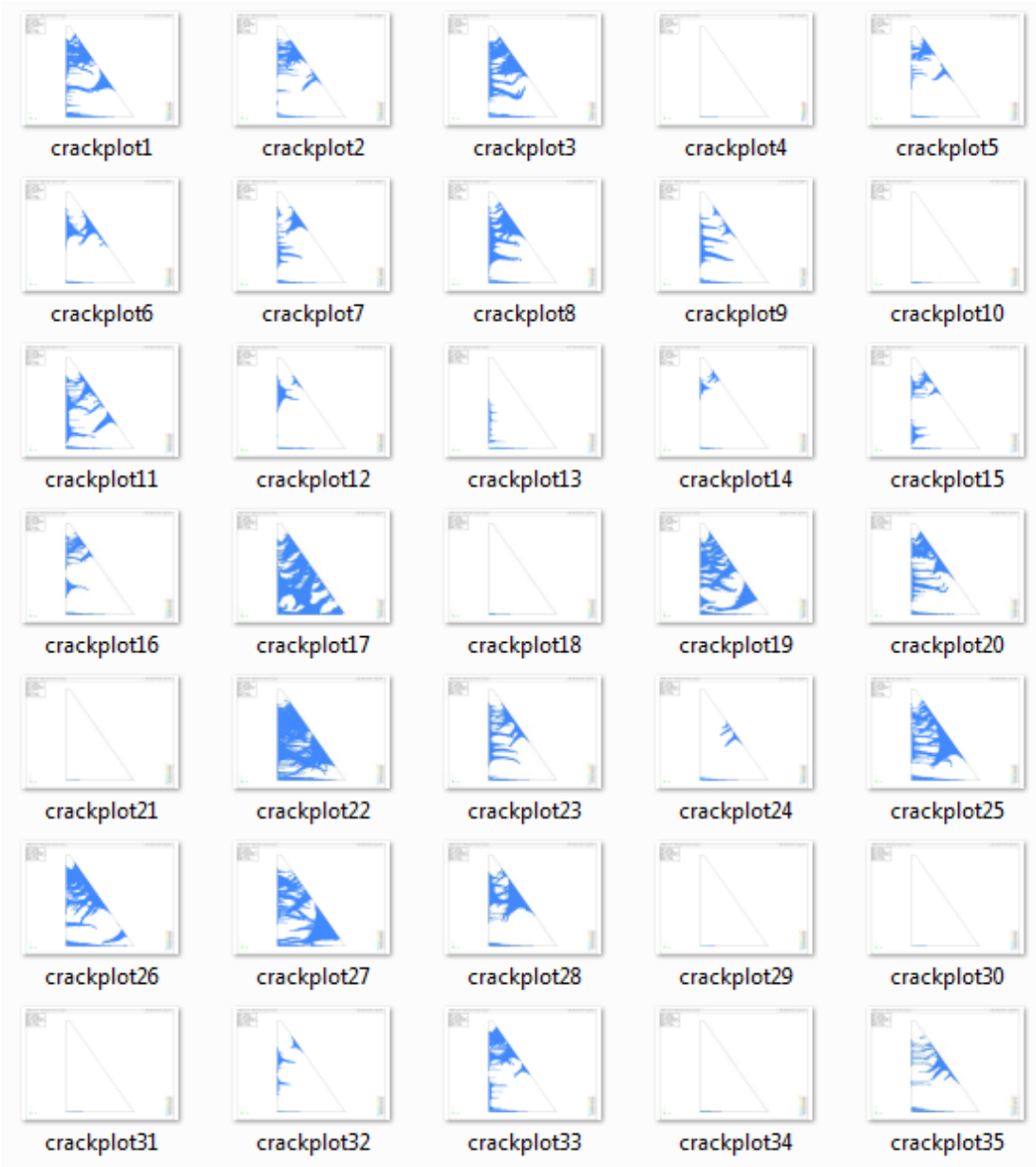**Figure A-7 Cracked Area Plots for MIV Analyses (h=50m , R=2)**

crackplot1   crackplot2   crackplot3   crackplot4   crackplot5

crackplot6   crackplot7   crackplot8   crackplot9   crackplot10

crackplot11   crackplot12   crackplot13   crackplot14   crackplot15

crackplot16   crackplot17   crackplot18   crackplot19   crackplot20

crackplot21   crackplot22   crackplot23   crackplot24   crackplot25

crackplot26   crackplot27   crackplot28   crackplot29   crackplot30

crackplot31   crackplot32   crackplot33   crackplot34   crackplot35

Figure A-8 Cracked Area Plots for MIV Analyses (h=50m , R=1.5)
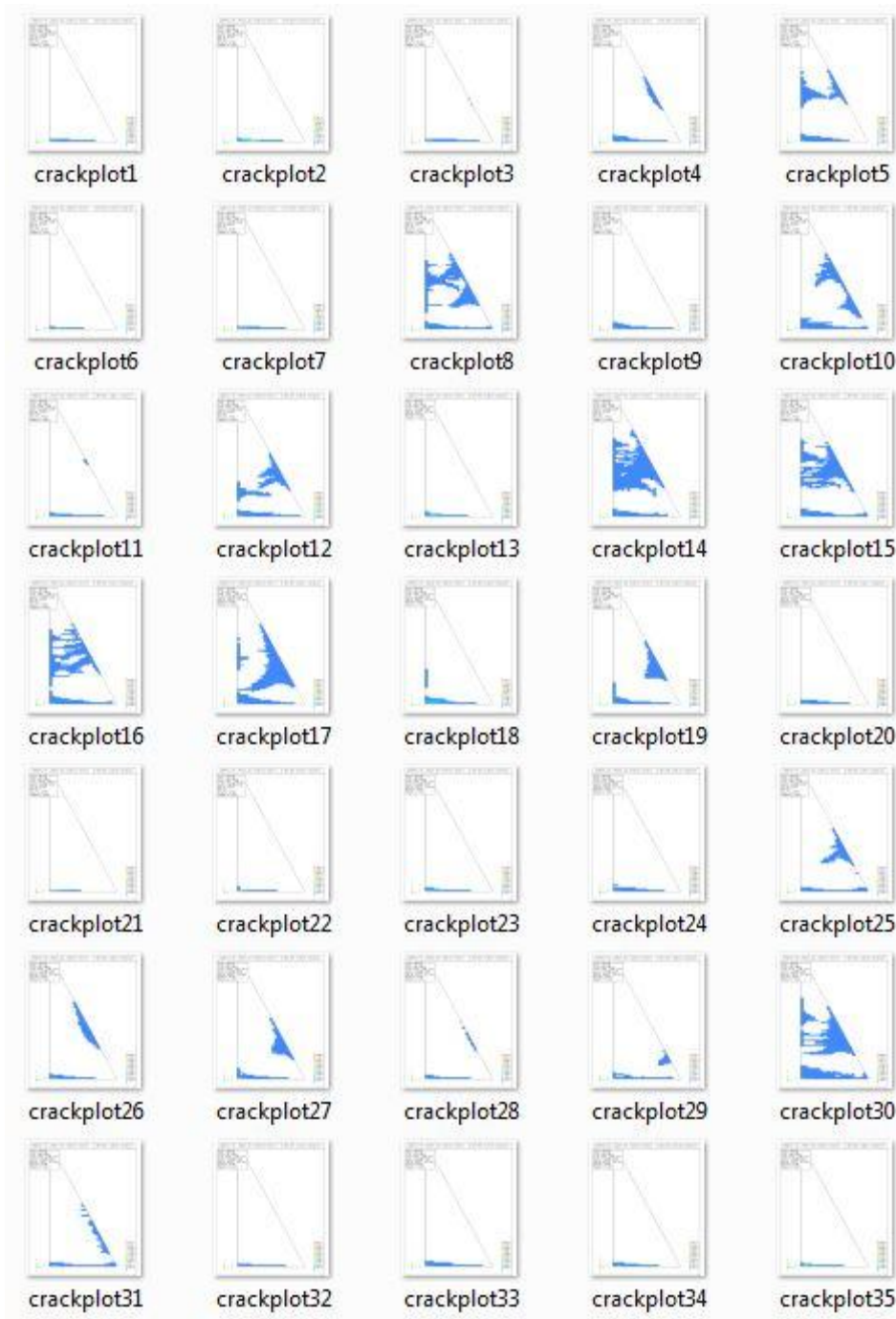
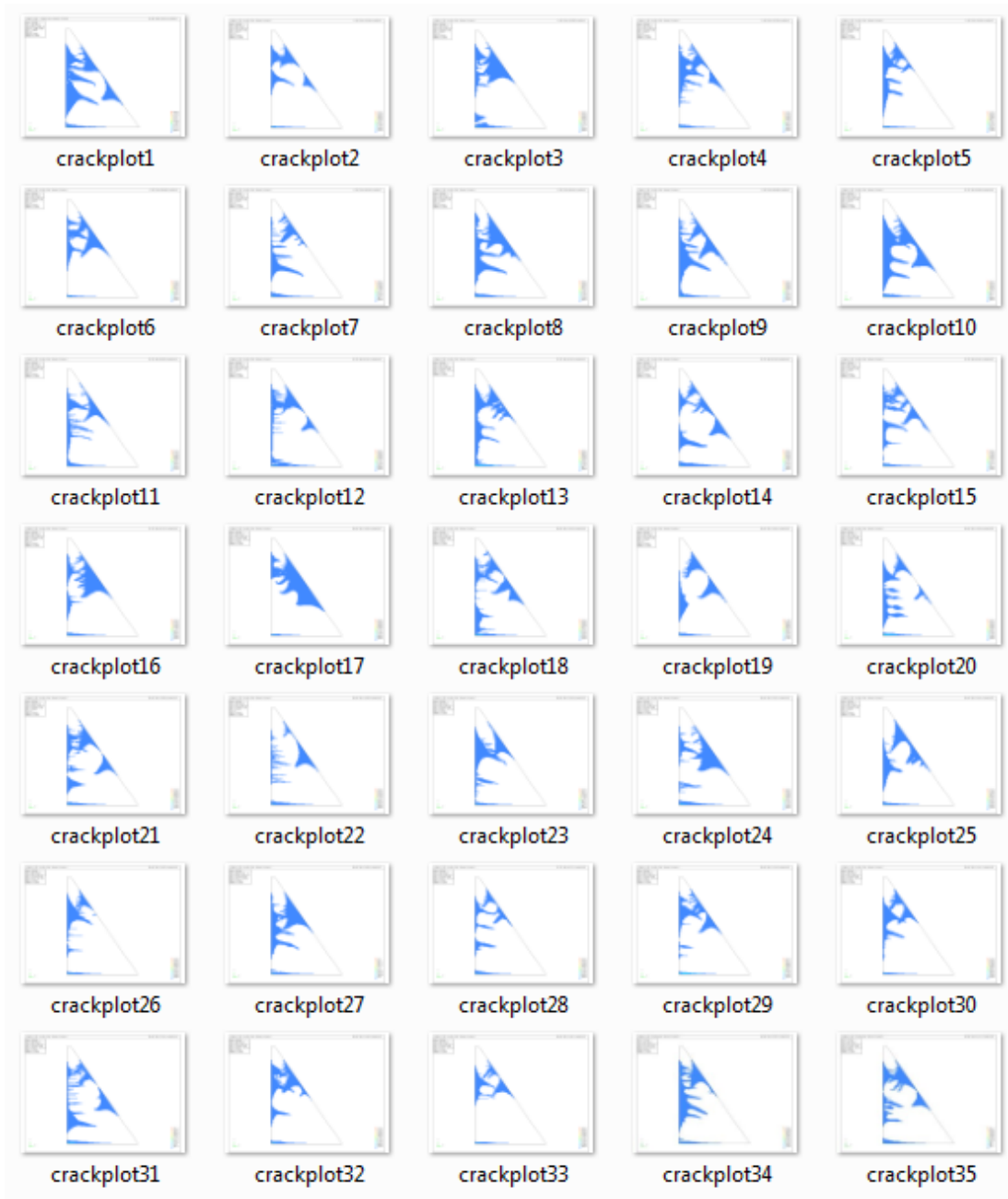**Figure A-9 Cracked Area Plots for MPS Analyses (h=50m , R=2)**
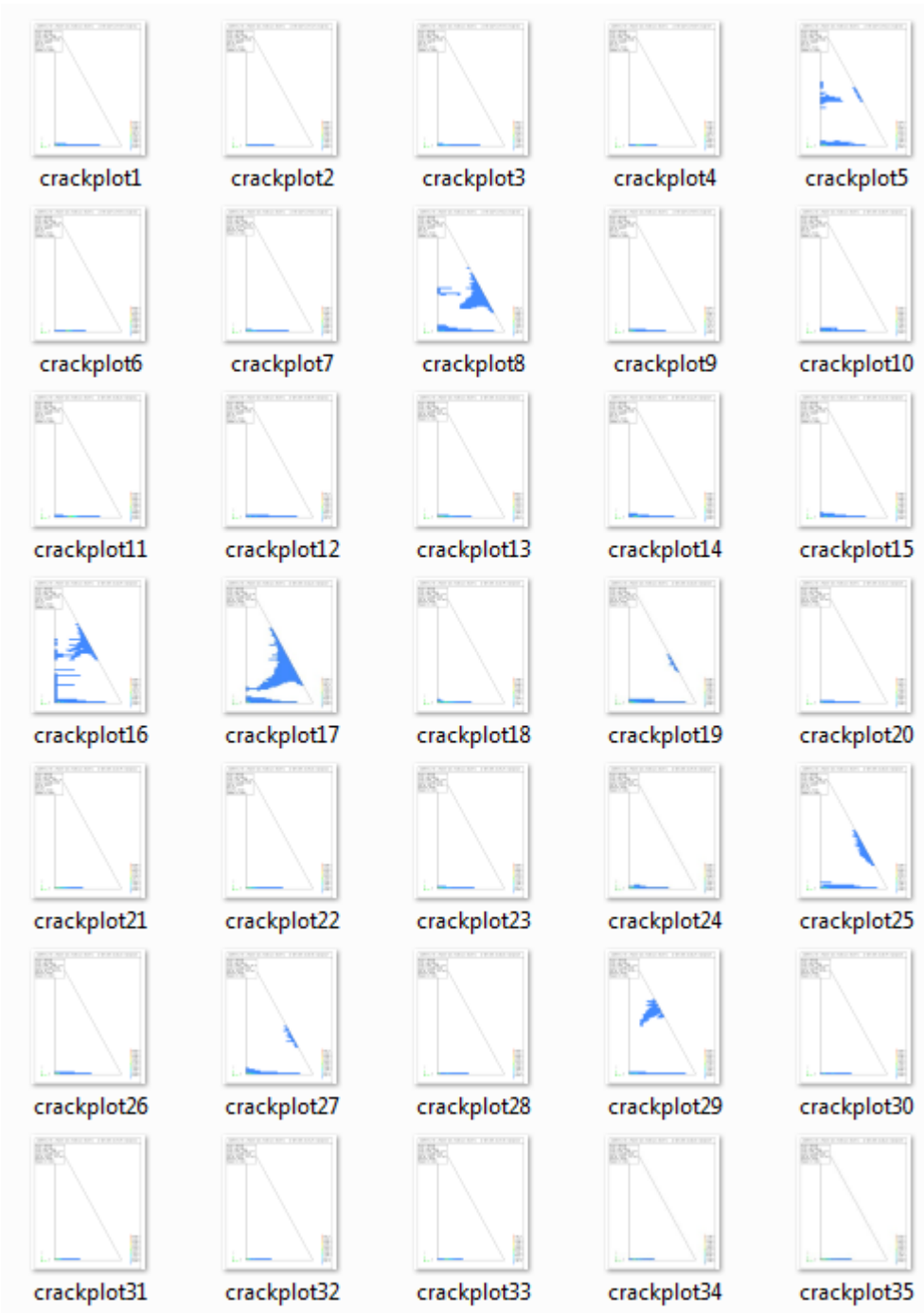
Figure A-10 Cracked Area Plots for MPS Analyses (h=50m , R=1.5)
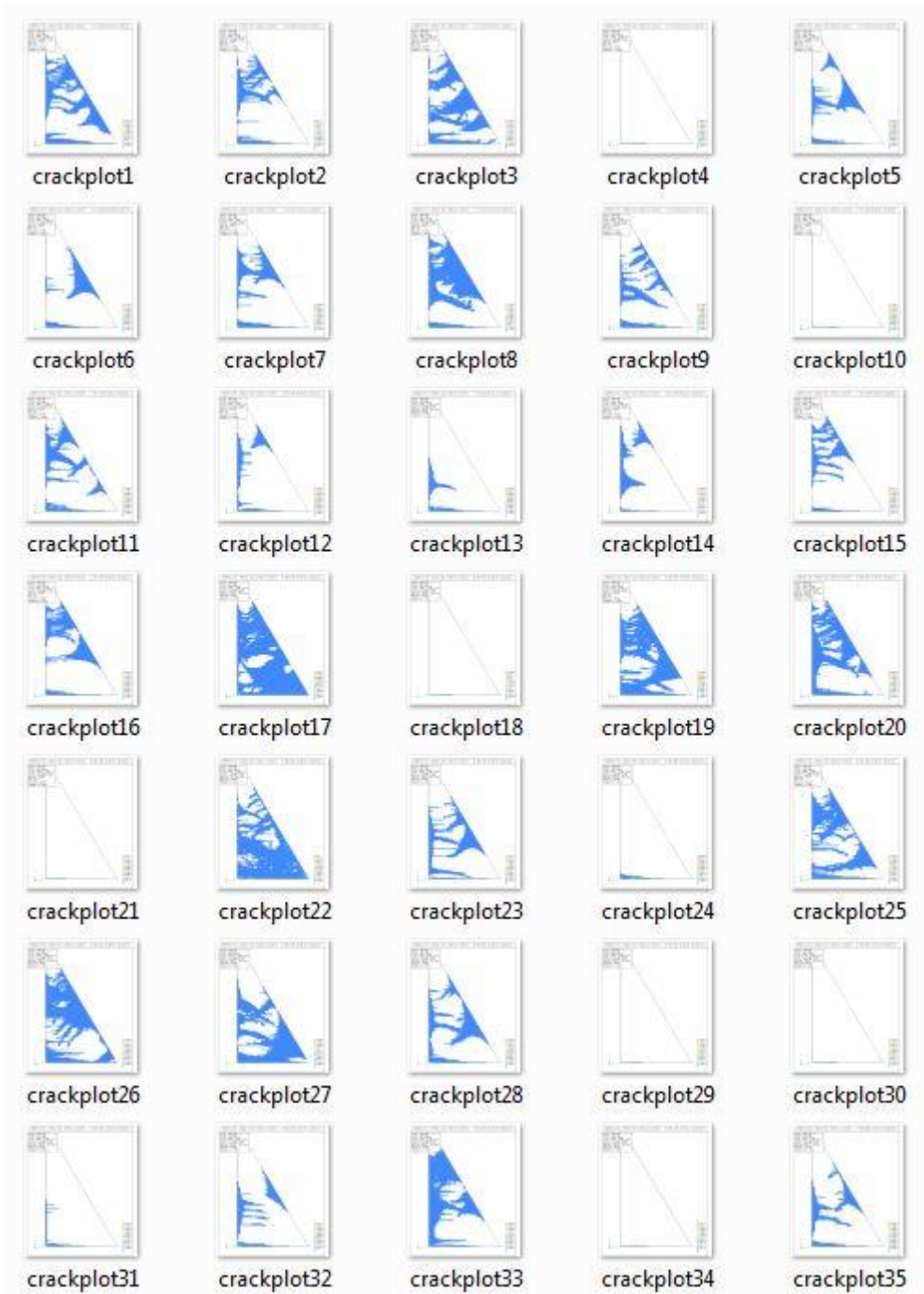
**Figure A-11 Cracked Area Plots for Unscaled Analyses (h=100m , R=2)**
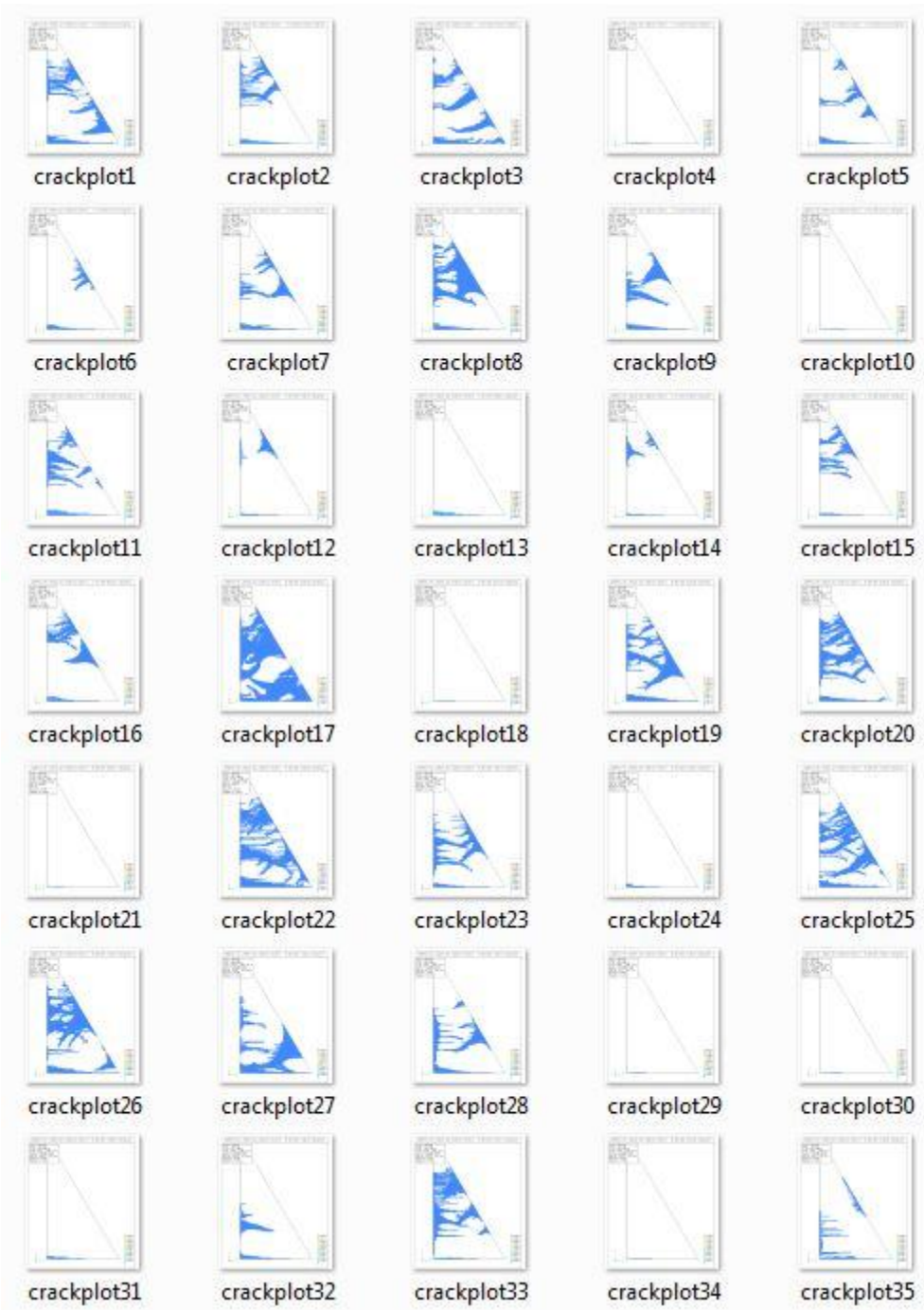
Figure A-12 Cracked Area Plots for Unscaled Analyses (h=100m , R=1.5)
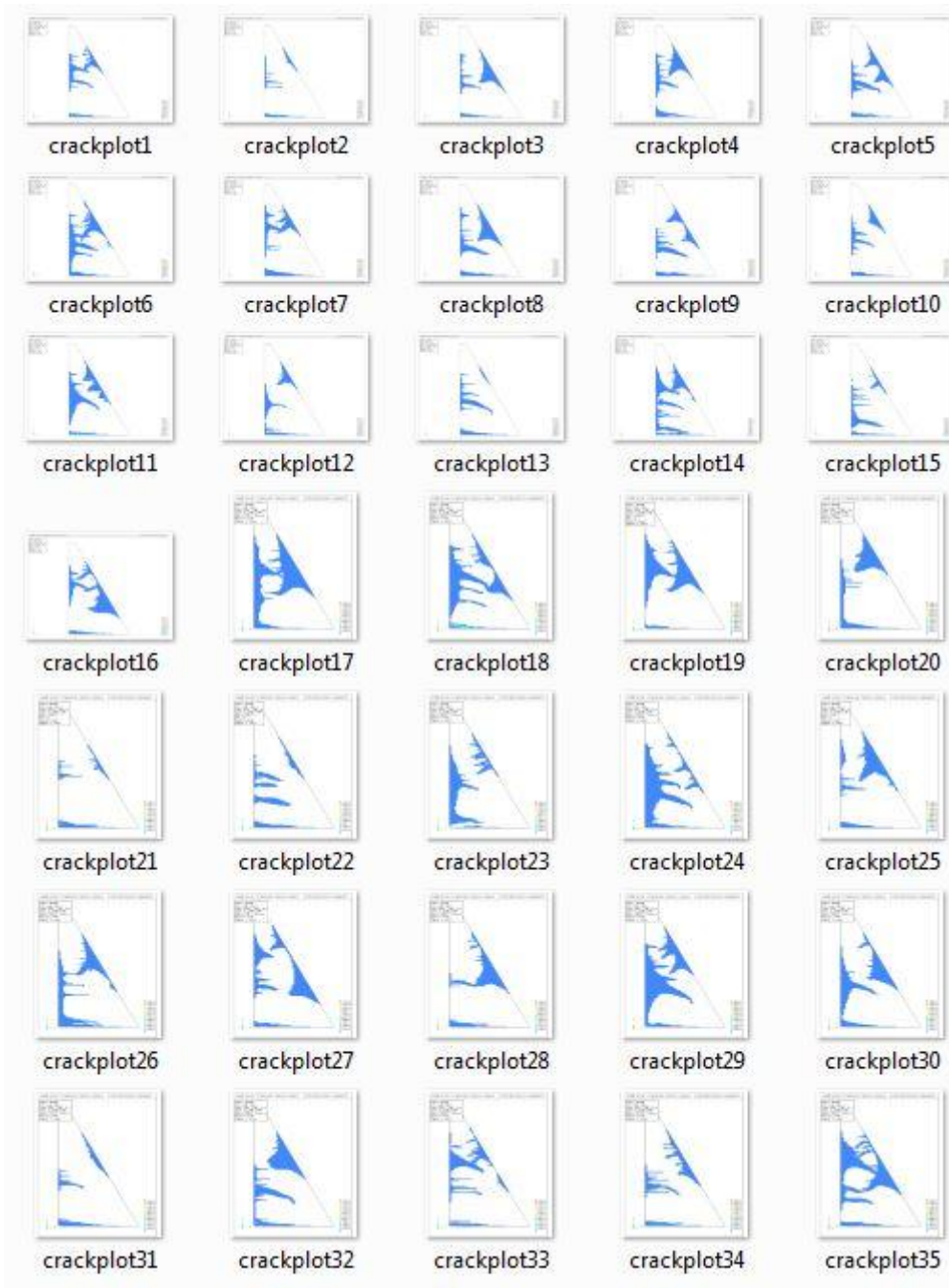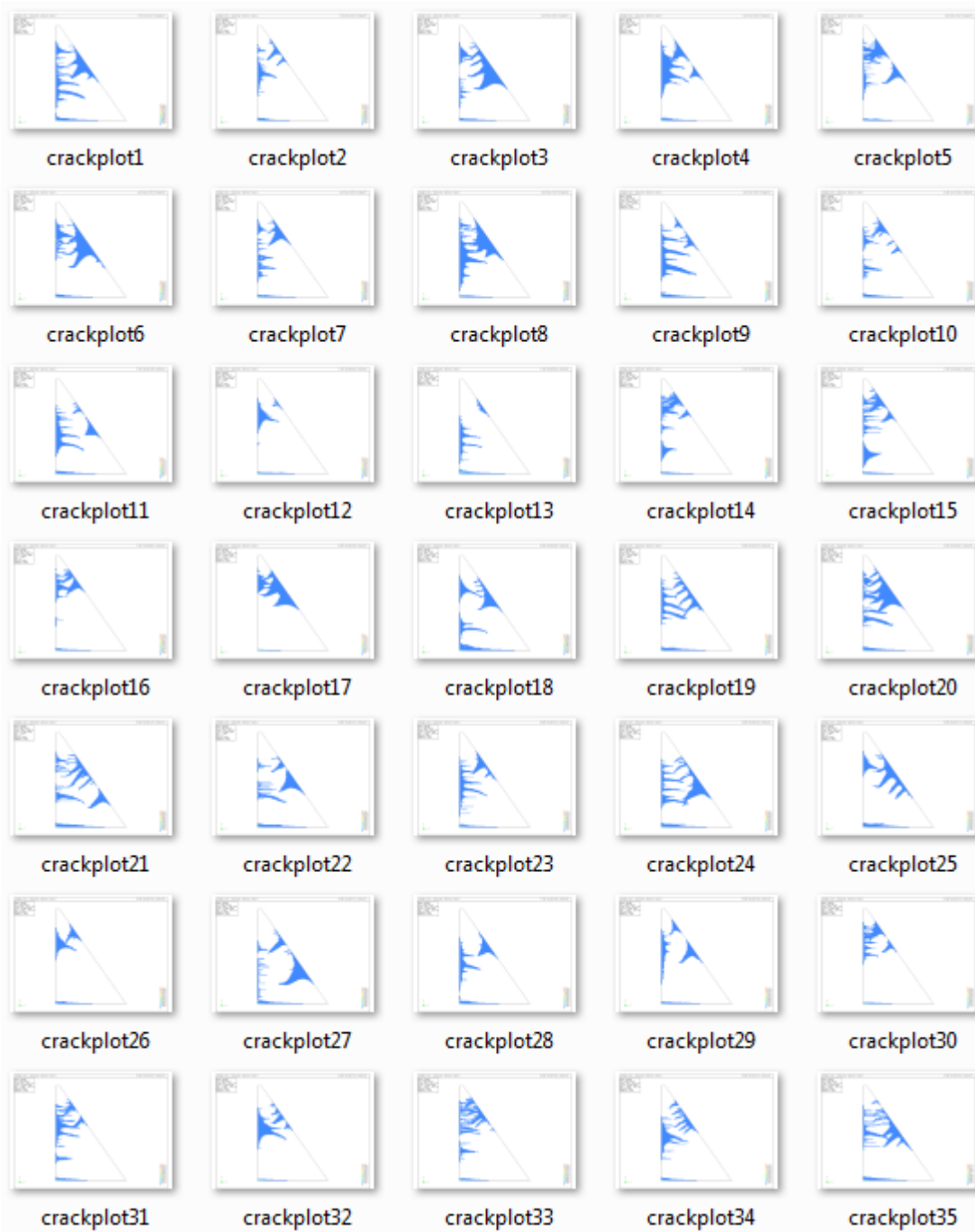
Figure A-13 Cracked Area Plots for RSPM Analyses (h=100m , R=2)
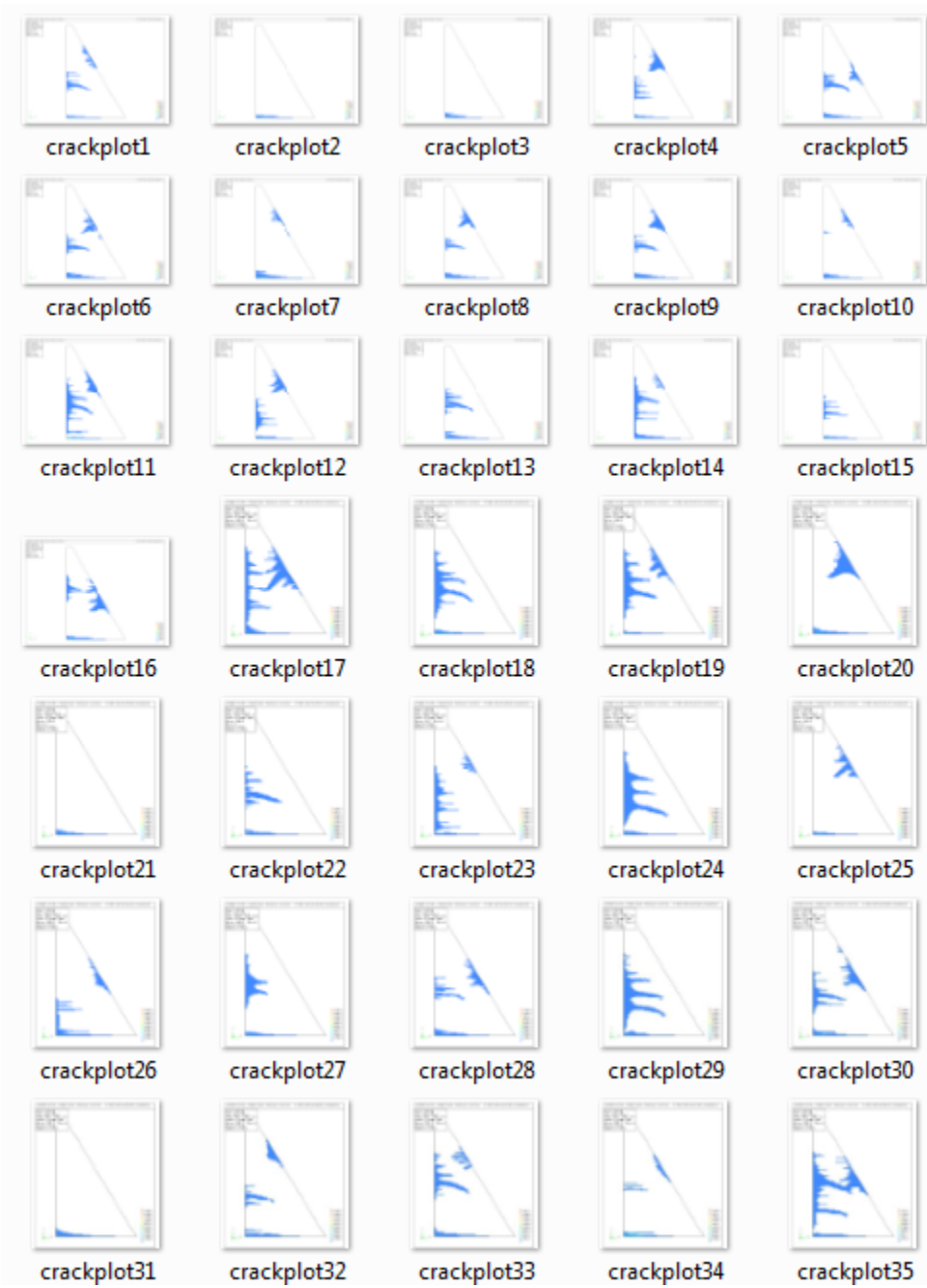
Figure A-14 Cracked Area Plots for RSPM Analyses (h=100m , R=1.5)
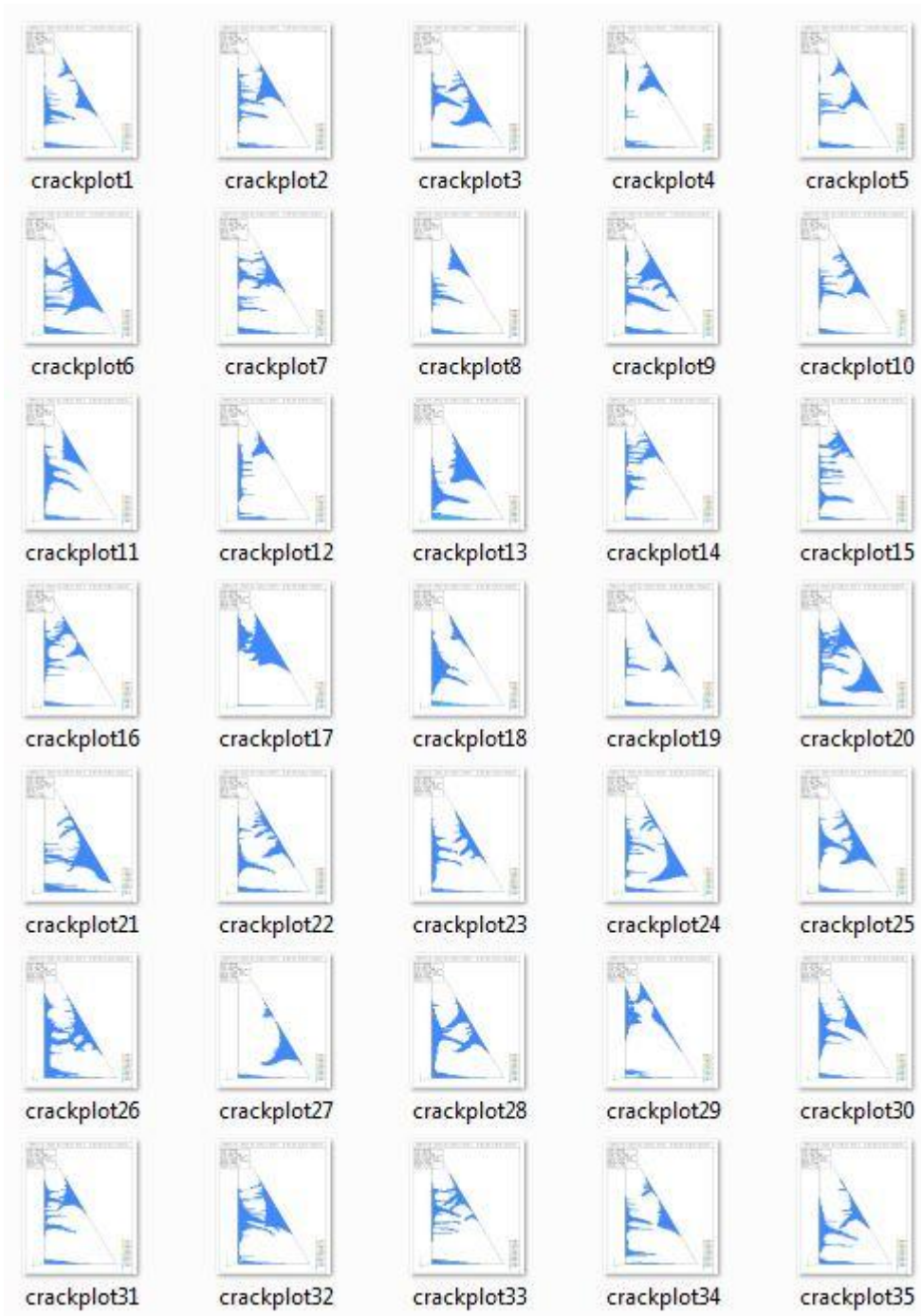
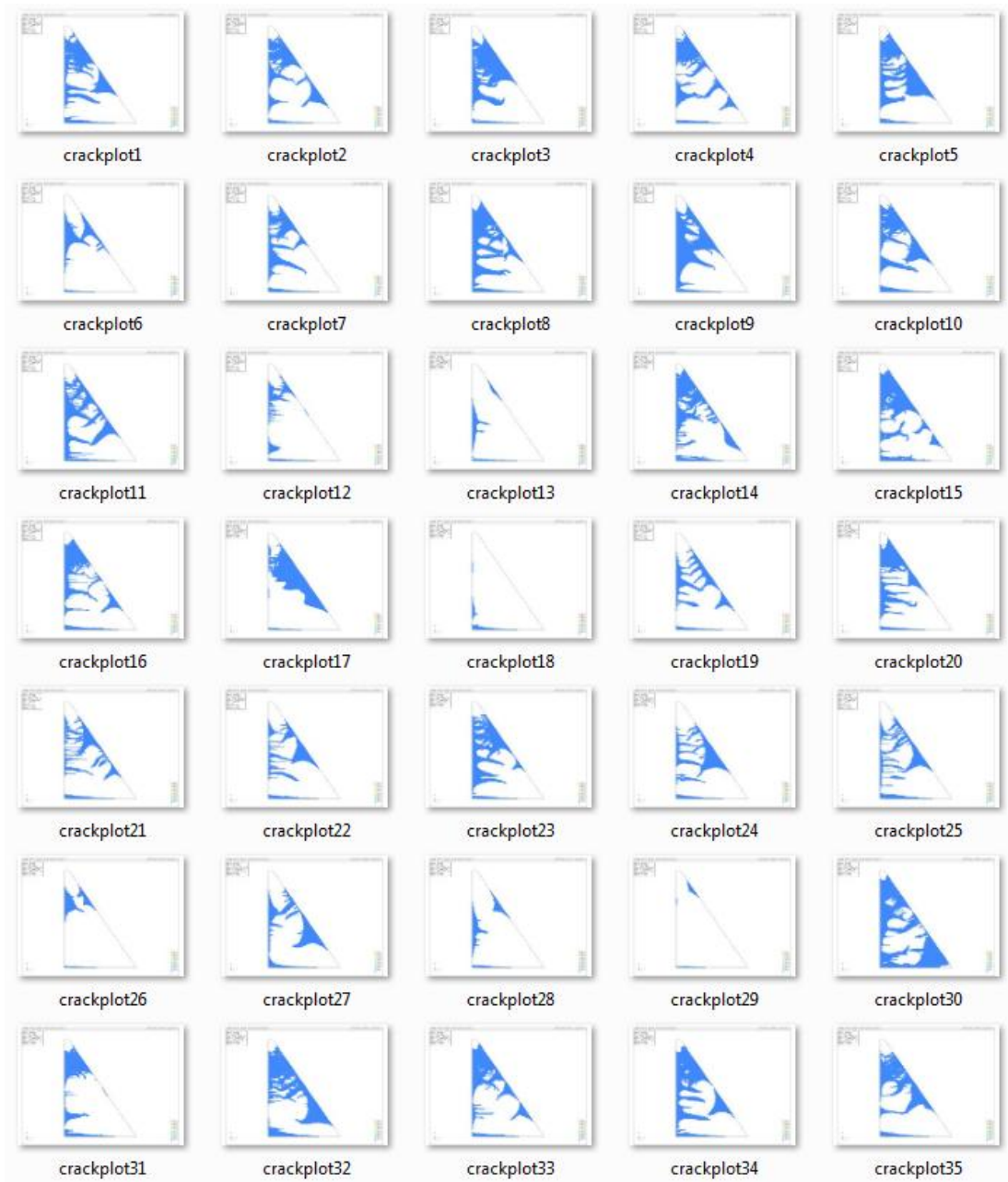**Figure A-15 Cracked Area Plots for ASCE Analyses (h=100m , R=2)**
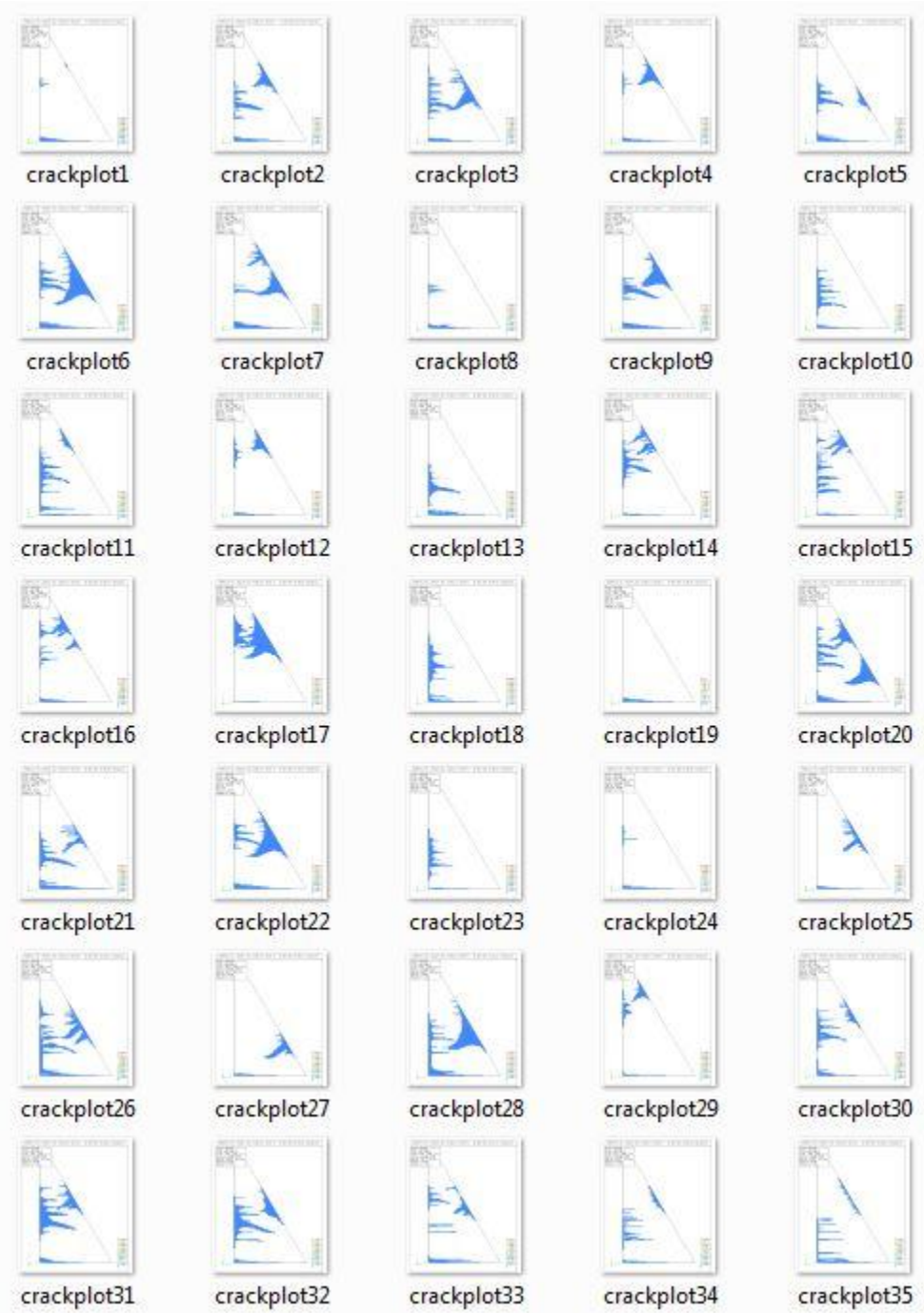
Figure A-16 Cracked Area Plots for ASCE Analyses (h=100m , R=1.5)
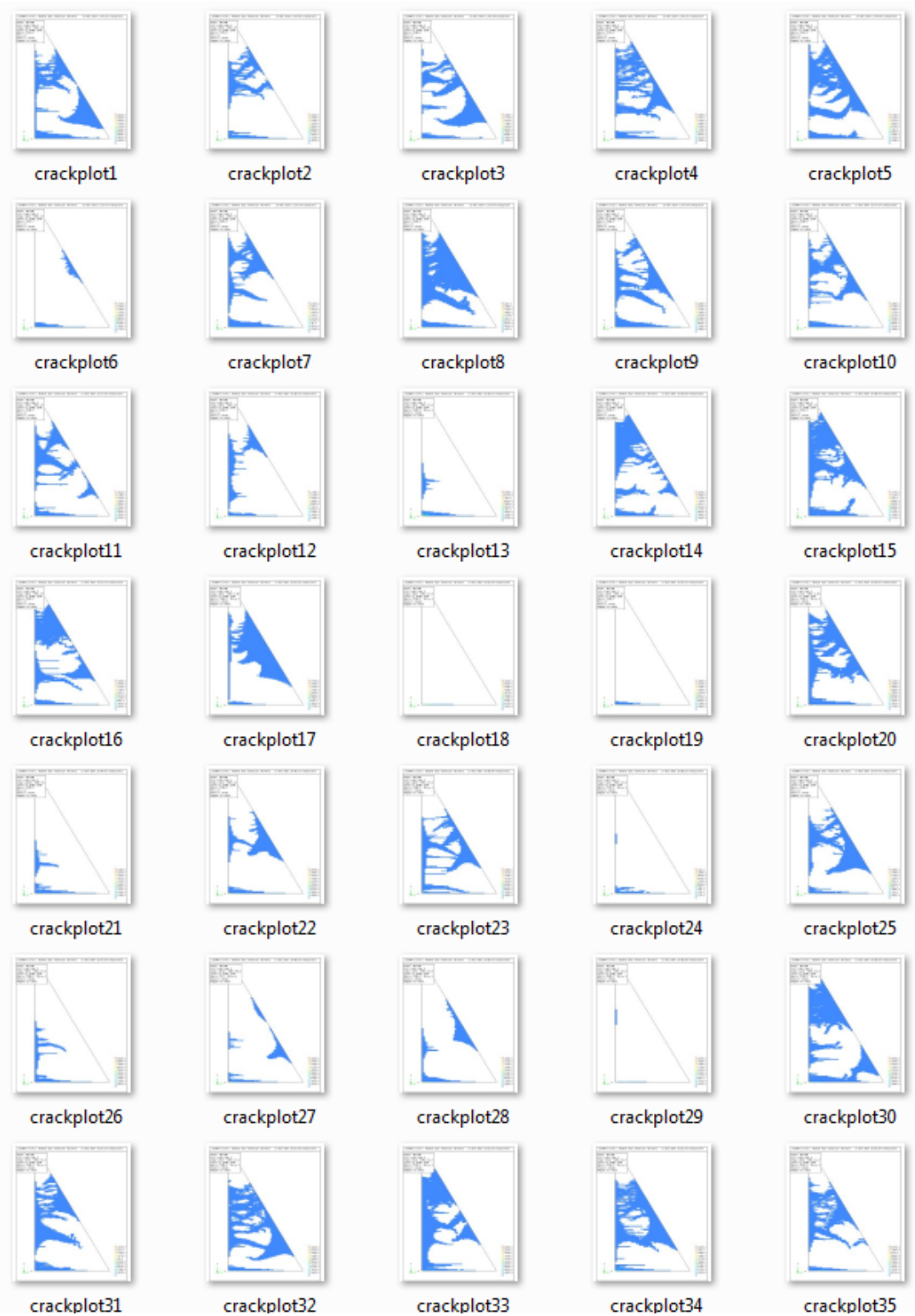
Figure A-17 Cracked Area Plots for MIV Analyses (h=100m , R=2)
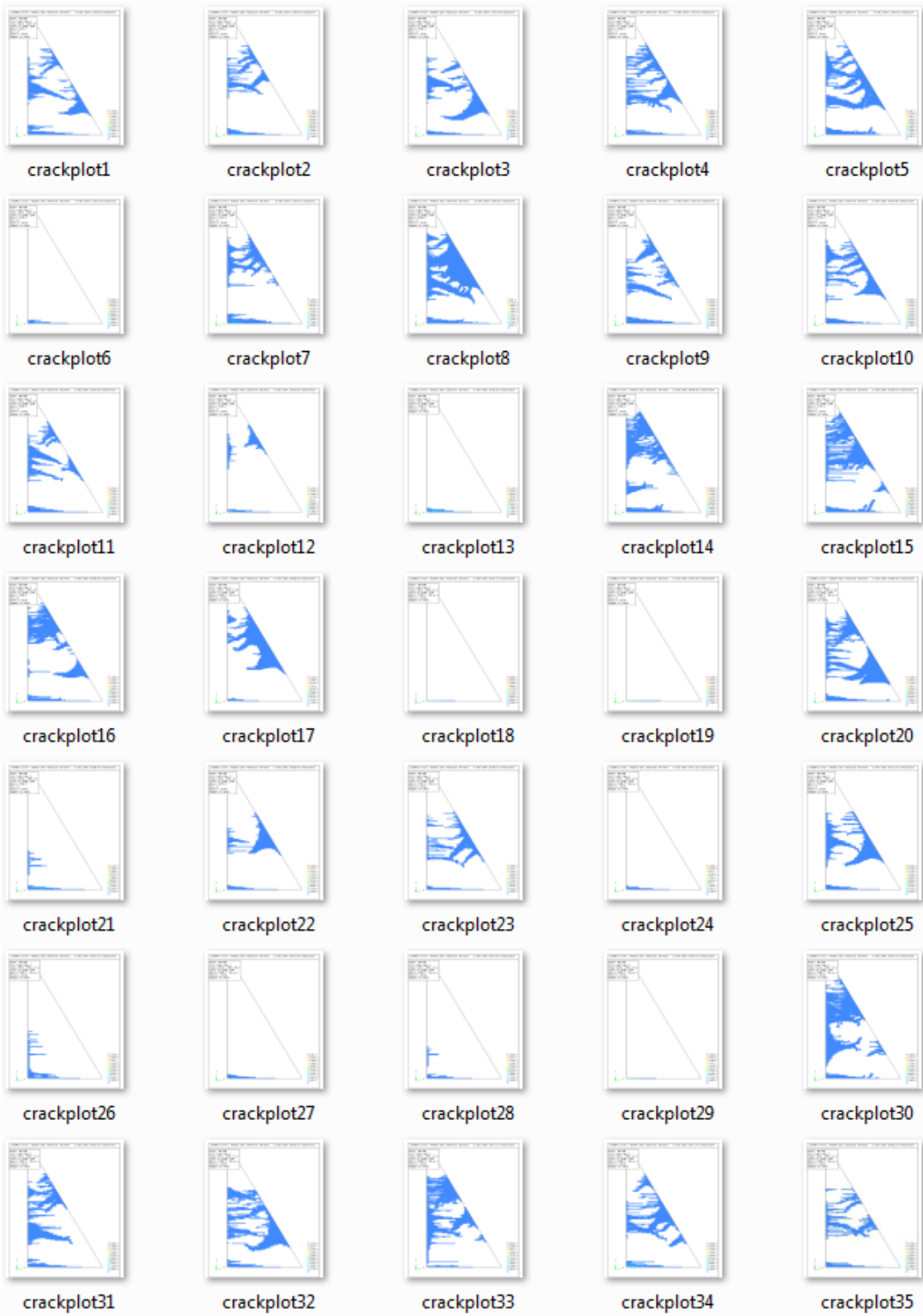
Figure A-18 Cracked Area Plots for MIV Analyses (h=100m , R=1.5)

Figure A-19 Cracked Area Plots for MPS Analyses (h=100m , R=2)

Figure A-20 Cracked Area Plots for MPS Analyses (h=100m , R=1.5)

Figure A-21 Cracked Area Plots for Unscaled Analyses (h=150m , R=2)

Figure A-22 Cracked Area Plots for Unscaled Analyses (h=150m , R=1.5)

Figure A-23 Cracked Area Plots for RSPM Analyses (h=150m , R=2)
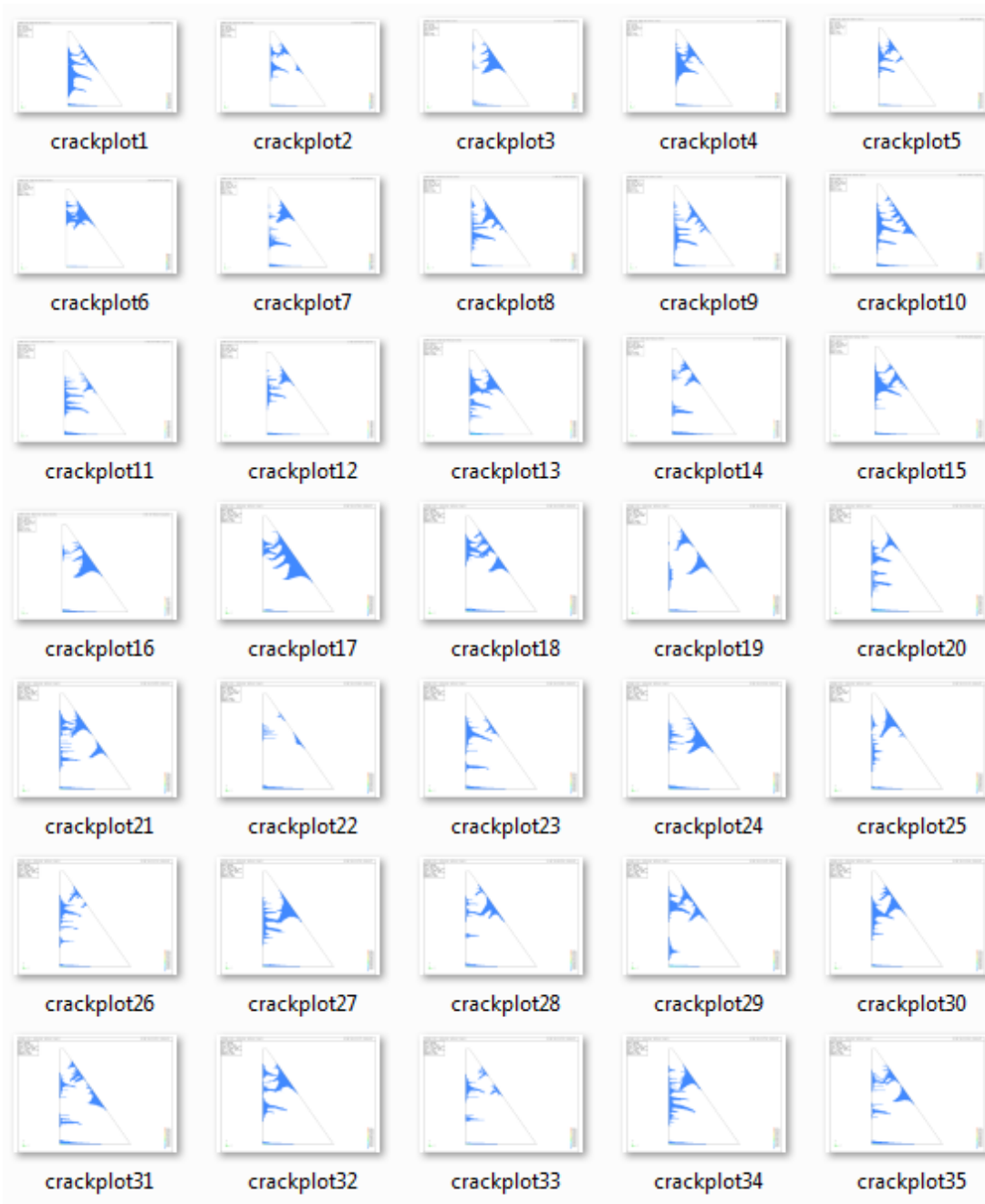
Figure A-24 Cracked Area Plots for RSPM Analyses (h=150m , R=1.5)
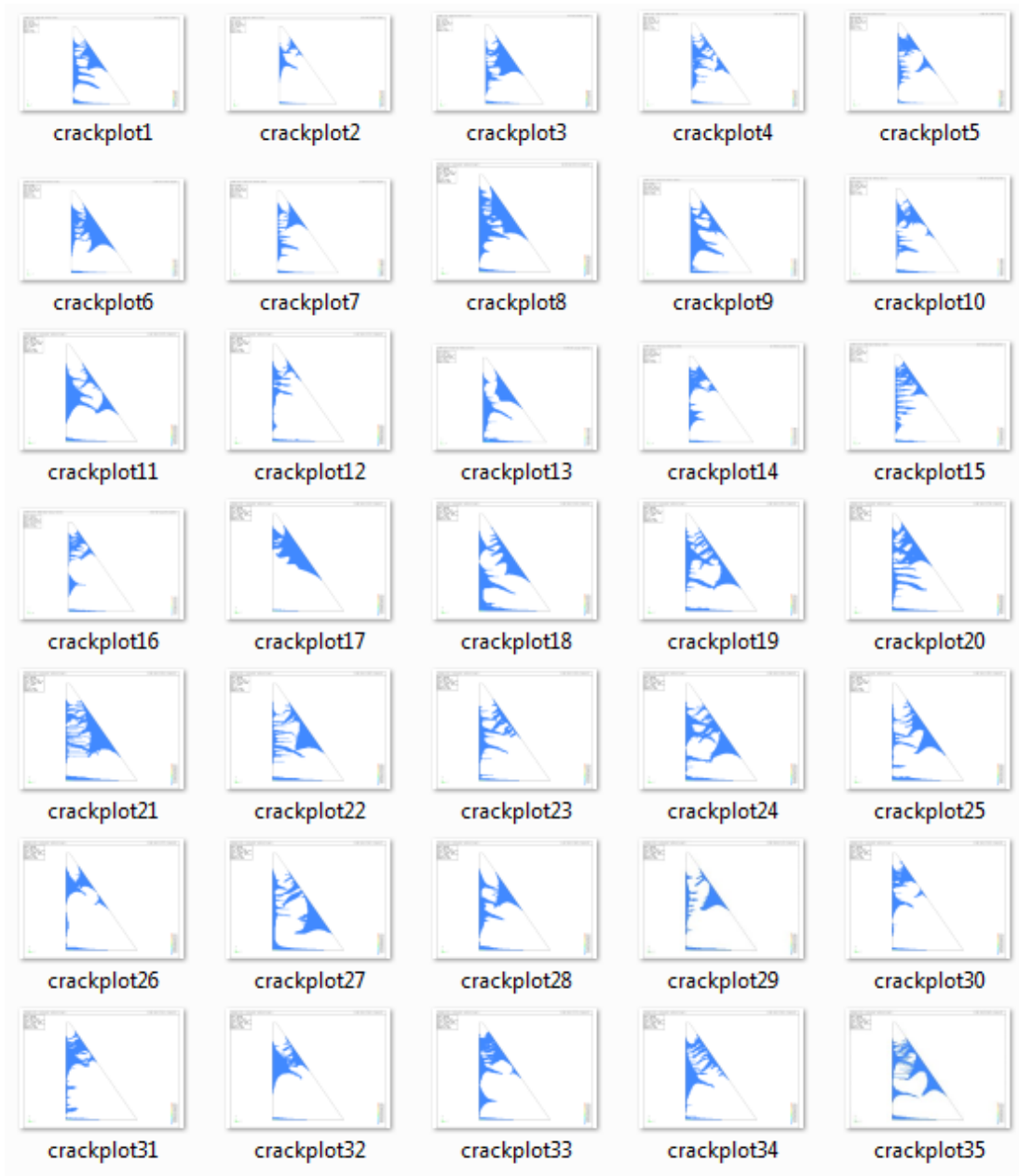
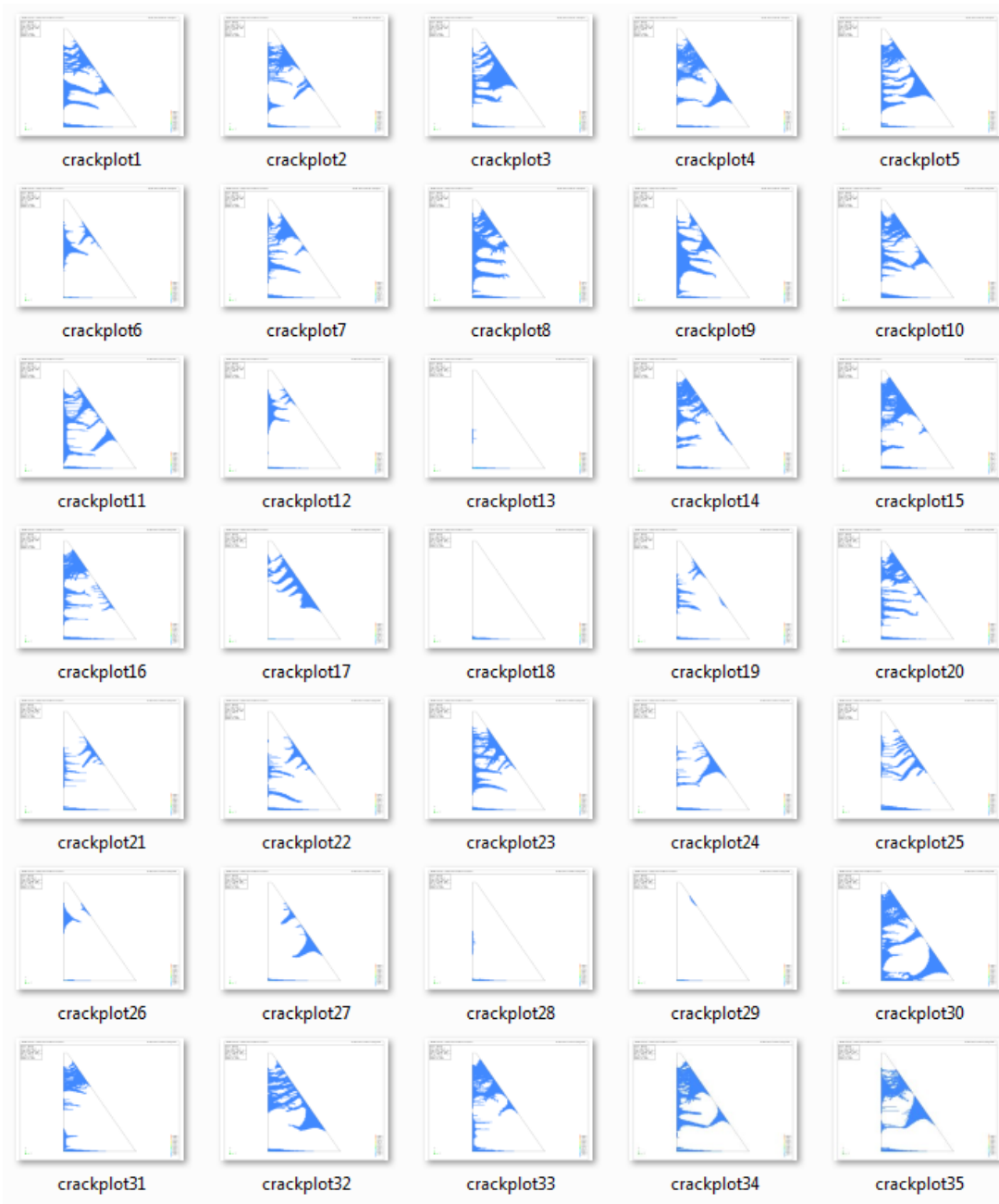**Figure A-25 Cracked Area Plots for ASCE Analyses (h=150m , R=2)**

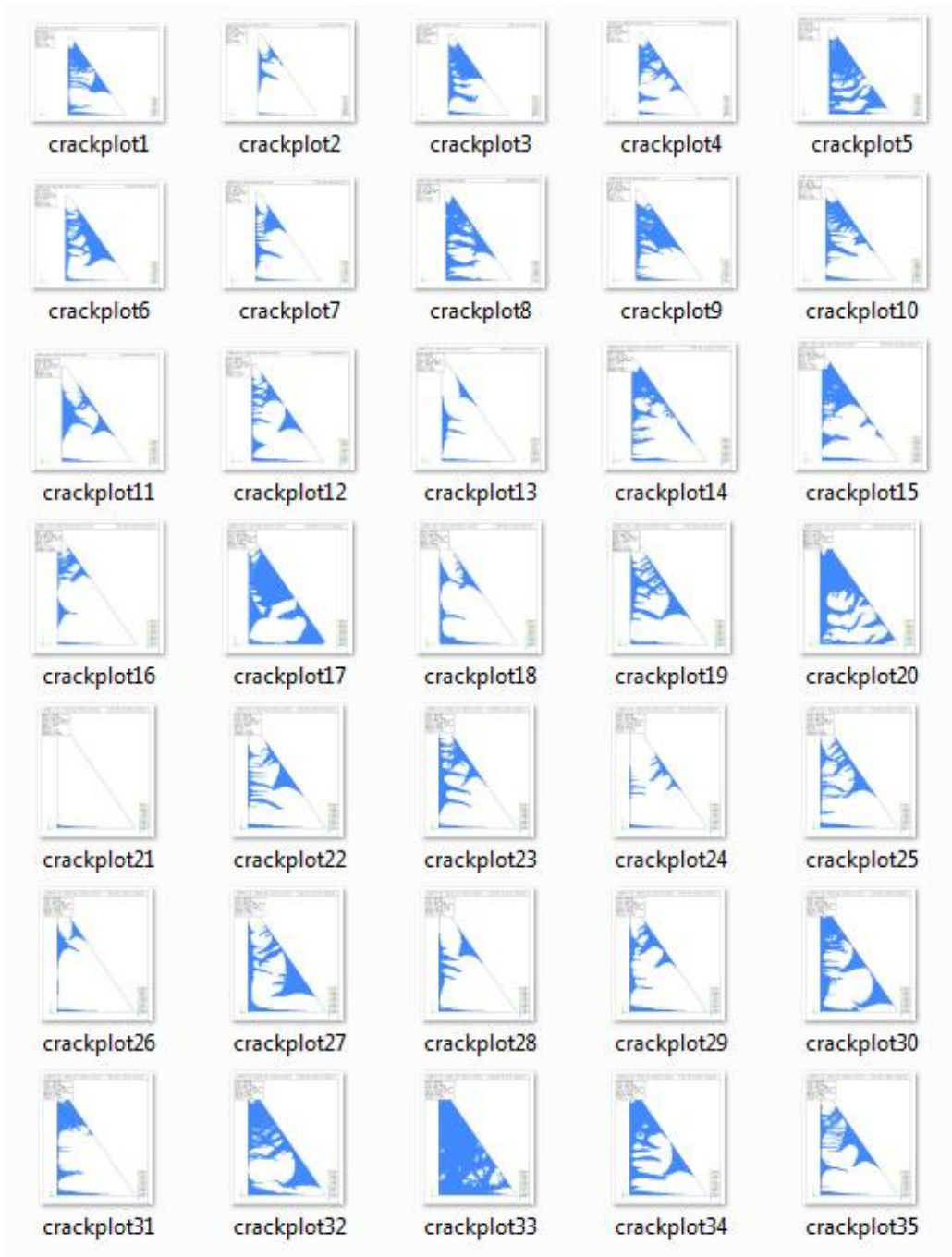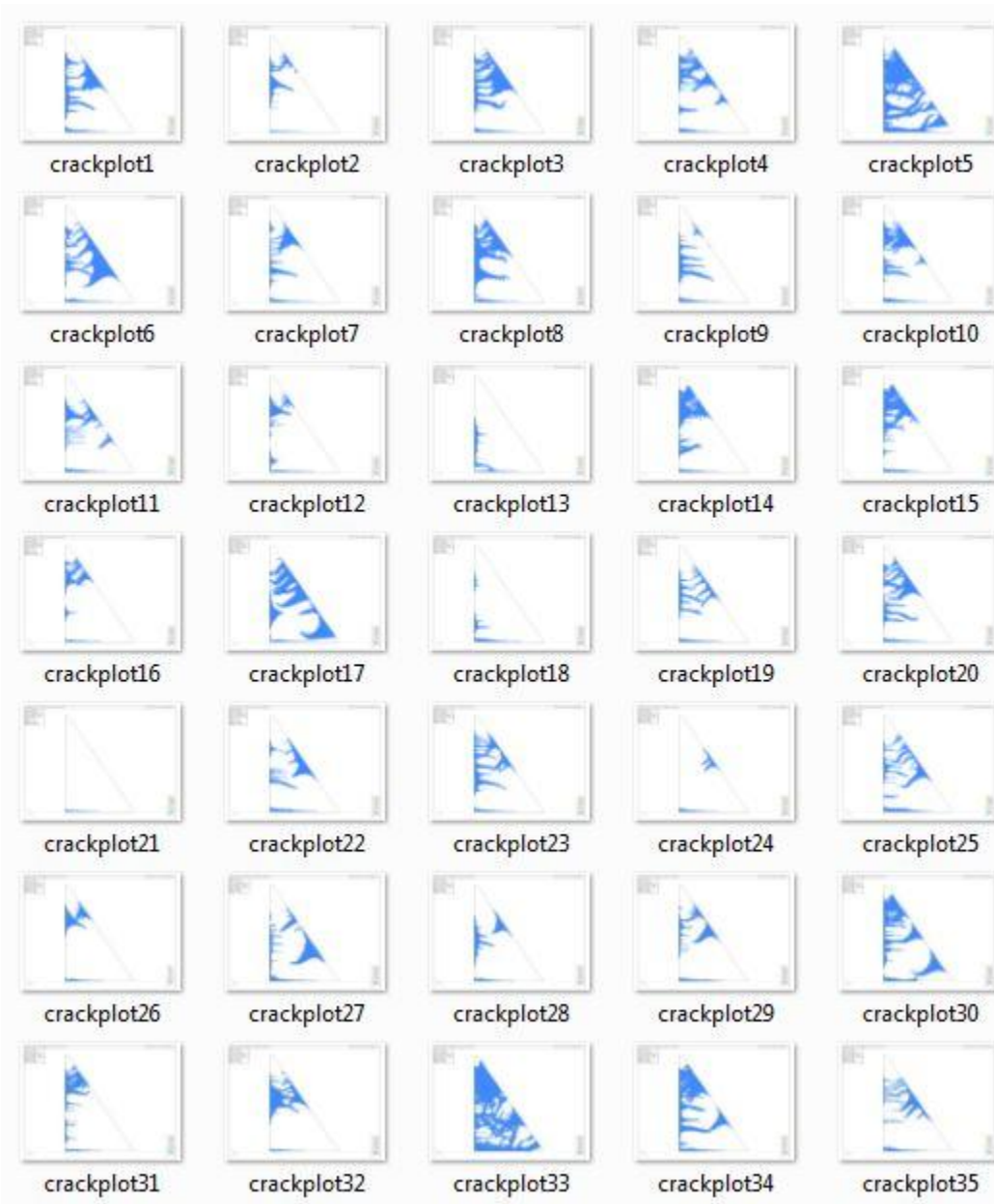**Figure A-26 Cracked Area Plots for ASCE Analyses (h=150m , R=1.5)**

Figure A-27 Cracked Area Plots for MIV Analyses (h=150m , R=2)

Figure A-28 Cracked Area Plots for MIV Analyses (h=150m , R=1.5)

Figure A-29 Cracked Area Plots for MPS Analyses (h=150m , R=2)

Figure A-30 Cracked Area Plots for MPS Analyses (h=150m , R=1.5)